Iii 83
4 85
5 111
9
22

DRL NO. 136
DRD NO. SE-7

9950-843

DOE/JPL 955733-6
DISTRIBUTION CATEGORY UC-63

CONTINUOUS CZOCHRALSKI GROWTH

DEVELOPMENT OF ADVANCED CZOCHRALSKI GROWTH PROCESS TO PRODUCE LOW COST 150 KG SILICON INGOTS FROM A SINGLE CRUCIBLE FOR TECHNOLOGY READINESS

FINAL REPORT
OCTOBER, 1980 - APRIL, 1982

CONTRACT NO. 955733

PROGRAM MANAGER - R. L. LANE
PROJECT LEADERS - B. R. BEZIO, J. BOOTHROYDE
L. M. POLSKY, C. M. JOHNSON

KAYEX CORPORATION
1000 MILLSTEAD WAY
ROCHESTER, NEW YORK 14624

"The JPL Flat Plate Solar Array (FSA) Project is sponsored by the U.S. Department of Energy and forms part of the Solar Photovoltaic Conversion Program to initiate a major effort toward the development of low cost solar arrays. This work was performed for the Jet Propulsion Laboratory, California Institute of Technology, by agreement between NASA and DOE."

ACKNOWLEDGEMENTS

The authors wish to thank the numerous people who contributed to this project. Special thanks go to:

Kayex Technology Center

D. Ewen - Process Technician

D. Rakover - Assistant Process Engineer

E. Roberts - Process Leader

N. Sarno - Process Engineer

W. Schaefer - Electronic Specialist/Designer

C. Schietinger - Mechanical Specialist/Designer

S. Shea - Assistant Process Engineer

Hamco Division of Kayex

D. Fanale - Equipment Engineer/Testing

S. Gilbert - Equipment Designer

Jet Propulsion Laboratory

M. Leipold - Deputy Manager - FSA Technology Development Area

A. Morrison - Technical Project Monitor

ABSTRACT

The goals of this contract are summarized as follows:

1. To design and construct a crystal grower capable of producing 150 kg of silicon crystal from one crucible (5 x 30 kg ingots).
2. Accelerated recharge and growth rate.
3. Microprocessor controls with improved sensors.
4. After-growth yields of 90%.
5. Throughput of 2.5 kg/hr.

Subsequently, a Technical Direction Memorandum was issued which placed emphasis on (1) the improvement of growth rates using radiation shielding and (2) investigation of the crucible-melt interaction for improved yields.

Growth runs were performed from both 15 and 16-inch diameter crucibles, producing 30 and 37 kg ingots respectively. Efforts to increase the growth rate of 150 mm diameter ingots were limited by temperature instabilities believed to be caused by undesirable thermal convections in the larger melts. The radiation shield improved the growth rate somewhat, but the thermal instability was still evident, leading to non-round ingots and loss of dislocation-free structure. A 38 kg crystal was grown to demonstrate the feasibility of producing 150 kg with four growth cycles.

After the grower construction phase, the Hamco microprocessor control system was interfaced to the JPL growth facility, including the sensor for automatic control of seeding temperature, and the sensor for automatic shouldering. Efforts focused upon optimization of the seeding, necking, and shoulder growth automation programs. Demonstration of these three crystal growth areas was accomplished with 150 mm diameter ingots and melts up to 40 kg. A laser beam reflection system for melt level sensing was installed on the grower and shown to function acceptably, although it was not interfaced with the microprocessor.

A gas analysis system was designed, built, and operated as a part of the analytical program of this contract.

Analyses of the crystal grower exhaust gas for CO, H_2O, and H_2 gas were performed on several crystal growth runs. Very high levels of CO accompany overheating of the crucible/melt, suggesting melt-down procedures should be controlled more closely to prevent excessive dissolution of the crucible. Graphite bakeout procedures have been improved by measuring CO and H_2 during the bakeout process to determine when graphite parts are sufficiently outgassed.

Solar cell efficiencies of silicon material produced during long recharge runs (run no. 10) showed no signs of deterioration from the first to the last crystal grown. These results tend to confirm results from previous contracts.

A best case economic analysis, based on actual growth parameters, yielded an add-on cost of $23.17/kg (or ¢16.34/wp) for the growth of 4 x 37.5 kg ingots from one 406 mm (16") diameter crucible.

Although all the goals of the contract were not met simultaneously, most of the goals were achieved either individually or in some combination. Information gathered and evaluated during this project has influenced the design and manufacture of a new Hamco crystal grower (CG 6000) intended to be a commercial machine with capacities in excess of those required during this project. The Hamco CG 6000 crystal grower was designed with the potential for meeting the goals of this project.

CONTENTS

CONTENTS (Cont.)

ILLUSTRATIONS

ORIGINAL PAGE IS
OF POOR QUALITY

ILLUSTRATIONS (Cont.)

TABLES

1.0 INTRODUCTION

This report describes the work performed by the Kayex Corporation Technology Center for the Jet Propulsion Laboratory under contract 955733. The contract was awarded on September 26, 1980, and was completed on April 30, 1982. The contract was part of the JPL/DOE Flat Plate Solar Array (FSA) project, the overall goal of which is to develop technology for the production of solar arrays at a cost of $0.70 per peak watt by 1986 expressed in 1980 dollars. It is also part of the JPL program to develop Technology Readiness in 1982 (TR-82).

This is the third program conducted at Kayex for JPL aimed at reducing the add-on cost of Czochralski (CZ) growth. It was a continuation of the effort toward developing a production method for continuous CZ growth. Continuous CZ growth is defined as the growth of large quantities of crystalline material from one crucible by serial ingot growth with either continuous or periodic melt replenishment.

1.1 Background

Since the inception of the DOE/JPL Flat Plate Solar Array Program several contractors have devised methods for melt replenishment in CZ growers and for continuous CZ growth.

Texas Instruments[1] proposed to replenish the melt with liquid silicon by the use of a resistance heated premelter. In the T. I. System, the auger feeder introduced silicon into the premelter, and the liquid silicon then flowed into the crucible, thereby maintaining a constant melt level during growth.

If the liquid temperature were reasonably controlled, it was expected that there would be no harmful thermal perturbation of the melt. Ingot size would only be limited by the pull length of the equipment.

It was found that the operation of the premelter was a very difficult task, primarily because (1) the refractory quartz liner of the premelter devitrified rapidly, and (2) the uniform flow of silicon was nearly impossible due to the high surface tension of the liquid. Considerable effort was made on premelter design.

Also, T.I. reported that the auger feed system worked poorly for chunk silicon, as it tended to crush the silicon. Concern was expressed that the abrasive nature of silicon was probably causing contamination of the silicon from the stainless steel auger.

The T.I. work, however, was significant, in that it illustrated the extreme difficulty in handling both solid and liquid silicon in a controlled manner without contamination.

Varian, Inc.,[2] adapted an auger system to their standard CZ grower. The Varian system was quite similar to the T.I. except that recharging was performed intermittently between ingot growth cycles. The auger system was adapted to feed lump silicon directly into the crucible.

Varian had good success with this recharging system and reported several fairly large runs completed, up to about 60-70 kilograms.

Perhaps one of the most valuable results from the Varian work was an experiment performed very early in the JPL program. A 100 kg run simulation was performed, by the growth of five 20 kg ingots sequentially from the same crucible and same charge of silicon. After each ingot was grown, it was remelted into the crucible and the cycle was repeated.

This experiment proved that the crucible would survive for long periods of time through severe thermal cycling. It was an encouraging result for all contractors involved in continuous CZ.

Siltec Corporation[3] developed a method of continuous liquid feed from a secondary melting chamber through a heated transfer tube.

The Siltec effort was very significant in that it pointed out a way to overcome or avoid the effect of the high surface tension on the pouring of silicon. A siphon principle was used. Once the transfer tube was filled with liquid, uniform and continuous flow could be achieved by simply raising the level of the supply crucible.

Simultaneous crystal growth and continuous liquid feed replenishment were demonstrated. Also, the possibility of growing an extremely large ingot from a relatively small crucible was demonstrated by the growth of an ingot of over 60 kg.

Although the Siltec method is not well enough developed for commercial application, its potential for low cost ingot growth probably surpasses the other approaches, primarily because its throughput should be the highest.

The demonstration of continuous liquid feed was an excellent technical accomplishment and may very well have a significant future application.

Previous Kayex Corporation projects related to continuous CZ growth, supported by JPL, are as follows:

JPL 954888 Continuous Czochralski Growth
Silicon Sheet Growth Development of the
Large Area Silicon Sheet Task of the
Low Cost Silicon Solar Array Project
October 1977 - December 1980

JPL 955270 Low Cost Czochralski Crystal Growing Technology
Near Term Implementation of Flat Plate
Photovoltaic Cost Reduction of the Low Cost
Solar Array Project
March 1979 - September 1980

The general objectives of contract 954888 were to:

- modify a commercial Hamco/Kayex CG2000 crystal grower for continuous CZ.
- develop a suitable continuous CZ process which met the cost allocations and solar efficiency goals of the JPL Solar Array Project.

Key modifications and accessories to the CG2000 equipment considered to be important to achieving the goals were as follows:

a. vacuum-tight isolation valve between furnace chamber and pull chamber to permit (1) removal of grown ingots and (2) replenishment of feed silicon.
b. automatic recharging mechanism, capable of handling either polycrystalline rods or lump silicon.
c. enlarged pull chamber for the storage of one charge of silicon feed material.

d. increased capacity to 356 mm (14-inch) diameter crucibles, and 12.5 cm (5-inch) diameter crystals with suitable automatic diameter controls.

e. ingot/silicon handling equipment for efficient crystal removal and recharging.

The optimized process which was developed on contract 954888 utilized the modified CG2000 machine with a 14-inch diameter crucible. One hundred kilograms of 5-inch diameter ingot were grown from the crucible with a target ingot size of 25 kilograms.

Major problems were encountered in achieving the throughput rate required to meet the cost goals. Also, the yield of monocrystalline vs. polycrystalline ingot was low.

The solar efficiency of cells produced from the monocrystalline grown material met the goal of 14% AM-1 but the polycrystalline material was typically in the range of 12% AM-1.

The results showed that, for monocrystalline ingots, solar efficiency did not change significantly from the first material to the last when grown from the same crucible. This indicated that the accumulation of impurities in the residual melt was not sufficient to degrade solar efficiency, at least up to 100 kg.

In addition, although polycrystalline ingot material showed somewhat lower solar efficiency, it too remained constant through 100 kg grown.

The work performed on contract 955270 was aimed at improving throughput by increased melting rate and by increased growth rate. The approaches to this effort were to:

a. utilize additional heating methods to accelerate the the meltback of the polysilicon.

b. utilize a conical radiation shield or cooled heat sink above the melt to cool the crystal and maintain a sharper thermal gradient in the melt, thereby permitting increased growth rate.

In order to increase the melting speed of polysilicon rod feed stock, an induction coil was placed in the furnace around the poly rod to provide the extra heat required for melting.

As the poly rod was lowered into the crucible, it was heated sufficiently to couple with the induction coil. This method allowed the crucible to be maintained at a lower temperature to prevent degradation while permitting very rapid melting.

To accelerate melting of lump silicon, a cold crucible premelter was constructed into which the lump silicon could be fed. It was designed to attach to the side of the grower so that silicon was actually poured into the crucible in the recharging operation. Again, the extra heat required for melting was provided separately by the induction coil, allowing the crucible to be maintained at a lower temperature.

Little success was obtained in premelting the poly rod due to arcing and cracking of the rods. However, it became apparent that low cost silicon would probably not become available in rod form, and the effort was therefore dropped. The cold crucible was found to melt and pour silicon successfully. Due to time and budgetary constraints, an actual recharge operation was not performed on the grower using the cold crucible premelter.

Considerable improvement in growth rates was realized with the radiation shield. This was concluded to be a reasonable method for production growth and would, therefore, result in reduced cost of growth.

The above experiments and the development of an economic model for continuous CZ showed that further reductions could be realized by:

a. growth of 150 kg from one crucible
b. increased ingot diameter (150 mm) for greater solidification rate
c. larger ingots, meaning fewer recharge cycles
d. automation by computer for better yields with cheaper labor cost
e. lower machine cost

After a preliminary study of the various alternative methods to implement melt replenishment, the present project was proposed to JPL which addressed the above areas of cost reduction. The intermittent recharge of lump silicon with a hopper developed on the first Kayex

contract was subsequently chosen as the preferred method for achieving the objectives. The program plan was developed to address the specific goals.

1.2 Project Goals And Program Plan

The specific objectives which were required to achieve the cost objectives were as follows:

a. Continuous growth of 150 kg or more of multiple single crystal ingots from one common crucible with melt replenishment.
b. Resistivity of 1 - 3 ohm-cm p type, in all crystals.
c. Dislocation density below 10^4 per cm^2.
d. Diameter of 15 cm or greater.
e. Growth rate of 15 cm or greater.
f. Orientation: 1-0-0.
g. Pulled yield of greater than 90%.
h. Equipment suitable for high volume continuous Czochralski production, transferable directly to industry.
i. Solar cell efficiency $\geq$ 14% at AM1.

The original program commenced in October 1980 and was scheduled for completion in 13 months. In April 1981 a request was received from JPL to minimize expenditures for fiscal year 1981 and to extend the program six months into FY82. The new completion date was March 31, 1982. The following program plan (figure 1-1) represents the revised one.

The Program Plan was divided into five tasks, which are described below:

Task 1. Equipment Construction and Test

A standard Hamco CG2000 crystal grower will be modified in a number of areas to make it suitable for advanced CZ growth of the parameters specified in the RFP. These areas will include at least the following:

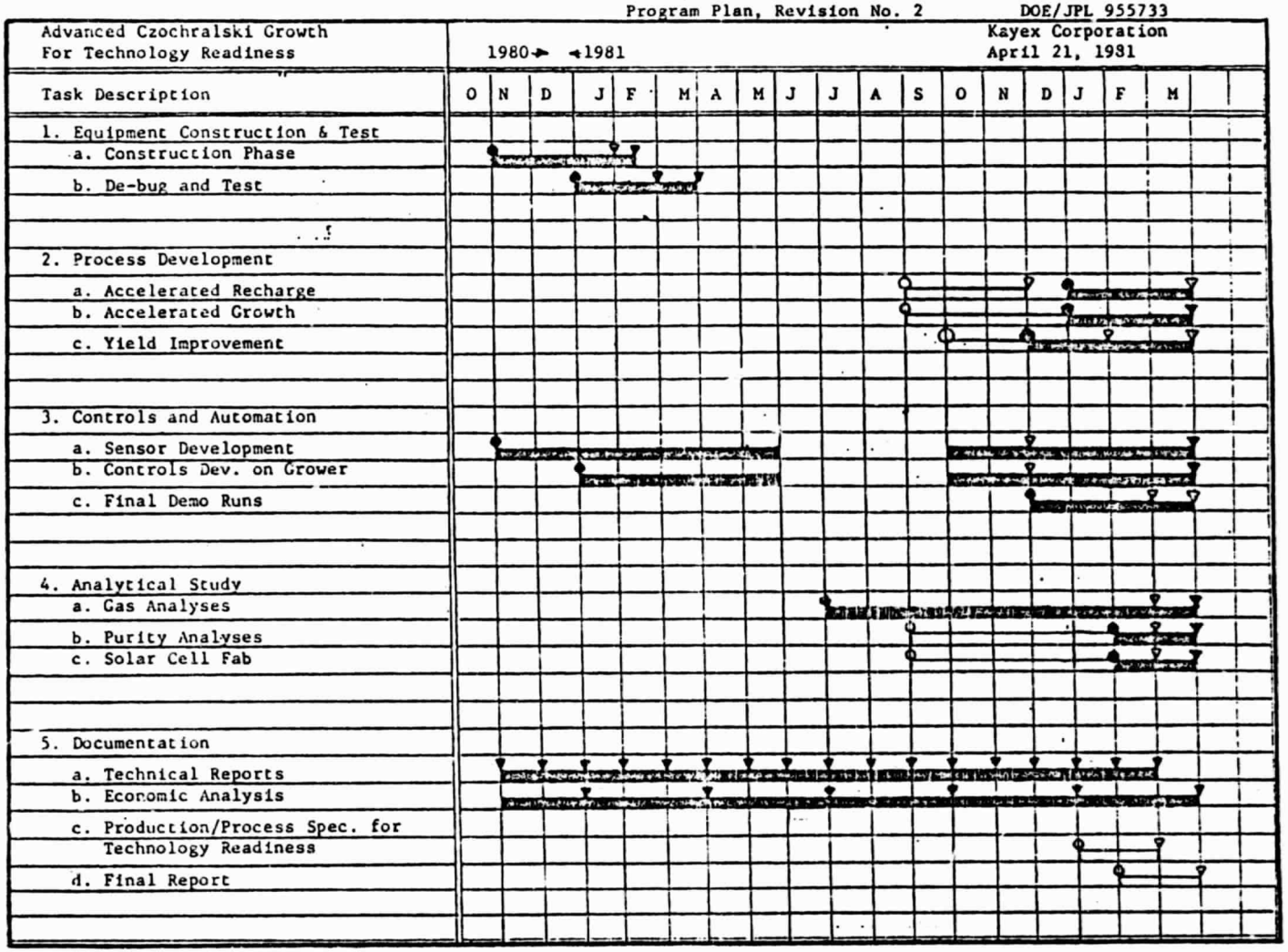

PROGRAM PLAN

FIGURE 1-1

- o Increased Chamber Size--A CG2000 chamber will be designed capable of accepting up to a crucible size of 16-inch diameter by 14-inch high. This will allow ingots of at least 30 kilograms to be grown.
- o Increased Hot Zone Capacity--15- and 16-inch diameter crucibles will be accommodated. Graphite parts will be designed to minimize as much as possible graphite losses due to breakage and degradation.
- o Recharge Hopper--A larger hopper will be designed to accommodate the larger recharge size.
- o Pull Mechanism--A standard Hamco cable lift mechanism and weight system will be upgraded to a 50 kg capacity.
- o Control Console--A Hamco control console will be adapted for plug compatability with the computerized control system. The control system will consist of a Kayex-Hamco Automatic Grower Logic (Agile) diameter control system and a sensor system to be developed.

Task 2. Process Development

Improvement in yields, throughput, and labor costs must be demonstrated in order to establish the suitability of advanced CZ growth for meeting goals. The major risk areas will be investigated independently and, after optimizations, will be demonstrated simultaneously.

Task 3. Controls Development and Process Automation

The Kayex-Hamco microprocessor-based controls currently available replace elements of the analog circuitry with programmed, digital logic and automate time dependent steps of the crystal growth process. However, significant operator judgment and input are still required during the initial stages of crystal growth prior to at-diamter growth of the crystal body. Operator attention and judgment are required because of the lack of adequate sensors for key parameters including melt temperature, melt level, and crystal diameter.

The proposed program includes implementation of sensors for these parameters and a controller for processing sensor output and

replacing operator judgment during the critical initial steps of crystal growth.

Task 4. Analytical Study

4 (a) Purity Analyses of Silicon

Control of silicon purity will be monitored by chemical impurity analysis of selected samples, including silicon feedstock, grown ingots, and residual melt. All analyses of silicon will be performed by outside vendors.

4 (b) Solar Cell Fabrication and Analysis

Grown ingot material will be selected from 150 kg runs for slicing into wafers to measure solar efficiency.

4 (c) Analysis of Furnace Atmosphere

Earlier Kayex-funded research attempted to analyze the atmosphere of the furnace during ingot growth utilizing a quadrapole mass spectrometer. A commercial residual gas analyzer was leased and a series of runs was made with the analyzer attached to the grower gas outlet. Although the results were highly qualitative, it was established that several gaseous species exist in the growth atmosphere. In the proposed work, the furnace atmosphere will be analyzed quantitatively and correlated with materials and process variables. Instead of the mass analyzer, a gas chromatograph will be used because it is more quantitative.

Task 5. Documentation

In accordance with the statement of work, Kayex will, in addition to the usual periodic technical reports, provide information for rapid technology transfer to industry. Equipment suitable for the economic production of solar material will be offered for sale to the industry as a means of technology transfer. Written procedures for the production of solar ingot material will be included.

A Technical Direction Memorandum (TDM) was issued by JPL in September 1981 which directed Kayex to place emphasis for the balance of the program on:

a. Increasing throughput rate by the use of a radiation shield.

b. The study of crucible-melt interactions by continuing the effort to analyze ambient gas in the furnace as a function of cycle time and temperature.

c. Preparation of a cost analysis of a "cheapest machine" configuration as it would be used in a production facility.

Thus, the balance of the work consisted primarily of single runs and the associated analytical and evaluation efforts, rather than simply attempting to make more 150 kg runs.

2.0 CRYSTAL GROWER CONSTRUCTION AND TESTING

In order to have a crystal grower capable of meeting the process, automation, and analytical tasks of this contract, a modified Hamco CG2000 grower was designed under a unilateral modification to JPL Contract No. 954888. This design phase occurred from June to December, 1980. When the present contract started in September, 1980, the construction/testing phase of this contract and the design phase program of the previous contract were planned to dovetail in order to minimize lead times for the grower construction. The Mod CG2000 was scheduled to be ready for test by March 1, 1981.

2.1 Design Specification

The Mod CG2000 used the Hamco CG2000 RC grower as the basis for the modified crystal grower. The modular subsystem concept, ease of access to furnace and electrical controls, interlocks, and other safety features were all maintained and/or improved.

The furnace chamber design included:

- All the anticipated ports in the cover for crystal diameter, melt temperature, and melt level sensor development.
- Increased size for accepting both 15-inch diameter and 16-inch diameter hot zones.
- Improved weld designs that minimize the chance of water leaks due to thermal cycling and stress corrosion.
- Easier access for subsystem servicing.

The hot zone designs were improved to minimize losses due to breakage and degradation.

The pull mechanism (seed motion mechanism) was designed for a 50 kg crystal rating and weight readout. Improved rotation seals for longer life and increased process reliability were included.

The crucible motion mechanism was improved by the use of a stainless steel bellows/rotary seal to minimize the potential for air leaks and increased process reliability.

The water cooling, argon, and vacuum subsystems were designed for increased functionality, reliability, and serviceability.

The control console was modified for interfacing with, and switchover to, the Kayex-Hamco Automatic Grower Logic (AGILE) computer control system. This allows for more automation and less operator attention.

The power supply was increased from 125 kW to 150 kW maximum output to provide for the larger zone size, faster meltdown and recharge rates. This was a vendor-supplied prototype obtained by modification of a standard 125 kW supply.

A molybdenum radiation shield/purge cone was designed to increase growth and recharge rates.

The Mod CG2000 is a larger grower. (See figure 2-1 for size comparison.) It is 21 inches taller, but requires only two square feet more floor space than a CG2000. The increased height was necessary for the longer crystals which would be grown from the larger melts.

2.2 Construction

The designs of the longest lead items for the Mod CG2000 were done first under JPL Contract No. 954888. Quotations for the pull chamber, furnace tanks, baseplate, frame, power supply, and hot zones had already been received and evaluated in anticipation of this contract.

When the contract started in Sepember 1980, purchase orders were issued immediately in order to minimize the time for grower construction. By November, all long-lead items were on order or being manufactured by the Hamco Division of Kayex. Design and release for manufacturing of ancillary modifications continued until December for the expected completion by February, 1981.

The grower was located in its own room to ensure an uninterrupted utilities supply. All utilities (argon, water, electrical, vacuum pumps) were installed. Some modifications from the original design were necessary for the water, vacuum, and argon systems because of the dedicated room (e.g. vacuum pumps were located outside the room).

Hamco testing personnel, along with Kayex Technology Center, completed the installation and function system checkout by the expected time in early March 1981. (See figures 2-2 thru 2-4 for photographs of the installed Mod CG2000.)

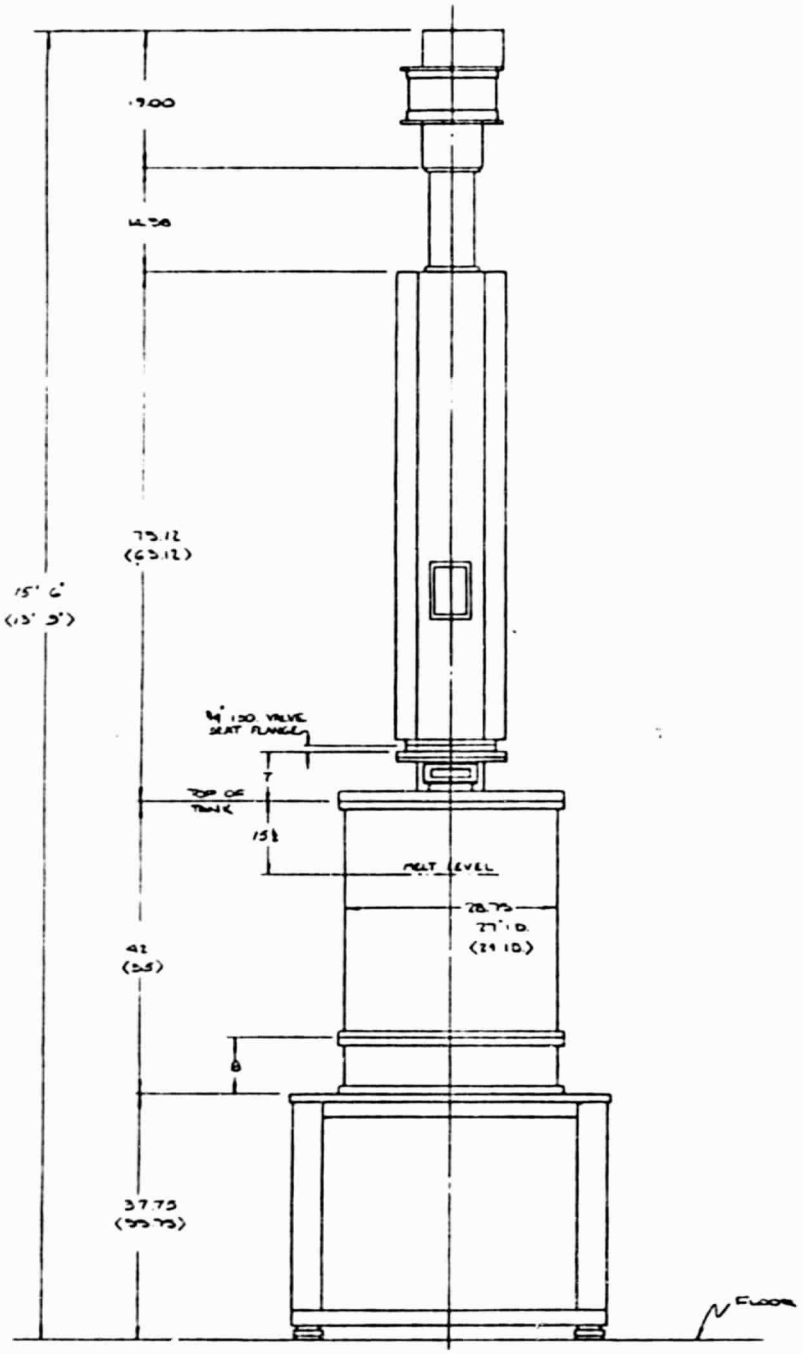

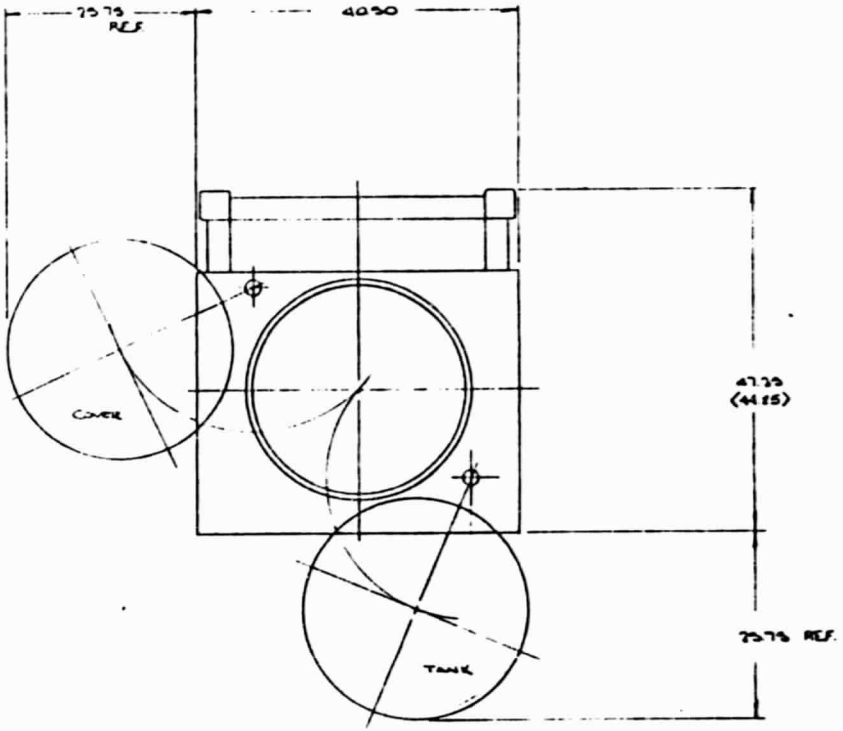

NOTE : DIMENSIONS IN ( )
ARE FOR CG 2000 STD.
NO ( ) INDICATES NO CHANGE.

MOD CG2000 CONFIGURATION

FIGURE 2-1

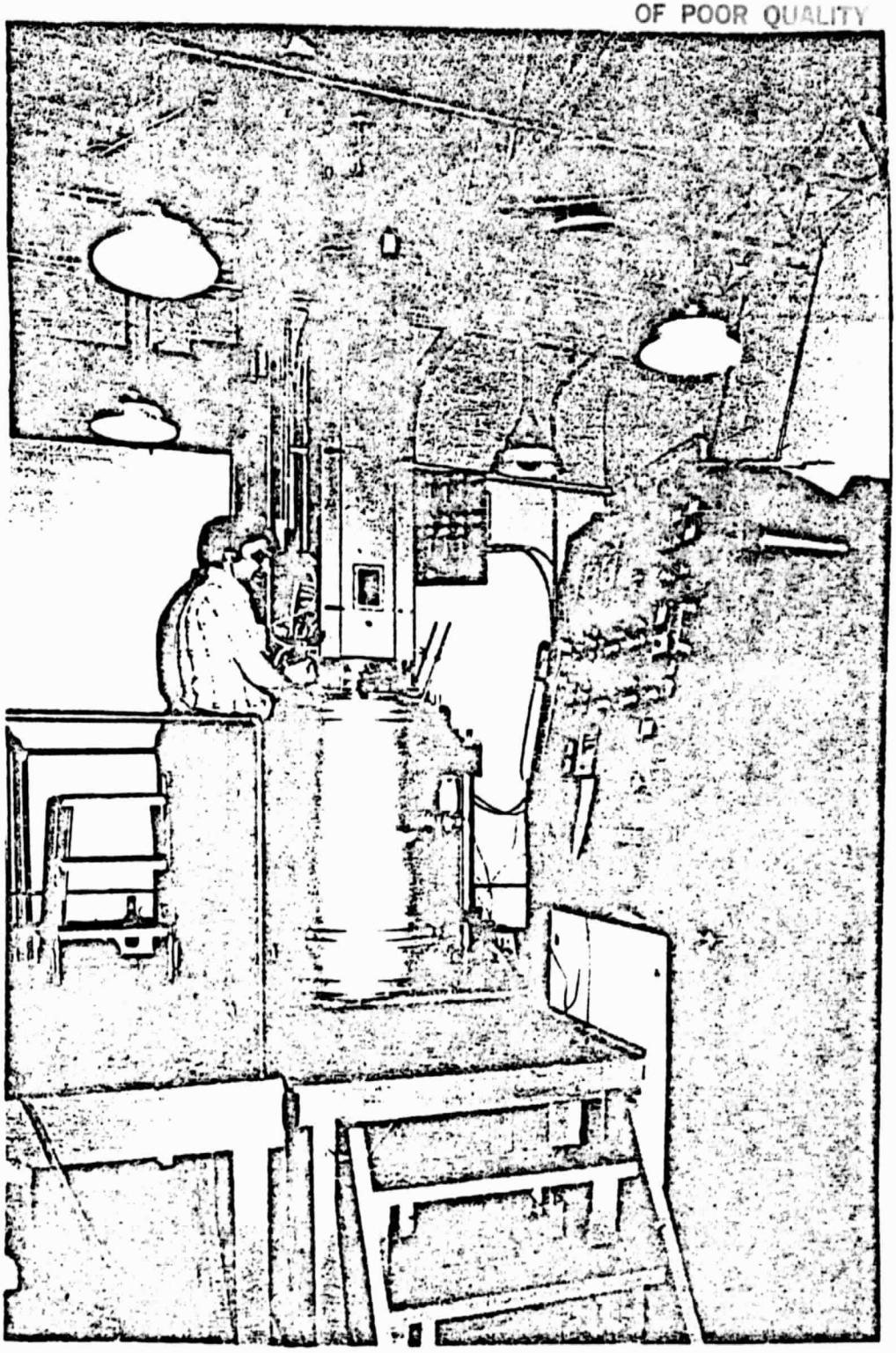

MOD CG2000, COMPLETE

FIGURE 2-2

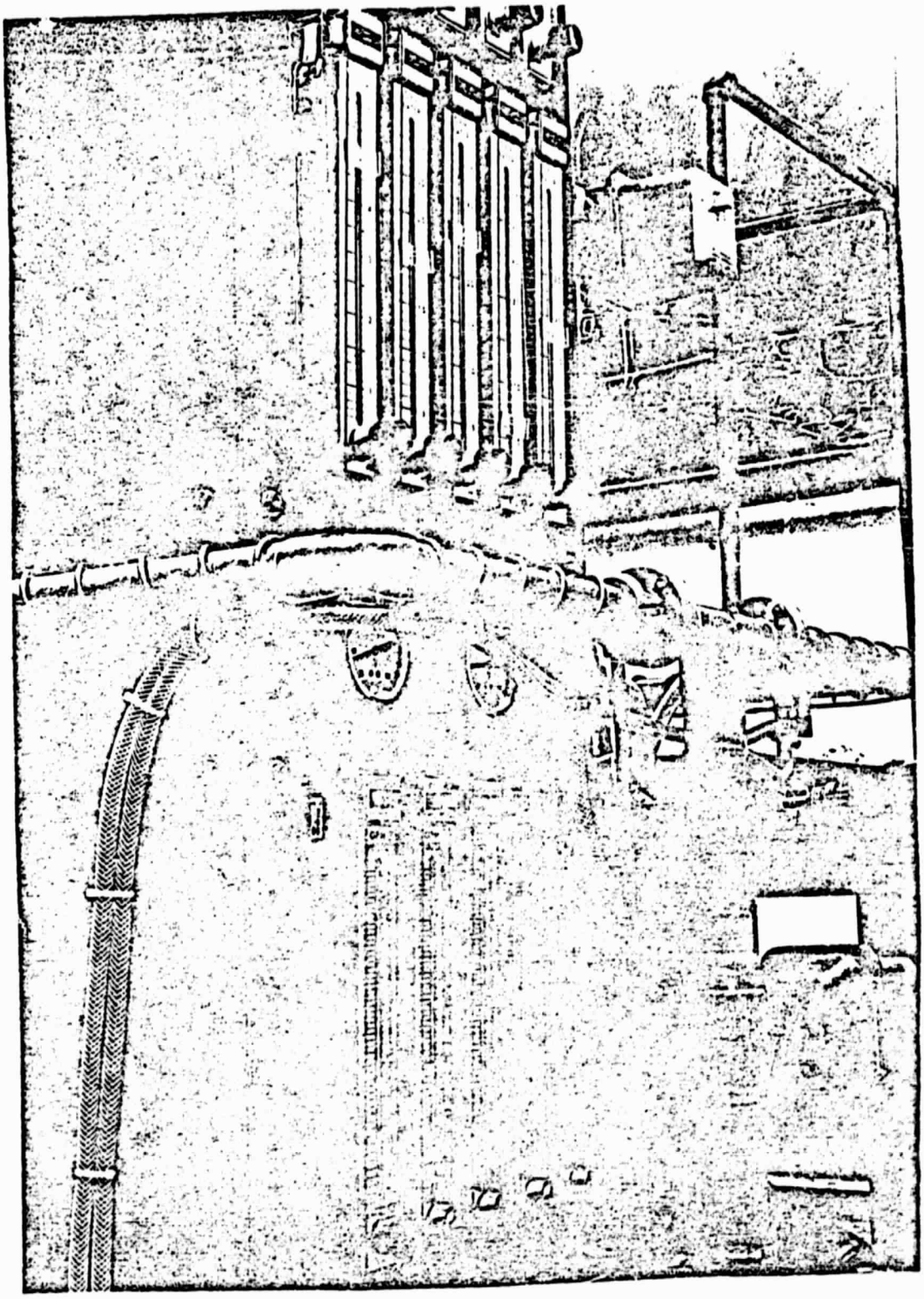

MOD CG2000, REAR VIEW

FIGURE 2-3

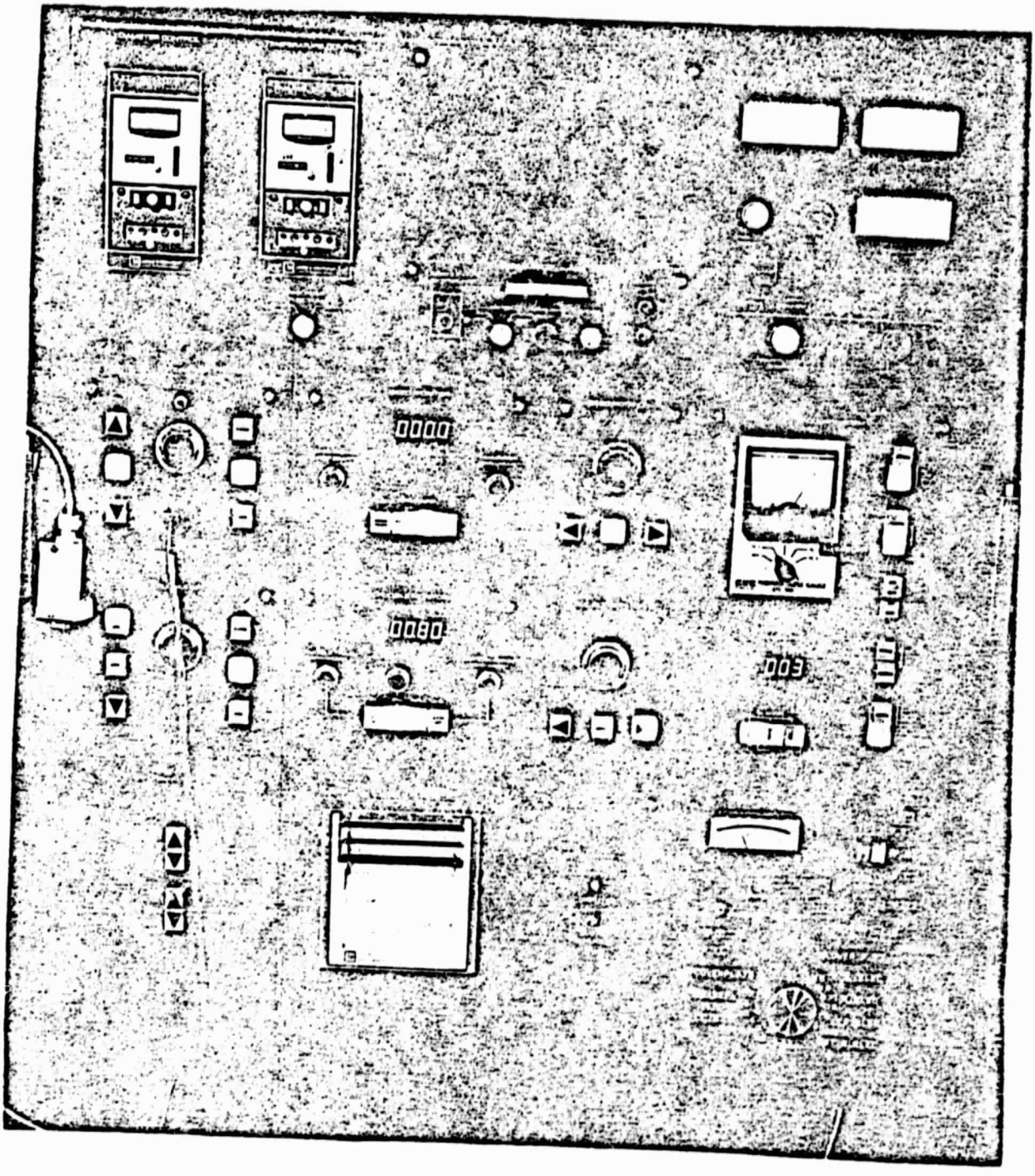

MOD CG2000, MAIN CONTROL PANEL

FIGURE 2-4

2.3 Testing

Process development personnel conducted several "dry runs", baking-out graphite, checking for leaks, and other process related checks under "hot furnace" conditions. Several problems were corrected including calibration of the PCC power supply readout and a noting of the high acoustical noise of the prototype 150 kW power supply.

The modified CG2000 chamber and hot zones were designed to accommodate 15- and 16-inch crucibles and included substantial design changes from their predecessor, the CG2000. The objectives of the first several growth runs were to debug the grower and provide baseline information on the performance of the machine and expected process parameters.

On March 19, 1981, the first growth run using 30 kg of re-cycle silicon was tried. An apparent misalignment of the cable lift mechanism prevented correct imaging of the crystal/melt meniscus under vacuum. Also, it was noted that smoking and excessive oxide build-up indicated a possible leak in the chambers. Several other problems were also noted and corrected.

During April, 1981, four more trial runs were performed. (See table 2-1) These runs continued the process check-out and de-bug of the grower and hot zones. All problems discovered were corrected or noted for future changes. Several parts were returned to vendors for correction.

After these five trial runs, the Mod CG2000 grower construction and testing was deemed to be finished, and the equipment ready for the process development portion of the program.

Run No.	Date	Charge weight recycle silicon (kg)	Pulled weight (kg)	Melt down time (hrs)	Crucible size (in)	Hot zone size (in)	Power supply used	1/xtal attempts for "O-D"	Smoke-in furnace	Oxide coating on xtal/crown	Crucible wall freeze/ dirty with oxide	Taper of xtal	Water/air leaks	ble Devitrification - excessive	Comments
2	4/2/81	31.8	23	2	15	15	PCC 150 kW	2	Excessive	Yes, heavy	Yes, freeze caused xtal size to exceed auto-control limit	Yes, 5.7" to 6.2" over 8 inch length	Yes, water near argon port	Yes	2nd attempt for O-D resulted in 4" xtal; growth loop reversed, caused structure loss; water leak in throat.
3	4/9/81	30	20.7	3	14	15	Robicon 125 kW	2	Excessive	Yes, heavy	Yes, freeze; also heavy oxide coating	Yes	Suspected	Yes	1st attempt for O-D, 3" xtal; 2nd attempt, lost on crown. Power readout not available due to Robicon supply; water leak suspecred; air leak found with later testing.
4	4/21/81	25	19	3	14	15	Robicon 125 kW	1	Moderate	Yes, but moderate	No, clean and freeze-free	No	No	Yes	No - spill tray; crucible melt vibration caused structure loss at 8 kg (8"); control diameter okay previous to melt vibration. Crucible shaft bearings replaced after run.
5	4/28/81	25	18	3	14	15	Robicon 125 kW	1	Excessive	Yes, heavy	Yes - wall freeze	No	Suspected site observed		No - spill tray - 1st attempt was O-D, until 5" of xtal; Wall freeze occurred.

TEST RUNS 2-5
TABLE 2-1

3.0 PROCESS RESEARCH AND DEVELOPMENT

3.1 Established Technology

In the previous contracts, the ability to grow ingots at a diameter of 150 mm, and to produce 150 kg of ingot from one crucible by means of recharging, was demonstrated. Continuous growth of 150 kg was carried out in a standard CG2000 crystal grower fitted out with a 355 mm (14-inch) diameter crucible and hot zone, which constitutes the size limit for that particular piece of equipment. It was also established on these contracts that the preferred approach toward recharging was the use of a recharge hopper containing silicon in small chunk form (in the range 5-25 mm). In addition, the advantage of increased pull rate, and hence throughput, with the use of an inverted cone type heat shield, had been demonstrated.

The aim, therefore, in the present contract was to consolidate the previous technology and then examine how far it could be extended toward achieving a revised set of goals, with lower anticipated cost per kilogram.

3.2 Process Objectives

3.2.1 Machine Capacity

The basic requirement was for a modified CG2000 crystal grower capable of pulling a minimum of five crystals, each of approximately 30 kg in weight and 150 mm diameter, from a single crucible with periodic melt replenishments. As already discussed in the section on machine construction (Section 2.0), the furnace tank size was selected to accommodate hot zone configurations suitable for 381 mm (15") and 406 mm (16") diameter crucibles. These crucible sizes with cold charge capacities of appproximately 35 and 45 kg, respectively, offer the opportunity of pulling 150 kg of crystal in less than five individual ingots. The hot fill capacity of a 16-inch crucible, for example, is 60 kg which would make 3 x 50 kg ingots a possibility. The impact on throughput,

and hence, the economic analysis of these solidification schemes is discussed in Section 6.0.

3.2.2 Material Specification

Ingots were required to be 15 cm diameter with a resistivity of 1 to 3 ohm cm, p-type, orientation (100), and dislocation density of less than $10^4/cm^2$. Diameter, orientation, and resistivity are straightforward parameters to control (resistivity during this contract being determined by doping with commercially available dope cells at the rate of approximately one cell per kilogram of silicon). In the Czochralski method, however, the standard practice is to aim for "dislocation-free" single crystal, which is material containing less than 500 dislocations per square centimeter. A density of $10^4/cm^2$ would constitute dislocated single crystal and would invariably be the precursor to twinning and ultimately polycrystalline formation. Throughout the contract it has been assumed that both dislocation-free and dislocated single crystal constitute an acceptable solar grade material.

The majority of crystal growth runs were made with (100) orientation seeds, but in a few instances a (111) orientation was tried. It is well known that the growth characteristics of the two orientations are different, and it is an advantage of (111) that retention of crystal singularity is prolonged in comparison with (100).

3.2.3 Throughput

The basic throughput goal was to achieve 2.5 kg per hour of machine operation with a pulled yield in excess of 90%. In support of this goal, a recharge/melt-down rate of 25 kg per hour was called for. The majority of machine cycle time, however, is actually dedicated to crystal body growth, and, therefore, the most immediate impact on throughput is by growth rate. As stated in Section 3.1, the effect of a radiation shield in accelerating growth rate has been demonstrated in a previous contract and remained the favored method for the present work.

The implication of a 2.5 kg/hr throughput in terms of growth rate is presented in Section 6.1 for three different solidification schemes. Bearing in mind the machine capacity, the possibility of producing 150 kg as 3 x 50 kg, 4 x 37.5 kg, or 5 x 30 kg crystals exists. The advantage of pulling fewer, but larger, crystals is that it cuts down the number of recharge/melt-down operations per cycle. If this can be allied to increased growth rate then the benefit to throughput should be significant.

It should perhaps be pointed out at this stage that accelerating melt-down time simply by applying more heater power is likely to increase crucible deterioration with a consequent degradation of single crystal yield. The influence of the crucible is discussed in Section 3.3.6.

3.2.4 Process Automation

Although process automation and sensor development is discussed elsewhere in this report, a note about its relationship to the process goals is appropriate at this point.

Any improvement in sensors and control functions will benefit the implementation of the process. However, significant improvements to yield and to throughput are brought about primarily by experiment, and therefore require that a process be defined before it can be automated. Thus, automation of the process can only have an impact on yield and throughput by virtue of its reproducibility from run to run. The obvious cost area which automation should improve is that of manpower requirement, both skill level and hours.

3.3 Process Investigation

3.3.1 Preliminary Growth Trials

In preparation for the development program, a few preliminary growth runs were carried out in order to commission the grower, correct any mechanical problems, and set some bsic growth parameters. Runs numbered 1 to 5 were necessary to identify and correct a number of faults, and these are discussed in more detail in Section 2.0.

After considerable effort to trace and rectify air and water leaks, two further runs were made utilizing a 381 mm (15") hot zone but with 355 mm (14") crucibles. Run 6 demonstrated the grower's capability for producing dislocation-free material, but oxide smoke evolution still persisted at an unacceptable level until the argon partial pressure was raised to 30 torr. The resulting crystal was significantly cleaner in appearance than any from the previous five runs. Run 6 data are shown in Table 3-1.

It was felt that the larger diameter furnace tank of the Mod 2000 was making argon flow at 20 torr less effective. Future use of a conical radiation shield would certainly improve the situation, but in the interim it was decided to utilize a light-weight cylindrical sleeve positioned on the top heat shield and extending up to the furnace tank cover. The sleeve was 48.3 cm diameter (compared to the furnace tank internal diameter of 68.5 cm) and fabricated out of laminated grafoil.

The grafoil sleeve was employed in run 7 for which a 25 kg charge was melted in a 355 mm crucible. Thermal conditions for growth had obviously been changed by the new arrangement, but an operating pressure of 20 torr was maintained and both crystal and crucible at the end of the run were considerably cleaner than in all previous runs. Zero-dislocation crystal was not achieved during this run, but the benefit of improved argon distribution had been proved and; therefore, the next step was to commence process development with 15" crucibles.

3.3.2 Crystal Growth in 381 mm (15") Diameter Crucibles

Use of 381 mm x 305 mm crucibles enabled a standard charge weight of 35 kg to be melted suitable for pulling 30 kg crystals. The short term objective was to build up to a 150 kg run (5 x 30 kg crystals from one crucible).

Two preparatory runs were scheduled, the first of which (Run 8) was designed to determine the conditions for dislocation-free growth using a 381 mm crucible in combination with the grafoil purge sleeve. In addition, the operation of the isolation valve and recharge hopper

ITEM	UNITS	PROCESS DATA										
Run #	-	6	7	8		9	9	10	10	10	10	10
Date	-	5/5/81	5/12/81	6/10/81		6/16/81	6/17/81	6/22/81	6/22/81	6/23/81	6/24/81	6/25/81
Crystal #	-	1	1	1		1	2	1	2	3	4	5
Charge - Cold Fill	kg	25	25	25		28.5	-	35	-	-	-	-
Charge - Hot Fill	kg	-	-	10.25		6.5	25	-	30.1	30.1	28.9	28.7
Crucible Diameter	cm	35.5	35.5	58.1		38.1	38.1	38.1	38.1	38.1	38.1	38.1
Silicon - New/Recycle	-	Recycle	Recycle	Recycle		Recycle	New	New	New	New	New	New
Seed	-	1-0-0	1-0-0	1-0-0		1-0-0	1-0-0	1-0-0	1-0-0	1-0-0	1-1-1	1-1-1
Meltdown Power	kW	110	110	106		83	106	88	110	110	110	100
Total Meltdown Time	hr	2	2	2.25		4.5	2.5	3.0	2.4	2.1	2.16	2.16
Start Neck Power	kW	78	77	74		70	71	72	72	72	73	70
15" Body Power	kW	81	82	88		74	75	74	75	75	74	73
Crystal Diameter	cm	13.7	14.0	14.0		14.86	15.0	14.9	15.1	15.5	15.7	15.7
Pulled Weight	kg	20.0	17.5	32.5		25.3	24.7	30.4	30.6	29.1	28.4	27.0
Residual Melt	kg	5.0	7.5	2.75		9.7	10.0	4.6	4.1	5.1	5.6	7.3
Zero-D - Length	cm	53.3	0	39.4		62.5	5.1	64.8	47.0	0	0	0
Zero-D - Weight	kg	20	0	14.0		25.3	2.0	26.2	19.6	0	0	0
Body Growth Time	hr	11	9.2	15		9.5	8.0	11.37	12	12.25	11.25	11
Cycle Time (Power On-Power Off)	hr	15	15	25.25		→	31.5	→	→	→	→	100
Pulled Yield	%	80	70	92.2		→	83.3	→	→	→	→	95.2
Average Pull Speed	cm/hr	5.3	5.1	5.8		6.4	7.6	6.3	6.25	5.7	5.7	5.4
Zero-D Yield	%	80	0	43.1		→	54.6	→	→	→	→	31.5
Machine Throughput	kg/hr	1.33	1.17	1.29		→	1.59	→	→	→	→	1.46

GROWTH RUN DATA, RUNS 6-10

TABLE 3-1

was checked out by hot filling 10 kg of polysilicon into an initial melt of 25 kg. The hot-fill operation worked well, although there was a suspicion of some air leakage through the isolation valve during the pull chamber purging cycle. The growth run established a suitable melt level at which a dislocation-free crystal could be grown, although structure was only maintained for 14 kg.

Run 9 was the first run made using an Ircon sensor for automatic diameter control, so that one purpose of the run was to fine tune the ADC (Automatic Diameter Control) loop for optimum performance. It was also decided to make this a 2-crystal run in order to practice a complete recharge procedure. Two crystals were indeed grown, the first being all dislocation-free but the second becoming dislocated after 2 inches of body growth (growth run data are presented in Table 3-1). The reason for the loss of structure was undoubtedly due to chafing of the isolation valve O-ring during the recharging operation causing subsequent contamination of the furnace atmosphere. It was felt that the O-ring had not been properly seated and hence not adequately cooled, exposing it to high heat load during crystal removal. The O-ring was replaced and firmly seated prior to the next run.

3.3.2.1 150 kg Growth Run

The object of run 10 was to pull five consecutive 30 kg crystals from the same crucible utilizing the recharge procedure. The grafoil sleeve was retained, and the Ircon diameter sensor which had worked well in the previous run was employed again.

Five crystals were pulled totalling 145.5 kg in a time of 100 hours. The first two crystals were 90% and 65% dislocation-free respectively, but subsequent crystals did not retain structure in spite of repeated attempts to achieve it. The machine throughput was 1.46 kg/hr, but this would have improved to 1.56 kg/hr if repeated attempts at achieving structure had not been undertaken. Two main problems were encountered during this run.

(i) Air leakage through the isolation valve during the pull chamber purging cycle in the recharge operation. Any air leakage would, of course, contribute to structure loss problems. It was subsequently found that the isolation valve problem affecting runs 8, 9, and 10 was due to a slight misalignment of valve plate to valve seat during assembly. This fault was rectified by dismantling and realigning the whole assembly.

(ii) At a mean pull speed of 7 cm/hr, all crystals grew in a slightly twisted or spiral fashion (see figure 3-1). The short term solution to this problem was to reduce pull rate by approximately 1 cm/hr. This enabled the crystals to straighten out, but obviously reduced the overall throughput. The exact mechanism for spiral growth of crystals is not well understood but the effect is usually ascribed to thermal asymmetry. Several attempts were made in later runs to gain a better understanding of this phenomenon.

In a follow-up to Run 10, an attempt was made to shed some light on the reason for structure loss during multiple crystal growth runs. After Run 10, the furnace was opened and very carefully unloaded. Care was taken not to disturb the oxide deposit on the furnace parts. A new crucible was placed in the hot zone and loaded with 35 kg of silicon. The object of the exercise was to determine the grower's capability for producing dislocation-free crystal with a new crucible and silicon but no other preparation. In other words, it was a test of which is the more important factor causing structure loss--oxide build up in the furnace or crucible degradation. Unfortunately, a crucible support failure occurred during meltdown, and the run had to be aborted.

The problem of spiral crystals was first addressed by checking the mechanical alignment of seed cable to crucible shaft. A degree of misalignment was found, and when this had been rectified, a run was initiated (Run 12) to determine whether a crystal spiral condition still obtained. Although a full term crystal was not produced from this run, sufficient material was grown to demonstate that the spiral habit had persisted. The condition was evident after 20 cm of body

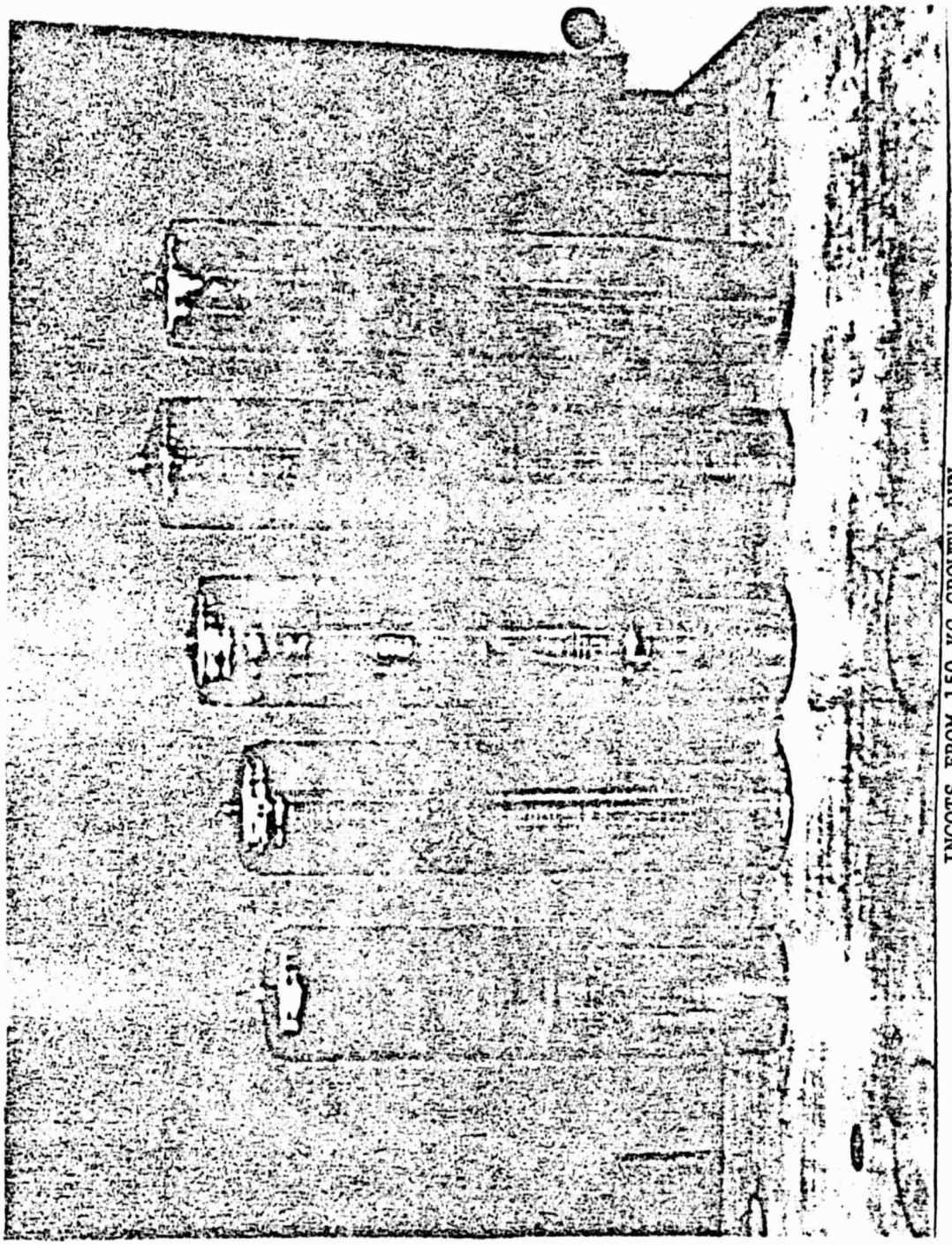

INGOTS FROM 150 KG GROWTH RUN

FIGURE 3-1

growth at an average pull rate of 7 cm/hr. Alignment was checked after the run and found to be unchanged. The indications at this stage were that the spiral problem was related to the combination of growth parameters and hot zone configuration being used.

3.3.3 Program Revision

Following a design and performance review and the issue of a subsequent Technical Direction Memorandum a change in emphasis for the remainder of the program duration was decided. The requirement for a number of 150 kg runs was relinquished in favor of the following areas of investigation.

(i) Methods for increasing throughput, particularly using a type of radiation shield.

(ii) Continued development and implementation of microprocessor control for the MOD 2000.

(iii) Consideration of the problem of crucible-melt interaction by continuing analysis of the furnace atmosphere, and by investigating the possibility of using synthetic quartz crucibles.

Although a design and material for a radiation shield had been chosen (see section 3.3.4) it was decided to dedicate a few runs beforehand to a continued investigation of crystal spiraling. At the same time, the microprocessor was interfaced with the MOD CG2000 grower to assess its performance and to familiarize the growing team with its operation. Runs 15 to 19 were made in 381 mm (15") crucibles with charge sizes of 25 kg; pertinent run data are presented in Table 3-2.

During the course of these runs, the hot zone/process changes made did improve the spiral situation somewhat, although the reason is not clear. Heater concentricity was improved, top heat shielding was lowered by approximately 12 mm, and growth melt levels were raised by 12 mm. The net effect was not an elimination of the problem, but an improvement to the point where average pull rates approaching 7.5 cm/hr could be achieved with minimal spiral.

ITEM	UNITS	PROCESS DATA								
Run #	-	15	16	17	18	19	20		21	
Date	-	12/1/81	12/8/81	12/10/81	12/15/81	12/21/81	1/11/82		1/15/82	
Crystal #	-	1	1	1	1	1	1		1	
Charge - Cold Fill	kg	25	25.5	25	25	20.1	41		40	
Charge - Hot Fill	kg	-	-	-	-	5	-		-	
Crucible Diameter	cm	38.1	38.1	38.1	38.1	38.1	38.1		38.1	
Silicon - New/Recycle	-	Recycle	Recycle	Recycle	Recycle	Recycle	Recycle		New	
Seed	-	1-0-0	1-0-0	1-0-0	1-0-0	1-0-0	1-0-0		1-0-0	
Meltdown Power	kW	110	100	108	109	110	110		110	
Total Meltdown Time	hr	2.08	2.5	2.58	2.08	3.67	2.2		2.1	
Start Neck Power	kW	68	67	66	68	68	61		63	
15" Body Power	kW	70	67	-	70	72	62		68	
Crystal Diameter	cm	14.8	16.6	15.2	15.5	15.4	15-20		15.7	
Pulled Weight	kg	16.3	19.15	10.8	17.75	19.92	29.8		31.5	
Residual Melt	kg	8.7	6.35	14.2	7.25	5.18	11.2		8.5	
Zero-D - Length	cm	26.7	5.1	25.4	14.0	24.1	5.1		-	
Zero-D - Weight	kg	10.75	2.5	10.8	6.14	10.4	2.2		-	
Body Growth Time	hr	5.33	5.42	3.5	4.5	5.2	15.2		10.0	
Cycle Time (Power On-Power Off)	hr	14.58	12.42	9.75	11.37	14.85	30.0		21.25	
Pulled Yield	%	65.2	75.1	42.2	71.0	79.4	72.7		78.8	
Average Pull Speed	cm/hr	7.6	7.4	7.8	7.9	7.0	3.2		6.6	
Zero-D Yield	%	65.9	9.8	100	41.2	52.2	7.4		-	
Machine Throughput	kg/hr	1.14	1.54	1.08	1.56	1.34	1.0		1.48	

GROWTH RUN DATA, RUNS 15-21
TABLE 3-2

The conversion of the vital grower functions to microprocessor control was accomplished with no great difficulty. However, some shortcomings were experienced when trying to develop and implement crystal growth programs, e.g.:

(i) No provision in the meltdown program for raising power to melt off chunks of silicon stuck to the crucible wall. This operation had to be carried out manually and could affect the subsequent stabilization sequence if the melt became super heated.

(ii) Because of the open loop nature of neck growth, a long melt stabilization phase was required. This is not satisfactory from a throughput standpoint.

(iii) Neck and crown recipes were sensitive to hot zone or process changes (i.e. melt level) and obviously difficult to predict in advance. This is the sort of situation alluded to in Section 3.2.4.

Despite these shortcomings, all aspects of crystal growth, except for the taper which was troubled by wall-freeze problems, were carried out with microprocessor control from 25 kg charge sizes.

In order to determine the performance of the microprocessor control system with larger melts, it was planned to carry out two further runs in 381 mm crucibles with 40 kg charge sizes. Before carrying out runs 20 and 21 a new heater and pedestal were installed and baked out. In addition, a modification to the crucible lift mechanism was made in order to allow more down travel and thereby facilitate melting of the larger charges.

Meltdown time for Run 20 was just 2.2 hrs using the same meltdown recipe as for the previous 25 kg runs. However, the power level of 70 kW for Stabilization 1 was too high and had to be manually reduced for seeding. In fact, power levels for seeding, neck, and crown growth had to be about 5 kW lower for the 40 kg charge than for 25 kg. After four attempts, a zero-dislocation crown was grown and a good transition made from shoulder to body growth, but a high initial pull rate indicated that the power was now somewhat low as a wall-freeze problem occurred after about 5 cm of body growth.

In fact, it proved impossible to retain a reasonable pull rate without a recurring wall-freeze problem under automatic control. The crystal was therefore grown under manual control, at low pull speed, and with decreased crucible rotation.

After completion of Run 20, the crucible shaft was inspected and evidence of overheating and reaction between the metal shaft and graphite pedestal was observed. The shaft was replaced with a standared CG2000 RC shaft, and the assembly on top of the pedestal altered to include three additional insulator pieces. For growth Run 21, a higher growth melt level was chosen to steepen the radial thermal gradient and diminish the possibility of a wall-freeze problem. The resulting power levels were about 2 kW higher than at similar stages in the previous run, and even though some wall-freeze did occur, it was not such a serious problem. The crystal was not single, but was at least grown in a more controllable fashion, and no crucible shaft overheating occurred (see data in Table 3-2).

Because of the unfavorable thermal conditions evident during these two runs, it was difficult to assess the performance of the microprocessor control. However, to keep the program on course, it was decided to pursue the behavior of large melts in 406 mm (16") diameter crucibles and to incorporate the radiation shield, which had by this time been designed and built.

3.3.4 Crystal Growth in 16" Crucibles with Radiation Shield

3.3.4.1 Radiation Shield

As in a previous contract, the method chosen for increasing crystal growth rate, and possibly recharge rate, was the use of a radiation shield. The device was to be a conical shape and was designed to fit up to the furnace tank lid and extend down toward the crucible as shown in Figure 3-2. Support for the cone was provided by a graphite ring standing on support legs which in turn were carried by the top heat shield ring.

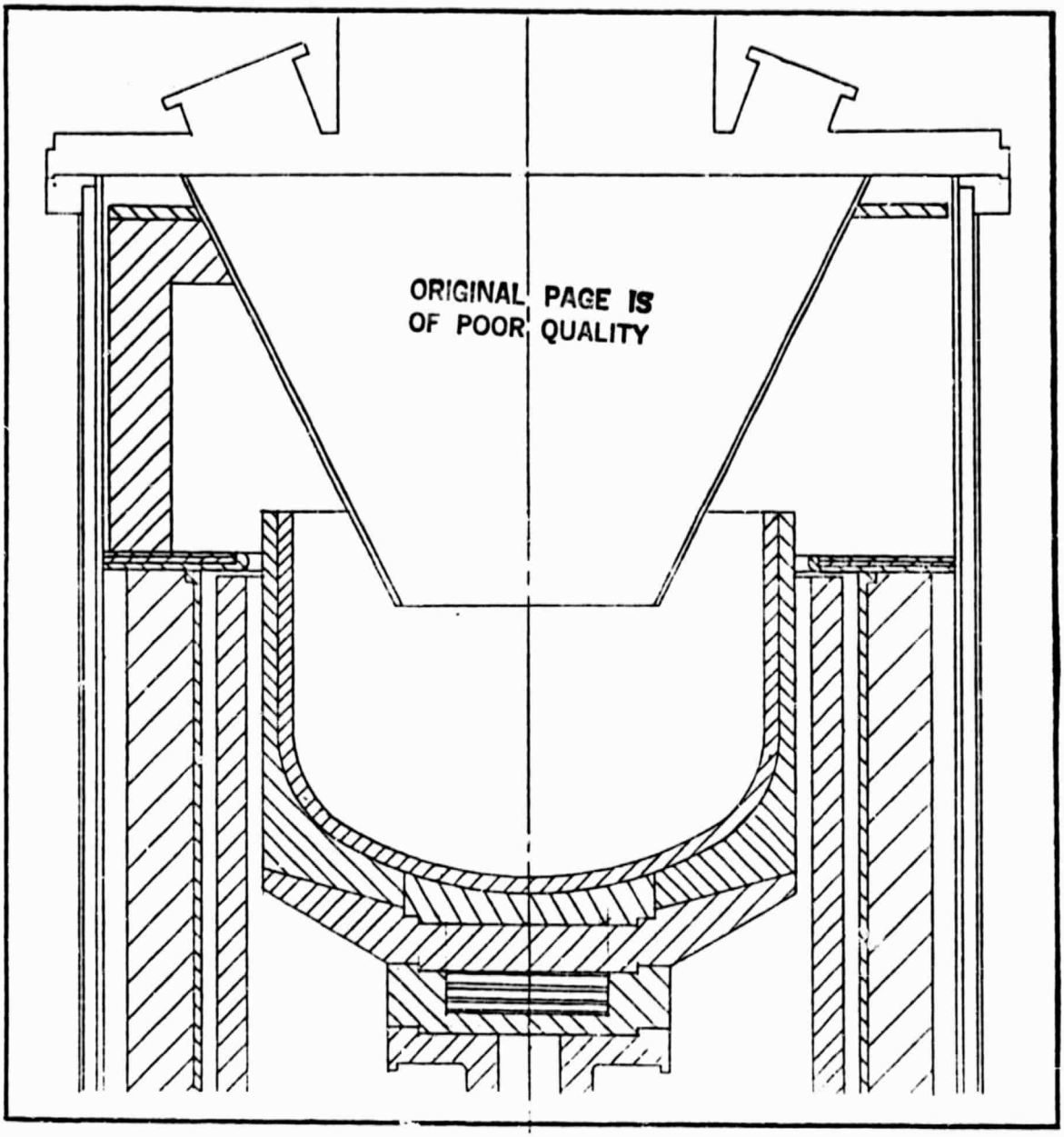

16-INCH HOT ZONE WITH RADIATION SHIELD

FIGURE 3-2

The materials considered for cone fabrication were molybdenum, graphite, and graphite coated with pyrolytic graphite. However, since the cone might operate in conjunction with the recharge hopper, it was decided to proceed with a molybdenum cone made out of 1.5 mm thick sheet. It was felt that possible bumping of silicon chunks on the cone during a recharge operation might cause graphite particles to fall into the melt if the cone were made out of graphite.

3.3.4.2 Growth Runs in 16" Crucibles

In preparation for Run 22, 40 kg of polysilicon was loaded into a 406 mm crucible. Because of the presence of the molybdenum cone, it was apparent that the crucible starting position for meltdown would have to be lowered to avoid contact between the bottom of the cone and the silicon charge. Melting proceeded quite normally, but because the cone obscured any view of the upper part of the crucible wall, it was impossible to see directly whether any chunks were sticking to the wall. In fact, by reflection in the melt surface, it did appear that one lump was adhering to the crucible rim and protruding inwards. Consequently, a decision was made to limit the extent of crucible upward travel during crystal growth in order to prevent the silicon chunk from interfering with the cone.

A zero-dislocation crystal was grown at the first attempt and although neck and crown growth was not fully automatic (because no computer program could yet be defined for the new set-up), the shoulder was turned and the crystal put into ADC with no problem. Because of the exploratory nature of this run, the pull rate was kept down by setting the growth loop (growth rate controller) at 7 cm/hr. When the crystal lost structure, its growth was continued and the resulting ingot was clear and oxide-free as a result of the purging action of the cone. The ingot exhibited a gradual taper from halfway down its length, where the crucible lift had to be turned off because of the decision to limit upward travel. Run 22 was accomplished with no wall-freeze problems and produced a crystal with minimal evidence of spiral character. For further run data, refer to Table 3-3.

ITEM	UNITS	PROCESS DATA										
Run #	-	22	23		24	24		25				
Date	-	1/27/82	2/3/82		2/9/82	2/10/82		2/25/82				
Crystal #	-	1	1		1	2		1				
Charge - Cold Fill	kg	40	40		40	-		35				
Charge - Hot Fill	kg	-	-		-	29.0		-				
Crucible Diameter	cm	40.6	40.6		40.6	40.6		40.6				
Silicon - New/Recycle	-	Recycle	New		New	New		New				
Seed	-	1-0-0	1-0-0		1-0-0	1-0-0		1-0-0				
Meltdown Power	kW	110	110		110	110		110				
Total Meltdown Time	hr	2.85	2.9		2.5	2.16		2.3				
Start Neck Power	kW	68	69		67	66		72				
15" Body Power	kW	68	72		65	65		-				
Crystal Diameter	cm	15.2	15.2		15.2	15.9		12.7				
Pulled Weight	kg	29.2	37.5		29.0	21.5		23.5				
Residual Melt	kg	10.8	2.5		11.0	18.5		11.5				
Zero-D - Length	cm	12.7	20.3		26.7	-		-				
Zero-D - Weight	kg	5.4	8.75		11.4	-		-				
Body Growth Time	hr	12.5	13.6		7.92	8.58		12.2				
Cycle Time (Power On-Power Off)	hr	19.6	21.8		→	36.0		33.45				
Pulled Yield	%	73.0	93.75		→	73.2		67.1				
Average Pull Speed	cm/hr	6.6	7.1		7.85	5.3		6.6				
Zero-D Yield	%	18.5	23.3		→	16.5		-				
Machine Throughput	kg/hr	1.49	1.72		→	1.40		0.70				

GROWTH RUN DATA, RUNS 22-25
TABLE 3-3

Run 23 was, therefore, planned under similar conditions with the object of increasing pull rate. Preparation for the run only involved raising the molybdenum cone slightly to insure contact with the furnace cover plate and installing new seed rotation lip seals.

A 40 kg charge was melted and zero-D crystal obtained at the first attempt. Structure loss occurred after 20 cm of body growth, but the crystal was pulled for a total weight of 37.5 kg, representing a pulled yield of 93.8%. The most significant aspect of this run was the pull rate achieved during the major portion of crystal growth. The growth rate control was set at 9 cm/hr pull rate for the first 35 cm of body growth, after which the computer would reduce the set-point to 7.6 cm/hr. In fact, for a period of three hours after the crystal was put into ADC, the pull rate was averaging 10 cm/hr. The average pull rate over the first 60 cm of crystal growth was 9 cm/hr, and the growth diameter was 152.4 mm. At 60 cm of body growth the crucible lift was turned off to avoid contact between the crucible supports and the radiation shield. With crystal growth still in ADC, this resulted in a gradual taper to the crystal. Eventually, the crystal was controlled manually and a decision was made to try and leave as little silicon residue in the crucible as possible. Although pull rates were much slower over this latter portion of manual growth, the average rate for the whole 37.5 kg of crystal was 7.1 cm/hr (See Table 3-3 for further run data).

Some spiralling of the crystal was evident, as shown in Figure 3-3, but this did not seem exaggerated for the high pull rate being used over the first half of crystal growth.

Run 24 was set up to determine whether a recharging operation could be successfully carried out with the conical radiation shield in position. A charge of 40 kg was melted and a first crystal grown of which 11.4 kg was zero-dislocation. This crystal was pulled for a final weight of 29 kg and then withdrawn. A recharge operation was carried out and two hopper loads of silicon, totalling 29 kg, were filled into the crucible. The recharge procedure worked as normal except that the recharged material was funnelled into the crucible by the molybdenum cone. This had a beneficial effect, since it tended

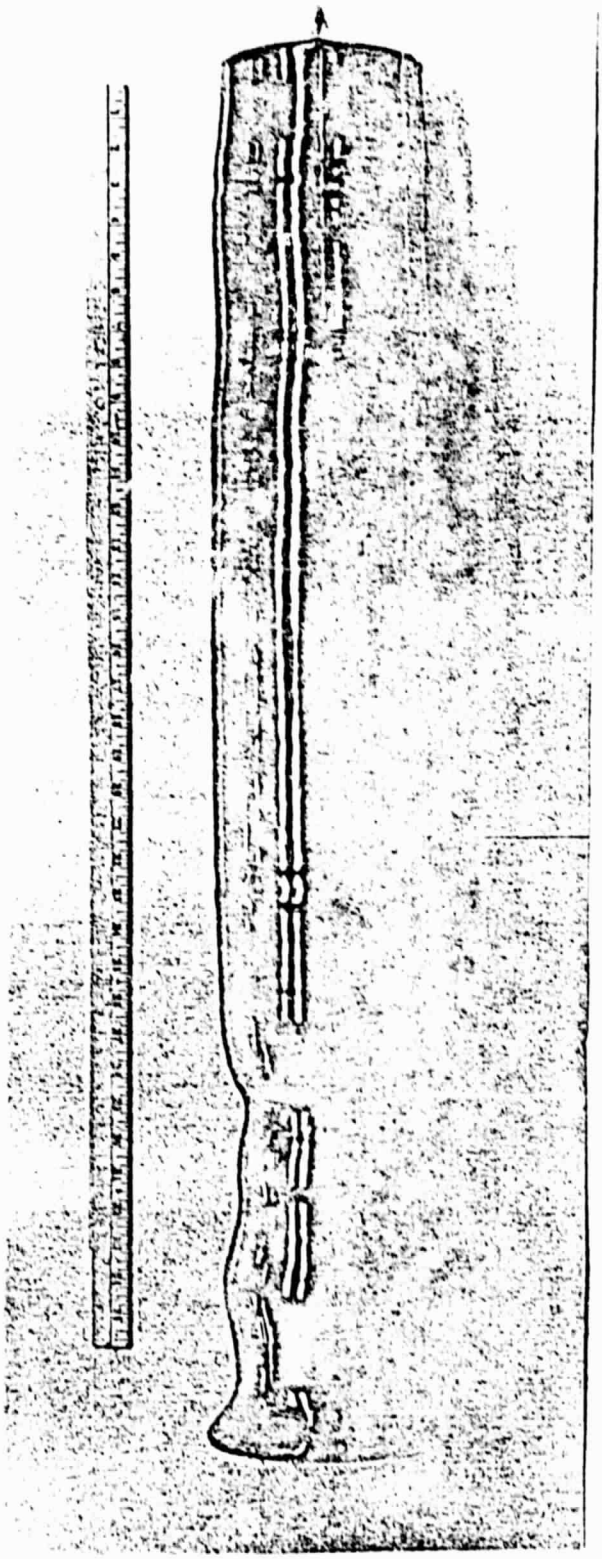

37.5 KG CRYSTAL FROM RUN 23

FIGURE 3-3

to keep material up in the center of the crucible, whereas previously, the recharged silicon heaped up against the crucible wall, increasing the chances of chunks sticking to the wall.

After meltdown of the recharge material and dipping of the seed, it was obvious from the excessive oxide build-up that a large leak of some sort had occurred. With some difficulty, an ingot was grown, but it was polycrystalline from the start and covered with a flaky deposit. At first, a minute water leak was suspected, but a post-run investigation revealed that the seed rotation lip seal assembly had been inadequately installed, and this began leaking severely after the recharge operation. Although no really meaningful data could be derived from the second crystal, an analysis of the data relating to the first crystal (See Table 3-3) shows that an average pull rate of 7.9 cm/hr was achieved.

Run 25 was set up primarily to test a laser melt level sensing system. A secondary objective was to determine what influence crystal diameter might have on spiral growth; therefore, a growth diameter of 125 mm was chosen. Because of the incident and reflected paths of the laser beam, the molybdenum cone could not be used for this run and instead the grafoil sleeve was employed (See Section 3.3.1).

A 35 kg charge was melted and several attempts made to hold zero-D structure with this changed configuration. However, since the object of the run was to track melt level variation and investigate crystal shape, it was decided not to persevere with the effort to obtain zero-D. As a result of growing 23.5 kg of crystal it appeared that the extent of spiralling was very similar to that exhibited by the 150 mm diameter crystals. However, the melt level system tracked quite successfully and could possibly form the basis of a very useful control device.

3.3.5 Thermal Instability in the Melt

Much discussion and background literature searching had gone on during the program in order to gain an understanding of the nature and causes of spiral growth tendency in Czochralski crystals.

The phenomenon has been ascribed to thermal asymmetry [4] in the furnace such that the thermal center of the hot zone does not coincide with the geometric center, where the seed is located. A spiral induced by thermal asymmetry might be expected to decay as the crystal lengthens because of the influence that a body of solidified silicon in contact with the melt has on heat flow. As the size of the crystal becomes significant it forms a heat sink at the geometric center and consequently pins the thermal center at the geometric center. From this point on, radial differences in heat loss encountered by the rotating crystal become less significant and the crystal straightens out. This seems to be the pattern exhibited by crystals grown during the program; a typical example being shown in Figure 3-4.

It is assumed that the thermal center of the melt should coincide with the geometrical center (rotational center) as long as the heater and insulation are placed concentrically about the crucible and crucible support, and that correct alignment is maintained between crucible shaft and seed cable movement. Having taken care to mainatin concentricity and alignments, it must be assumed that the continued problem of spiral growth was fundamental to the combination of hot zone configuration and growth parameters being used. Some support for this view is provided by the work of Kobayashi [5] who considers melt hydrodynamics and the interaction between free convection, due to melt density variation, and forced convections, due to crystal and crucible rotations. Depending primarily on which convection mode is dominant, it is possible for a thermal asymmetry to exist around the crystal, in which case the effect of the growth instability would be a spiral distortion . To pursue this line of thinking would require some crystal growth runs in which rotations could be varied to alter forced convection, and the hot zone could be modified to affect thermal gradients and hence free convection. Rotational variations could be made at any time during a run, but to make a hot zone change required that it be decided beforehand whether the change should increase or decrease heat losses from the zone. From an analysis of the results and observations of the runs so far, particularly wall-freeze problems and low power levels, it seemed that the way to go would be to increase heat loss from the hot zone.

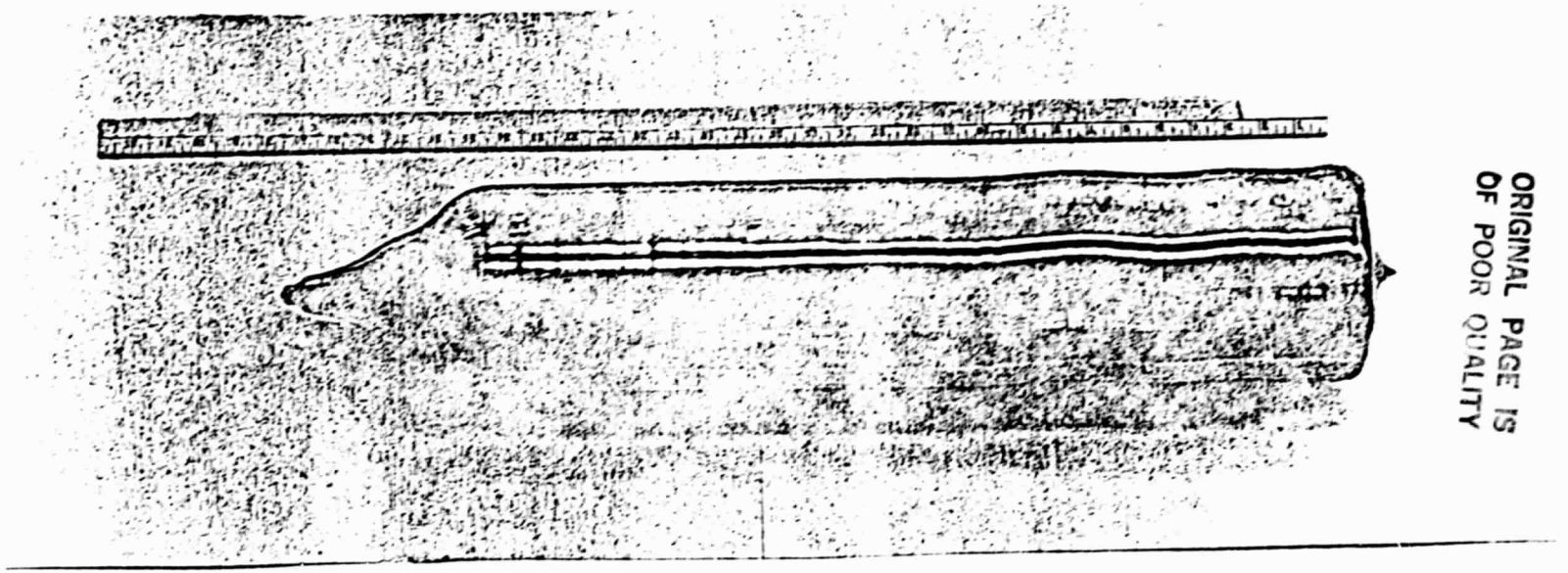

TYPICAL SPIRAL GROWTH

FIGURE 3-4

In setting up for Run 26, it was decided to remove the pedestal insulator from beneath the crucible support and to remove some insulation from the bottom heat shield. This was effective in increasing heat losses away from the bottom of the crucibles, as evidenced by increased power levels (See Table 3-4). However, it proved very difficult to maintain structure and many attempts during which crystals 1 and 2 were grown were made to achieve it. During the course of these attempts, crucible rotation changes were made to see if any change in melt stability could be observed. Starting from a nominal rotation of 6 rpm, the crucible was slowed down to 3.5 rpm, but at this, the rotation neck and crown growth became more unstable. Eventually the crucible rotation was brought back up to 10 rpm resulting in a more controllable neck and crown growth. Finally, crystal number 3 was grown for a pulled weight of 37.5 kg but, as can be seen from Figure 3-5, there was still evidence of a spiral appearance. The taper on this crystal, from about 55 cm of body growth onwards, was once again a consequence of turning off the crucible lift to prevent the crucible from colliding with the conical shield.

After the failure of Run 26 to produce any significant amount of zero-D material, it was felt that the heat loss may have been too drastic and so for the next run, the pedestal insulator was put back in. Run 27 was also set up to try out a new design of 381 mm (15") heater which had just been made available. This heater was approximately 7.5 cm shorter than the design used earlier in the program, and being only a 2-active terminal heater the number of pickets was less. In order to draw a comparison with the earlier 381 mm zone, the run was made with the grafoil sleeve in place of the molybdenum cone.

A 35 kg charge was melted and a 30.05 kg crystal grown with a mean diameter of 131 mm. Out of the pulled weight of 30 kg some 20.8 kg of material was zero-dislocation. This was achieved after several attempts to find the right melt level, seed dip temperature, and crucible rotation conducive to quality growth. As in the previous run, the variation of crucible rotation was found to lead to more stable growth at a higher rotation (12 rpm) than at a lower rotation (3 rpm). However, some spiral character is still obvious in this crystal (See figure 3-6).

ITEM	UNITS	PROCESS DATA					
Run #	-	26	26	26		27	
Date	-	3/2/82	3/3/82	3/4/82		3/18/82	
Crystal #	-	1	2	3		1	
Charge - Cold Fill	kg	40	-	-		35	
Charge - Hot Fill	kg	-	-	15		-	
Crucible Diameter	cm	40.6	40.6	40.6		38.1	
Silicon - New/Recycle	-	New	New	New		New	
Seed	-	1-0-0	1-0-0	1-1-1		1-0-0	
Meltdown Power	kW	110	-	115		110	
Total Meltdown Time	hr	2.42	-	1.0		2.27	
Start Neck Power	kW	77	79	77		63	
15" Body Power	kW	-	-	80		62.5	
Crystal Diameter	cm	15.5	15.5	15.2		13.1	
Pulled Weight	kg	5.86	9.0	37.5		30.05	
Residual Melt	kg	34.14	25.14	2.64		4.95	
Zero-D - Length	cm	3.8	3.8	-		68.6	
Zero-D - Weight	kg	1.65	1.65	-		20.8	
Body Growth Time	hr	2.0	3.5	14.1		14.23	
Cycle Time (Power On-Power Off)	hr	→	→	73.6		28.52	
Pulled Yield	%	14.7	26.4	93.4		85.9	
Average Pull Speed	cm/hr	6.4	5.84	6.25		7.0	
Zero-D Yield	%	28.2	18.3	-		69.2	
Machine Throughput	kg/hr	→	→	0.71		1.05	

GROWTH RUN DATA, RUNS 26 & 27
TABLE 3-4

ORIGINAL PAGE IS
OF POOR QUALITY

INGOT FROM RUN 26
UNSTABLE SPIRAL GROWTH AT TOP

FIGURE 3-5

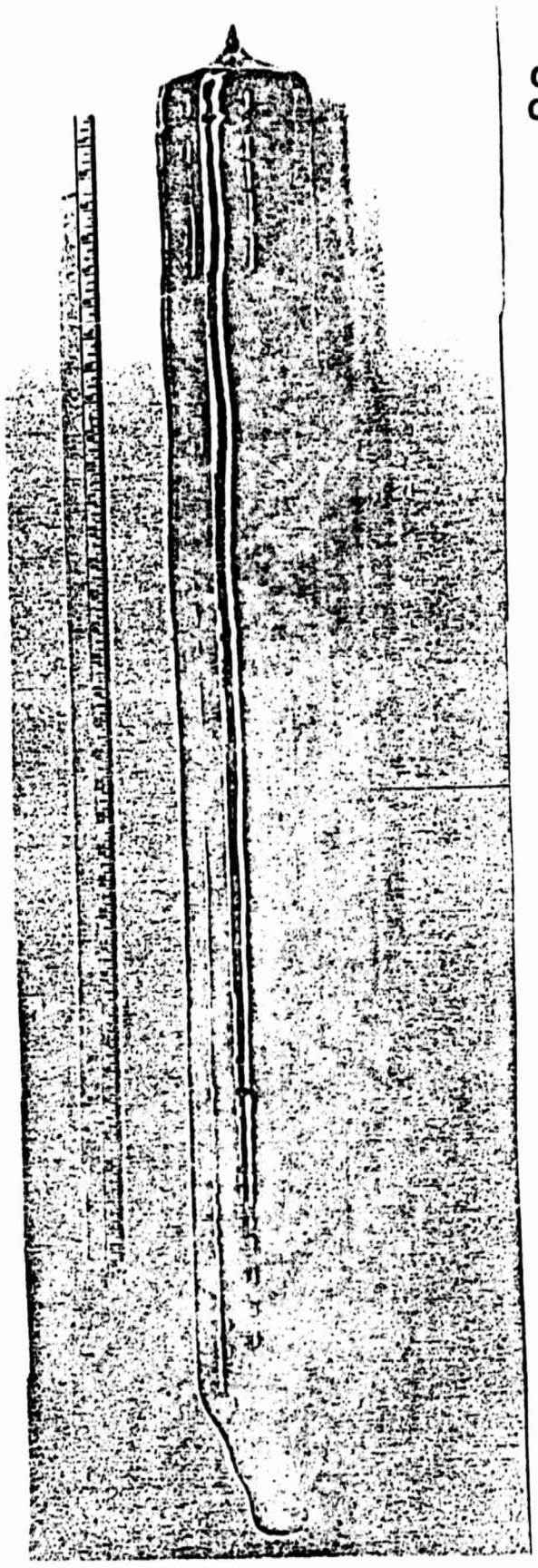

30 KG CRYSTAL FROM RUN 27

FIGURE 3-6

It is, perhaps, worth noting that there does not seem to be a direct correlation between ability to maintain dislocation-free structure and degree of spiral obtained. Therefore, if good structure were achievable every time, but at the expense of a small degree of spiral, this might be acceptable. The difficulty, however, is when increased pull speeds are required to improve throughput, because this has the tendency of exaggerating spiral.

3.3.6 Crucible/Melt Interaction

A prime suspect for the cause of persistent structure loss during multi-crystal runs is crucible deterioration. Although the exact mechanism is unknown, some sort of a picture has emerged from technical discussion with those involved with crucible manufacture. There is evidence that the typical "rosette" pattern on the inner crucible wall, where it has been in contact with molten silicon, is composed of an island of cristobalite surrounded by a ring of $SiO_{(2-x)}$. These rosettes grow and coalesce as time and the extent of crucible dissolution proceed. The problem in a multi-crystal run occurs when the molten silicon has dissolved away the inner glassy surface of the crucible (after, say, 40 hours) and starts to expose bubbles. The bursting of bubbles at the melt/crucible interface might then release cristobalite particles into the melt, leading directly to crystal structure loss.

To test this theory, it would be necessary to obtain some crucibles with zero, or at least greatly reduced, bubble content. Several possibilities exist and these are listed and commented on below, along with price information where available.

1. Synthetic quartz - this is a very high purity bubble-free material available commercially. The limiting factors with this material would be cost and size of crucible that would be manufactured. Some estimates as to cost for, say, a 305 mm diameter crucible, ranged from $2,700-$6,000.
2. Clear fused quartz - this material is available in tube form and can be fabricated into crucibles. Some examples

of sizes and prices are:

305 mm x 228 mm @ $435

355 mm x 267 mm @ $745

381 mm x 305 mm @ $1,015

The drawback with these crucibles is the thin wall (2.0 $\pm$ 0.5 mm), which is an inevitable consequence of the tube starting stock and the forming process.

3. Slip-cast, fused quartz - after slip-casting and drying these crucibles are given a heat treatment, to remove organics and moisture, before undergoing a fusion cycle. This technique produces a transparent, low bubble content crucible. Crucible cost is comparable to standard arc-fused crucibles, but the available size range does not go beyond 330 mm diameter crucibles.
4. Synthetic quartz lining - an alternative to the prohibitive cost of a synthetic quartz crucible might be a standard arc-fused crucible with a synthetic quartz lining. Manufacturers have been reluctant to respond to this scheme and so at this time, it is not certain that this is technically feasible.
5. 'Reglazed' crucibles - in this case, an extra fusing step is utilized to produce a thicker glassy layer on the inner surface of the crucible. Two sizes of reglazed crucibles have been quoted, i.e.

   305 mm x 228 mm @ $210 ($125)

   355 mm x 267 mm @ $330 ($210)

   --Figures in parenthesis are comparative costs for the standard arc-fused product.

Based on the above information, it would seem that any investigation of the effect on yield due to crucible type, particularly during multiple crystal growth runs, should be carried out using 305 mm (12") hot zones in order to encompass the greatest number of crucible variants. However, the time involved in setting up an alternative hot zone size and procuring crucibles, put such an investigation beyond the scope of the present program.

3.4 Technology Readiness Demonstration

At the end of the program using the Mod. 2000, three supplementary runs were made to assess the performance of the newly designed 15-inch "short" heater. These runs are described in Table 3-5. Although some improvement in melt stability was observed, the problems of zero-D yield and spiral growth tendency persisted. However, the change in hot zone geometry allied to rotational changes, to affect forced convection in the melt, was felt to be the direction to follow.

This approach was carried over to the process work in the production CG6000 grower. Process development on this machine was inevitably slowed down by equipment debugging problems, but in 15 runs, the zero-D yield was improved and the spiral problem was eliminated. These runs are detailed in Table 3-6. In all runs, the crucible size was 15-inch diameter, seed orientation was (1-1-1), and growth diameter was 130 mm. Recharging was performed on runs 5, 11, 13, and 14.

The CG6000 differs from its prototype, the Mod 2000, in that the main furnace tank has an internal diameter increase of three inches, and the pull chamber and throat diameters are smaller. In addition, a new generation seed cable mechanism was installed on this grower. It was confirmed early on in the CG6000 program that when using the larger diameter furnace tanks, some form of gas-directing device was necessary. It was also learned that a cylindrical sleeve resting on top of the hot zone could perform such a function as long as its mass was not too great.

In addressing the spiral problem, no outstanding breakthrough was accomplished; rather, a refinement of the hot zone configuration allied with growth parameter variations led to a diminution and subsequent elimination of the feature. Thus, no single cause was identified for a spiral growth tendency although several factors which can assist in reducing the problem were employed, for example, reducing pull speed, lower seed rotation, melt-level choice, and correct seed cable alignment.

RUN NO.	CRYSTAL NO.	SILICON CHARGE (kg)		PULLED WEIGHT (kg)	ZERO-D WEIGHT (kg)	AVG. PULL SPEED (cm/hr)	COMMENTS
		COLD FILL	HOT FILL				
28	1	35	-	5	4.5	6.6	Second run with new, "short" 15" heater. Crooked seed -- pulled out small crystal and reseeded.
	2	-	5	25.4	14.5	6.5	57% zero-D yield. Slight spiral appearance to crystal.
29	1	35	-	31.6	12	6.2	Same growth parameters as previous run but crucible slumped badly to one side.
30	1	35	-	25	0	7.1	Continuing work with Agile control and melt level detection system. Both crystals from this run have spiral.
	2	-	25	27.6	1.5	6.7	Appearance over the first 20 cm of body and then straighten out.

SUMMARY OF RUNS 28 - 30

TABLE 3-5

RUN NO.	CRYSTAL NO.	SILICON CHARGE (kg) COLD FILL	SILICON CHARGE (kg) HOT FILL	PULLED WEIGHT (kg)	ZERO-D WEIGHT (kg)	AVG. PULL SPEED (cm/hr)	COMMENTS
TR1	1	35	-	26.6	4.0	6.8	First run in production CG6000 - 15" hot zone Crystal dirty and spiralled.
TR2	1	35	-	31.4	25.3	5.6	Install thick graphite purge sleeve, remove pedestal insulator. 80% zero-D yield and cleaner crystal, but severe spiral with short period.
TR3	1	35	-	25	0	6.6	Bottom radiation shield lowered by 5". Insulator replaced. Isolation valve seat O-ring unseated during run and melted. Contamination caused polycrystal.
TR4	1	35	-	31.3	5	6.9	Addressed spiral problem by adjusting seed and crucible rotation rates. Reduction of S.R. from 15 rpm to 8 rpm has noticeable effect.
TR5	1	35	-	18.3	3.3	8.3	Run made to test recharge procedure in new machine and run some Agile recipes. Crystals grown with S.R. = 8 rpm are straighter than first two runs.
	2	-	5	17.2	1.2	7.6	Recharge worked well but considerable oxide buildup observed in furnace.
TR6	1	35	-	26.6	2.15	7.6	Difficulty obtaining structure linked to leakage of air through seal on isolation valve shaft.
TR7	1	35.3	-	30.4	7.3	7.35	Changed to overbraided seed cable. Raised bottom heat shield to 3" from bottom of heater. Seed rotation at 10 rpm. Crystal has slight spiral with longer period.
TR8	1	35	-	31.6	0	7.3	Raised bottom heat shield by 1.5". Crystal not zero-D but appeared single all the way. More oxide smoke than normal observed due to leak in pull chamber door viewport.

SUMMARY OF T.R. RUNS 1 - 15 ON COMMERCIAL HAMCO CG6000

TABLE 3-6

RUN NO.	CRYSTAL NO.	SILICON CHARGE (kg) COLD FILL	SILICON CHARGE (kg) HOT FILL	PULLED WEIGHT (kg)	ZERO-D WEIGHT (kg)	AVG. PULL SPEED (cm/hr)	COMMENTS
TR9	1	35	-	30.85	17	7.2	Fixed air leaks and removed pedestal insulator. Better zero-D yield but problems due to arcing around heater feet.
TR10	1	35	-	26	0	5.8	Ground faulting during meltdown - restarted but crucible badly sagged so pulled for recycle. Seemed to be excessive cable movement during this run.
TR11	1	35	-	29.14	18.7	7.5	Raised bottom heat shield by 3/4". Modified pull chamber argon inlet to reduce cable movement. Good success with first crystal but
	2	-	30	29.4	0	7.4	could not hold structure, after recharge, for second crystal. Sporadic seed cable movement and melt vibration occurring.
TR12	1	35	-	31.6	10.5	6.85	Checked cable mechanism and reassembled. Experimenting with melt level changes. Once again unbraided cable induces spiral with shorter period.
TR13	1	35	-	20.6	19.9	7.5	Braided cable installed with cable guide. Argon inlet changed. Heavy graphite purge sleeve removed. Good first crystal.
	2	-	22.3	28.8	0	6.7	Second crystal never more than 5 kg zero-D. Experimented with rotations and melt levels. Oxide depositing on viewport.
TR14	1	34.6	-	27.2	11.6	7.1	Still no purge sleeve. Crystal dirtier than normal.
	2	-	26.3	29.15	0	6.3	Oxide buildup occurs after recharge operation. Could not retain structure on body.
TR15	1	35	-	29.3	29.3	7.4	Installed 19" diameter grafoil purge sleeve. Seed rotation = 12 rpm, crucible rotation = 10 rpm. Full term zero-D crystal with no spiral.

TABLE 3-6 (CONT.)

4.0 CONTROLS AND AUTOMATION

4.1 Introduction

The modified CG2000 grower constructed under this contract is equipped with Kayex-Hamco Automatic Grower Logic (Agile) control system. The Agile program includes meltdown, stabilization and growth of the ingot neck, crown, body, and final taper based on information stored in process tables. A discussion of the Agile system is given in a following section.

Tasks performed under this contract addressed the addition of sensors to the Agile system to enhance its control capability for growth of large diameter material for solar cell application. Goals for these tasks included:

a. Melt temperature sensing and automatic dip temperature stabilization;

b. Implementation of a sensor to detect proper diameter for termination of crown growth and start of the crystal shoulder;

c. Implementation of a sensor for control of the growth of six-inch diameter material; and

d. Implementation of direct melt level sensing and control.

These tasks were performed in two major phases. The first phase included development of the melt temperature, shoulder and diameter sensors. This phase included the growth of a series of four-inch diameter crystals from 12-inch crucibles in a Hamco CG2000 RC grower. Upon completion of the development and test phase, the sensors were integrated with the Modified CG2000 grower constructed under this contract, and the system was released to the process group for use in process development.

The melt level sensing system requires optical access to the furnace tank that is not available on a standard CG2000. Therefore, the melt level system was installed and tested after the effort was transferred over to the Modified CG2000 grower.

4.2 Sensor Development

4.2.1 Melt Temperature

4.2.1.1 Background

Establishing the correct melt temperature prior to seed dip is a critical step in preparation for crystal growth. The acceptable range of melt temperatures for dip is approximately $\pm 3^{\circ}$ C. Seed dip and neck growth at lower temperatures result in excessively high seed lift rates to produce acceptable small neck diameters. Conversely, seed dip at higher temperatures results in melt back and undercutting of the seed. In manual grower operation, the melt temperature is set by the operator by adjusting the temperature set point for the grower heater while observing the wetting of the dipped seed. This procedure can be delicate and time consuming, particularly if the operator is of a relatively low experience level, and it is highly desirable to automate this critical step in the growth process.

The approach taken to automatic dip temperature setting is direct sensing of the melt temperature which then serves to close a loop which controls the heater temperature set point. Optical pyrometry was selected as the means of temperature measurement, and initial development employed a two-color pyrometer (type R supplied by IRCON, Inc., Skokie, Illinois).

The two-color pyrometer has the advantage of providing a temperature measurement that can tolerate large variations in the intensity of the radiation from the object whose temperature is being measured. This characteristic is a consequence of the two-color measurement technique which determines the radiant body temperature from the ratio of the intensity of radiation at two different wavelengths. Equal attenuation of the radiation at both wavelengths does not affect this ratio and consequently does not affect the temperature measurement. Insensitivity to large variations in overall intensity of the radiation was considered to be a desirable characteristic because of the common occurrence of silicon monoxide as "smoke" within a grower and as a deposit on the grower viewports.

4.2.1.2 Development

The two-color pyrometer was mounted on the top of the pull-chamber of the CG2000 grower used during the development phase. It viewed the melt at an angle approximately 5^{o} off vertical through a quartz window which replaced the solid aluminum blow-off port. This arrangement was used for melt temperature stabilization prior to seed dip for 8, 12 kg crystal growth runs in 30.5 cm diameter crucibles. In each case, acceptability of the resultant melt temperature was judged by growing a crystal neck with a standard process implemented in the Agile computer. Reproducibility of the neck profile within an acceptable range was taken as the criterion for acceptable reproducibility of the seed dip. After these initial tests, development efforts progressed to growth from 18 kg charges in 30.5 cm crucibles. The increase in charge size was intended to examine sensor and process reproducibility. Three crystals were grown from 18 kg charges in the CG2000 development grower with unsatisfactory reproducibility of the melt temperature at seed dip. The decrease in reproducibility was attributed to an increase in spurious reflections of radiation from hotter surfaces off the surface of the melt. The response of the two-color pyrometer is severely affected by such reflected radiation because the two-color technique favors the measurement of the temperature of the hottest object in the field of view, even if the radiation received from that object is only a small percentage of the total radiation being detected.

This problem was addressed by replacing the two-color pyrometer with a single-color unit mounted in a carefully controlled geometry that minimized reflections off the melt surface.

4.2.1.3 Implementation

The final implementation of the melt temperature pyrometer is illustrated in Figure 4-1. The pyrometer (IRCON type B, IRCON, Inc., Skokie, Illinois) mounts on a periscope that allows it to view the melt by reflection off of a gold, front-surface mirror. The periscope replaces the adapter normally located between the pull chamber and the cable lift

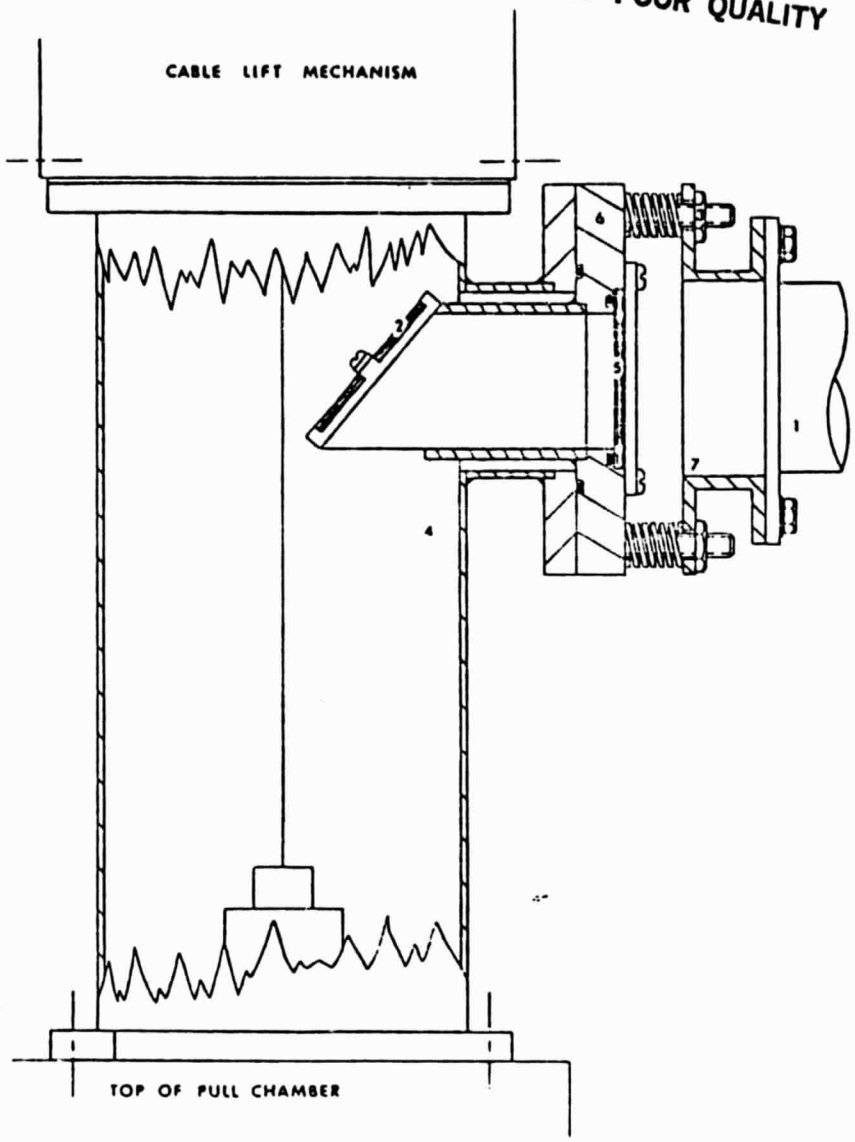

1. Pyrometer flange
2. Mirror
3. Adjusting Screws
4. Lift Mechanism Adapter
5. Quartz Window
6. Mounting Flange

MELT TEMPERATURE PYROMETER MOUNT

FIGURE 4-1

mechanism. Argon entering through an inlet (not shown in the figure) located in the periscope insures that, under normal operating conditions, monoxide created in the furnace chamber will not deposit on the mirror or quartz window of the periscope.

Spring loaded alignment screws located between the flange and pyrometer adapter allow precise alignment of the pyrometer field of view. The selected optics produce a 1.3 cm diameter field of view at the surface of the melt. This is centered on a point located 5 cm from the center of the crucible. The offset from the crucible center is necessary to allow the seed chuck to be lowered without encroaching on the pyrometer field of view.

Signal conditioning and linearization for the pyrometer is provided by an IRCON Series 220 electronic module with a linear output calibrated over the range of 900° C. to 1600° C. This module also provides signal filtering with a three second response time. The linearized output is then converted to a 12-bit binary input to the Agile computer system.

The output of the pyrometer electronics has a high noise content due to convection within the melt resulting in temperature variations in the melt surface. This can be seen in the chart record of melt temperature shown as A, Figure 4-2. The noise content is approximately 10° C. peak-to-peak and is excessive for a signal which is to be used as a process control input. The noise is reduced significantly by processing the signal with a digital filter implemented in the Agile software. The filter has a 60-second time constant and results in a typical output shown as B in Figure 4-2.

The control arrangement used for automatic melt temperature stabilization is illustrated in Figure 4-3. The control blocks in the figure represent PID control algorithms implemented in software. The cascade control configuration is closed after completion of meltdown and a soak of the melt at constant power. The control cascade is maintained until the melt temperature has been within a $\pm$ 2° C. band of set point for a 30-minute time period. This criterion assures that the melt is at the correct temperature and is stable before the start of neck growth.

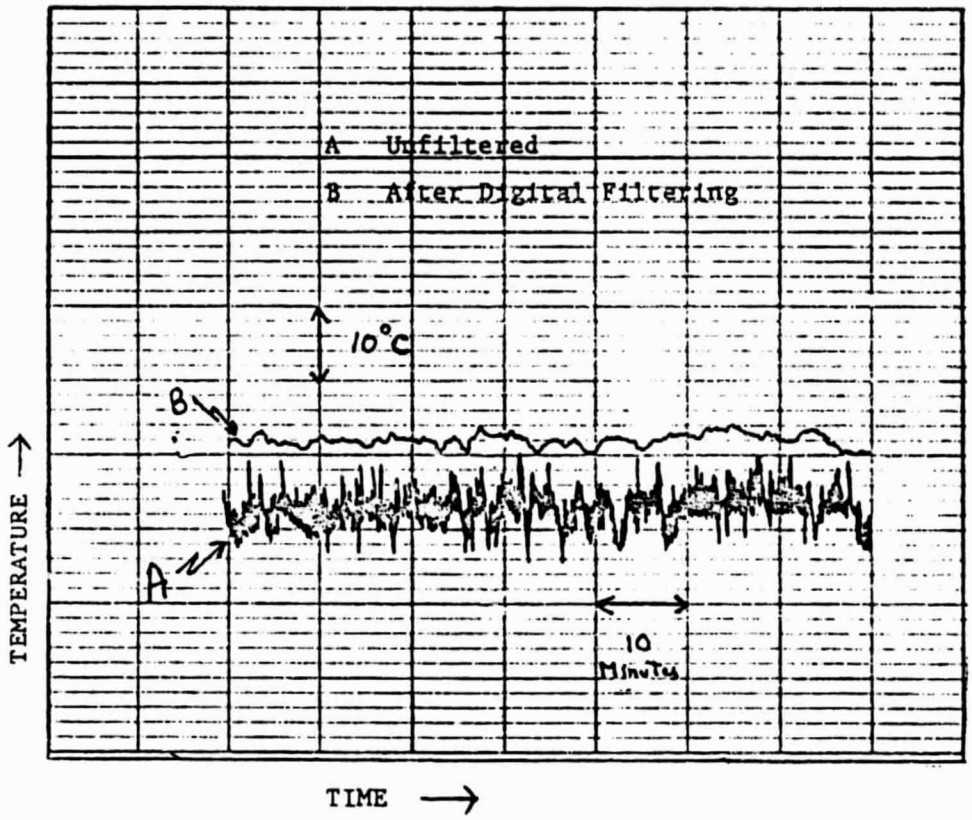

MELT TEMPERATURE CHART RECORDING
FILTERED AND UNFILTERED

FIGURE 4-2

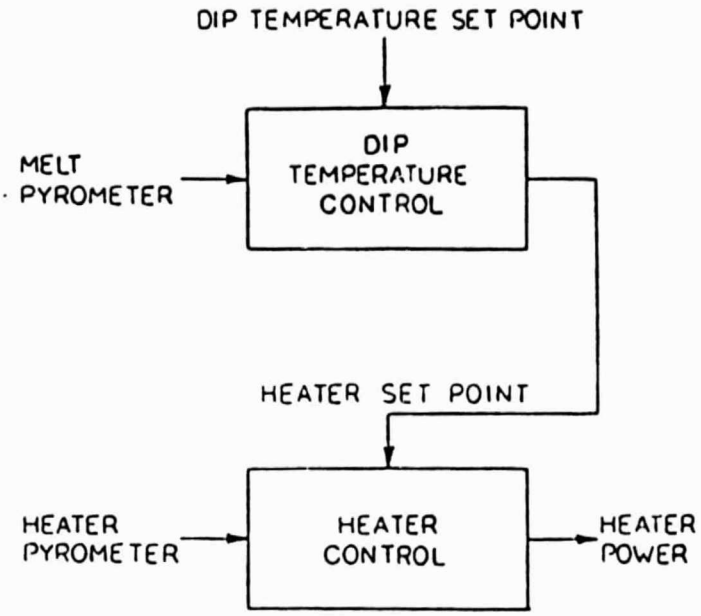

CONFIGURATION FOR AUTOMATIC
CONTROL OF MELT SEEDING TEMPERATURE
FIGURE 4-3

4.2.2 Shoulder Sensor

4.2.2.1 Principles of Operation

A critical step in ingot growth occurs at the transition from the relatively flat crown to growth of the cylindrical, at-diameter portion of the ingot. Performing this transition (or shoulder) requires that the seed lift rate be increased. The proper variation of seed lift rate is performed by the Agile computer upon receipt of an input at the proper time for the shoulder transition. This input is generated by sensing that the crown is at the correct diameter. This occurrence is detected by means of a focused optical pyrometer aimed at the crown diameter where the shoulder is to begin.

The solid silicon of the crown has an emissivity approximately three times higher than the emissivity of liquid silicon. Even though the crown is slightly cooler than the melt, the difference in emissivities results in an easily detectable increase in infra-red radiation when the crown increases in diameter to the point where it is seen by the pyrometer. Selection of pyrometer optics to give a small, well-defined field of view results in a sharp rise in electrical output as a function of increasing crown diameter. This signal is then compared with a threshold to determine the start of the shoulder threshold.

4.2.2.2 Implementation

The shoulder sensor is based on a Type Z pyrometer supplied by IRCON, Inc., of Skokie, Illinois. The pyrometer consists of three units: the detector assembly, a reimaging lens, and a flexible fiber optic cable for connecting the detector and lens assembly. This system was selected because the reimaging lens is physically small and is easily mounted on the grower. The reimaging lens assembly was modified as shown in Figure 4-4. The stock pin hole and lens are replaced with a .3 mm diameter pinhole and a 5.0 cm focal length lens. This combination gives a 3.3 mm diameter field of view at the surface of the melt.

The reimaging lens assembly and its mount are shown in Figure 4-5. A micrometer driven stage visible behind the lens assembly allows

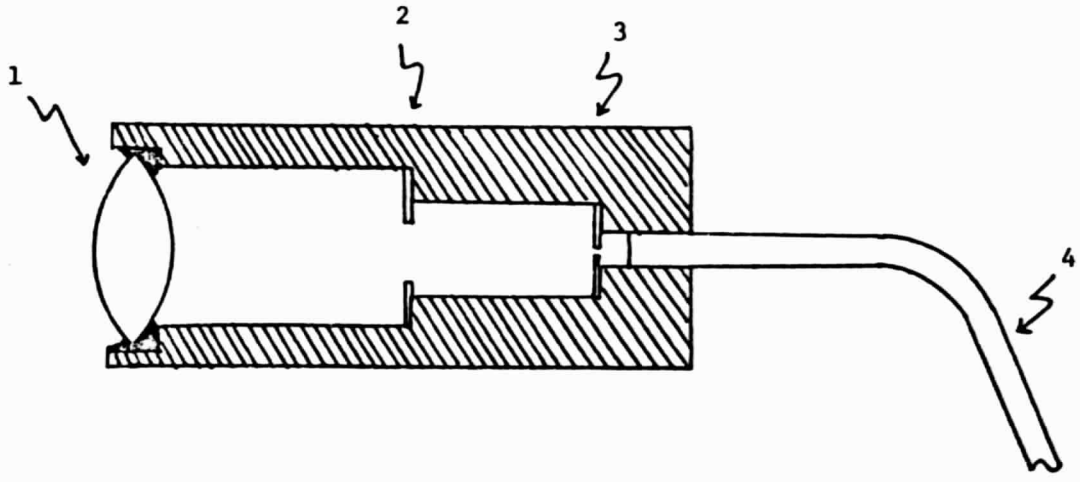

1. 50 mm Focal Length Lens
2. Optical Baffle
3. 0.25 mm Pin Hole
4. Fiber Optic to Detector

SHOULDER SENSOR OPTICS

FIGURE 4-4

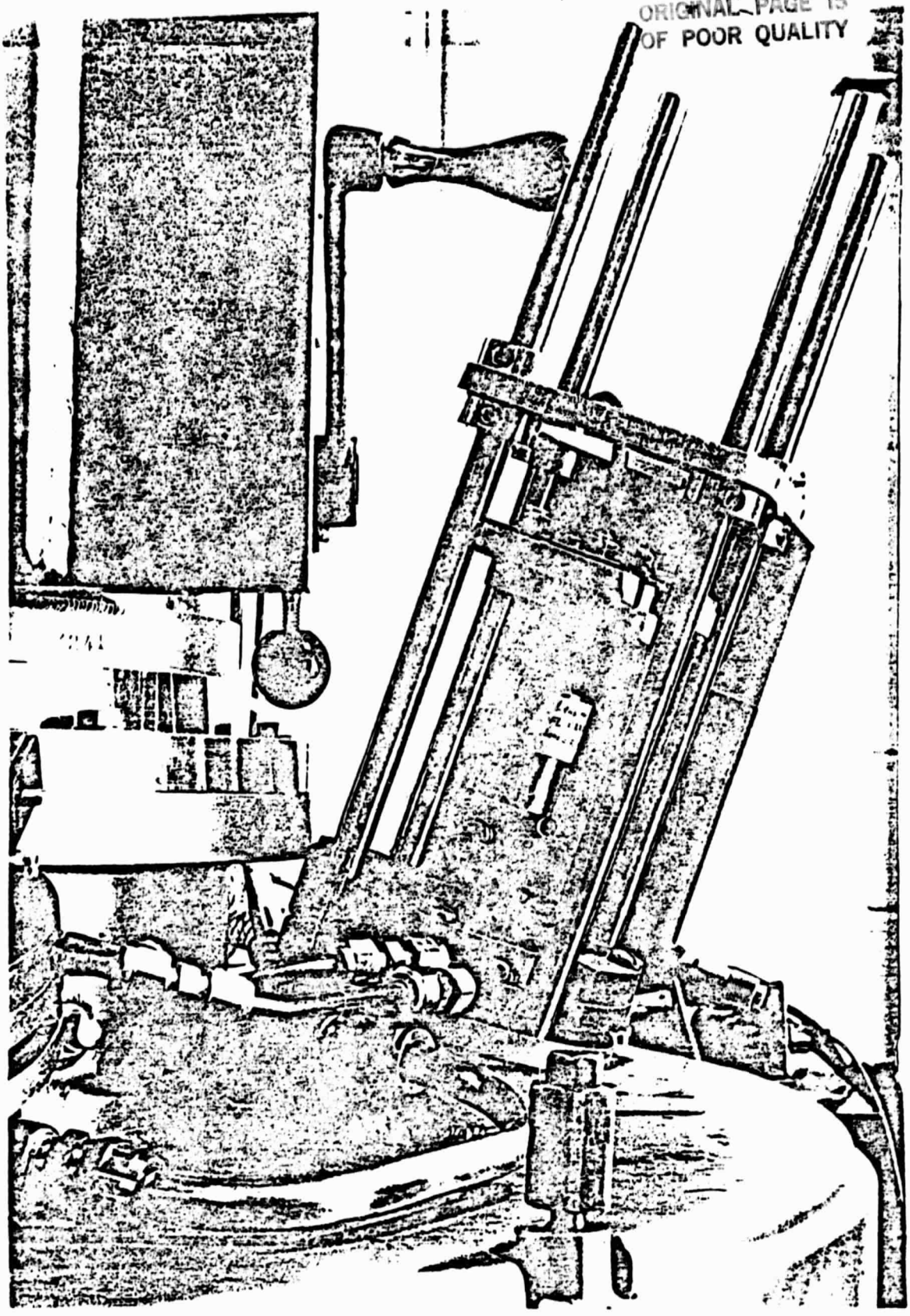

SHOULDER SENSOR REIMAGING LENS AND MOUNT

FIGURE 4-5

the aiming point of the pyrometer to be set. The aiming point is calibrated in terms of crystal diameter by replacing the detector with an illuminator that transmits light back through the fiber optics and reimaging lens. This allows an image of the pin hole to be projected onto an alignment target mounted on the crucible shaft.

4.2.2.3 Signal Processing

The output of the pyrometer detector is amplified by the circuit shown in Figure 4-6. The first stage is a current-to-voltage converter and the second stage is an active filter with a three-second response time. The output of the amplifier is fed to an analog input module of the Agile computer where it is converted to 12-bit binary. A digital filter implemented in software provides a sharp cut-off at 0.1 hz. The filtered signal is then compared to a fixed threshold. The 0.1 hz filter response reduces sensitivity to crown motion produced by seed orbiting to a negligible level, and it also provides a high level of immunity to transients in the pyrometer output that may be caused by spurious reflections from the crown or melt.

4.2.2.4 Operation

The response of the shoulder sensor was verified by using the micrometer stage to scan the field of view across the edge of a slowly growing crown. The relative location of the crown edge could be identified to $\pm$ 0.5 mm. The error in calibrating the position of pyrometer with the alignment target is estimated to be of the same magnitude. The total uncertainty in the shoulder trigger point is then better than $\pm$ 1.0 mm on the crystal radius for a given, fixed melt level.

4.2.3 Diameter Sensor

The diameter sensor is also a focused optical pyrometer. The optical and electronic implementation is identical to that described above for the shoulder sensor. Its operation is based on the classic

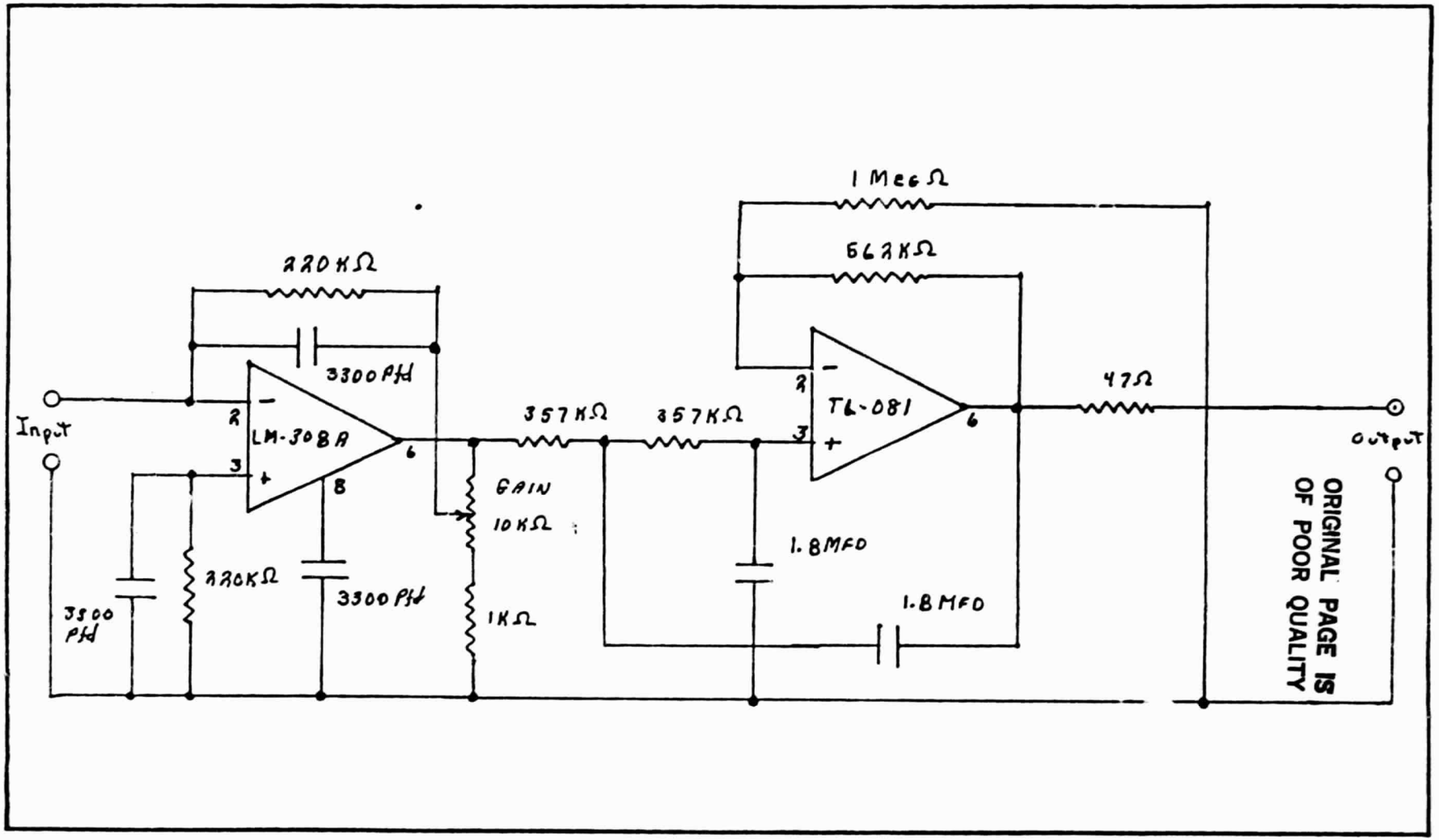

CIRCUIT DIAGRAM FOR SHOULDER SENSOR

FIGURE 4-6

technique of relative overlap between the pyrometer field of view and the image of the bright ring of reflections off of the meniscus near the crystal/melt interface. The overlap increases with the crystal diameter, resulting in an increase in the pyrometer output. This response characteristic holds over a range determined by the apparent width of the bright ring and the diameter of the pyrometer field of view.

The diameter sensor response was verified by growing a crystal out to nominal diameter and then manually controlling the seed lift rate to give stable growth at a constant diameter. This was verified by visually monitoring diameter with a cathetometer. The micrometer stage carrying the diameter sensor was then used to scan the pyrometer field of view across the bright ring and the filtered pyrometer output was recorded. The usable range of sensitivity was determined to be approximately 4.5 mm on the crystal radius.

4.2.4 Melt Level Sensor

4.2.4.1 Background

Maintenance of a constant melt level relative to the position of the heater is desirable for two reasons. Geometric considerations require that variations in melt level be minimized to avoid uncertainties in diameter control, and process considerations requie a known and constant melt level to minimize uncertainties in the thermal conditions within the melt.

In the past, melt level has been controlled indirectly by driving the crucible lift at a speed proportional to the seed lift. The proportion is a function of crystal and crucible diameters and departures from their nominal values result in a cumulative error or drift in melt level. The modified CG2000 design called for direct sensing of melt level and closed loop control of the crucible lift to give a controlled melt level throughout each crystal growth run.

4.2.4.2 Implementation

The melt level sensing technique is based on the system described by C.S. Duncan, et. al. in the March, 1981, Quarterly Report for DOE/JPL Contract 954654. The principle of operation is illustrated in Figure 4-7.

The output of the He-Ne laser enters the grower through a port and is reflected off the surface of the silicon melt to a second port. The receiver lens mounted just outside this port serves to reconverge the laser light that has been scattered by disturbances on the melt surface. An interference filter is used to eliminate light except for a narrow band centered on the laser wavelength. A linear, position-sensitive detector located at the focus of the receiver lens generates outputs which are processed by the electronics to give a signal proportional to the position of the spot on the detector being illuminated by the reflected laser light. A change in melt level results in a position change of the illuminated spot. The detector is a Model LSC 30-D manufactured by United Detector Technology of Culver City, California. The difference of the detector's output signals is proportional to the product of the illumination intensity and its position along the detector axis. The sum of the output signals is proportional to intensity only. The circuit illustrated in Figure 4-8 includes a divider whose output is proportional to position and is independent of intensity. This output is buffered and filtered to give the final melt level output.

4.2.4.3 Operation

The system was tested by tracking the level of water in a crucible while driving the crucible lift. Additional tests were performed by tracking the surface of a silicon melt during crystal growth Run 25. These tests indicated a system sensitivity to changes less than 0.5 mm over a range of 4 cm.

Further tests of the system were not possible because of interference between the laser sight line and the radiation shield installed in the grower in the later stages of process development. Consequently, the ouput from the melt level sensor has not been used as an input for closed-loop control.

ORIGINAL PAGE IS
OF POOR QUALITY

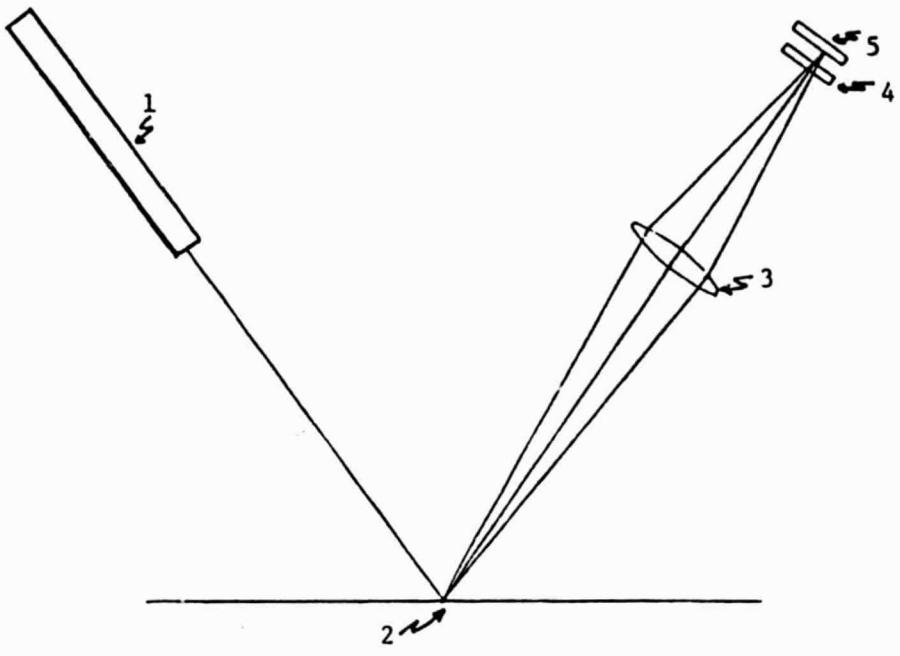

1 2-Milliwatt HeNe Gas Laser

2. Surface of Silicon Melt

3. Receiver Lens

4. Narrow Band Interference Filter

5. Position-Sensitive Photodetector

MELT LEVEL SENSING SYSTEM

FIGURE 4-7

ORIGINAL PAGE IS
OF POOR QUALITY

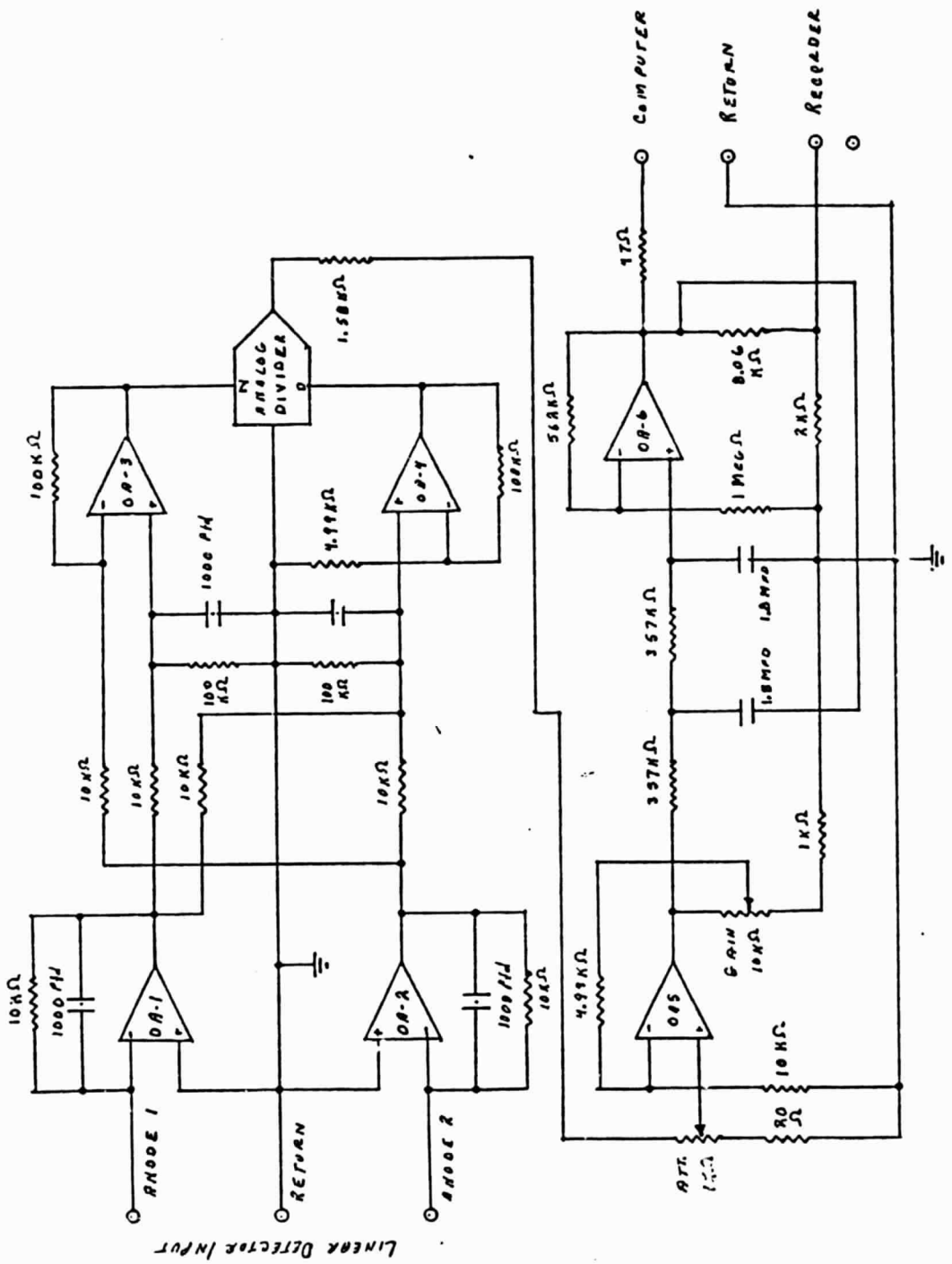

MELT LEVEL SENSOR ELECTRONIC CIRCUIT

FIGURE 4-8

4.3 Computer Control System

The automatic grower logic (Agile*) computer-based control system was integrated with the modified CG2000 grower and the sensor developed under this contract. The Agile system includes logic for controlling growth of the ingot neck, crown, body, and final taper with a minimum of operator judgement and input. The grower operator is required to make specific observations and decisions at a limited number of discrete points in the process. However, the operator input is limited to Yes or No responses as prompted by the computer system. Process reproducibility is achieved by taking process parameters from tables in the computer program. These tables are structured so that all entries are in familiar format and notation and are field changeable without knowledge of programming techniques.

The computer system includes digital implementations of the PID controllers for diameter and heater control and the Kayex-Hamco Growth Control.* An additional control loop is used for automatic setting of the melt temperature prior to seed dip as described in 4.2 above. Growth of the neck and crown are controlled by programmed variations in Seed Lift Rate and the Heater Control set point. These programmed variations are determined by process table entries.

The level of operator attention is significantly reduced by having the computer sound an audible annunciator and present messages to the operator at specific points in the process. Controls available to the operator are minimized. All controls for process tuning and modifications are included in a separate Engineer's Station which plugs into the grower control system when needed for development purposes.

The Agile system includes 72-hour battery backup of the computer memory, which avoids reloading the program after short-term shutdown. The Engineer's Station includes a digital cassette recorder if reloading should be necessary. The system also includes built-in self-test and diagnostic program for troubleshooting and maintenance.

*A proprietary development of the Kayex Corporation.

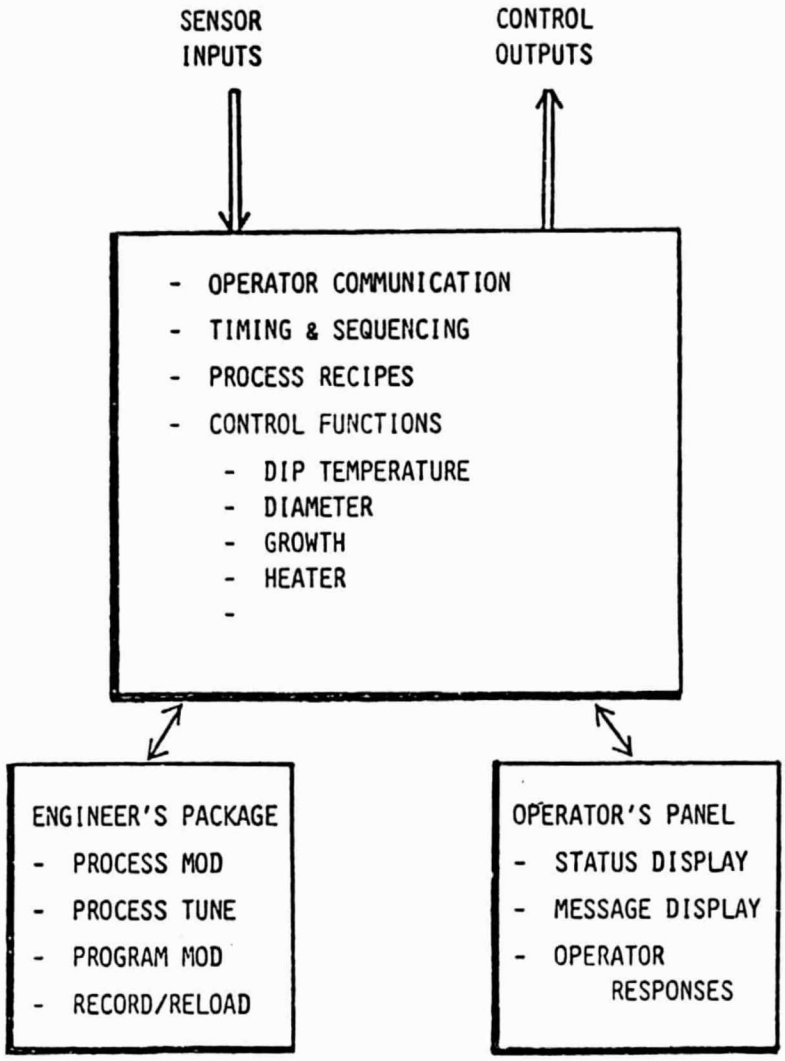

OVERVIEW OF THE AGILE CONTROL SYSTEM

FIGURE 4-9

4.3.1 Configuration

The Agile System includes the computer enclosure and the interface assembly. The computer enclosure houses the Texas Instrument PM550 computer, input/output electronics and the Operator's Panel. The interface assembly mounts in the grower console and includes relays and isolating amplifiers that allow the grower to be controlled by either the analog console controls or the Agile computer system. The control mode is determined by a front panel switch.

The separate Engineer's Station includes modules for process development and modification. The modules are plug coupled and are normally not connected during grower operation.

4.3.2 Functional Organization

4.3.2.1 Overview

A functional overview of the system is shown in Figure 4-9. The central box represents functions performed within the Agile computer. The boxes at the bottom of the Figure represent functions performed through the Engineer's Station and Operator's Panel. These are illustrated in Figure 4-10 and 4-11.

A more detailed representation of the internal system organization is given in Figure 4-12. Inputs, outputs, and functions are discussed below.

4.3.2.2 Inputs

a. Crucible Height - The output of the crucible height encoder potentiometer is an input to the Agile system. This input is monitored to raise the crucible to the correct starting position for crystal growth.

b. Shoulder Sensor - This output of the sensor described in 4.2.2 is used to determine when the crown is at the correct radius to begin turning the ingot shoulder.

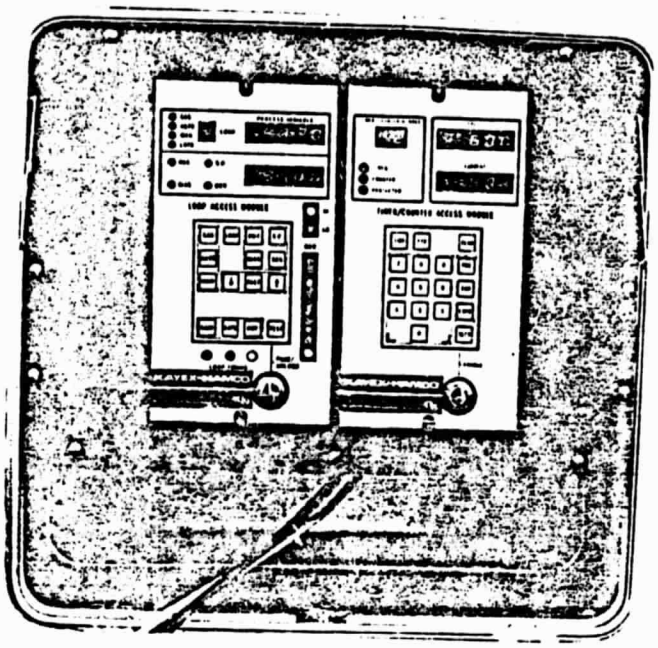

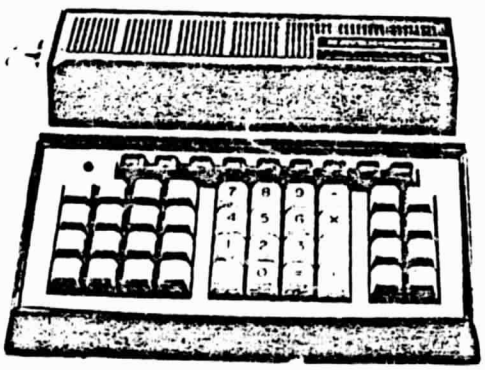

AGILE ENGINEER'S STATION MODULES

FIGURE 4-10

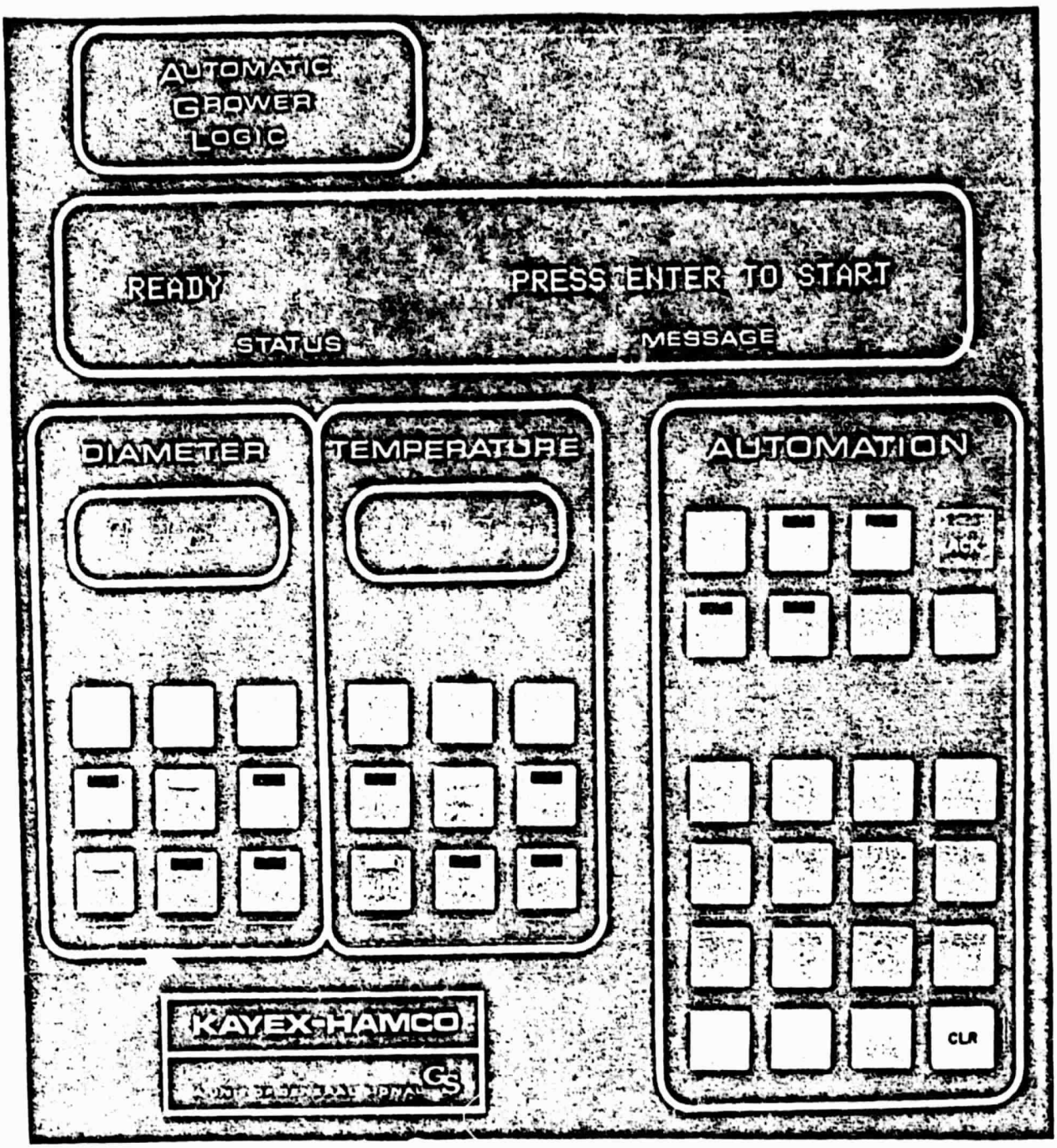

AGILE OPERATOR'S PANEL

FIGURE 4-11

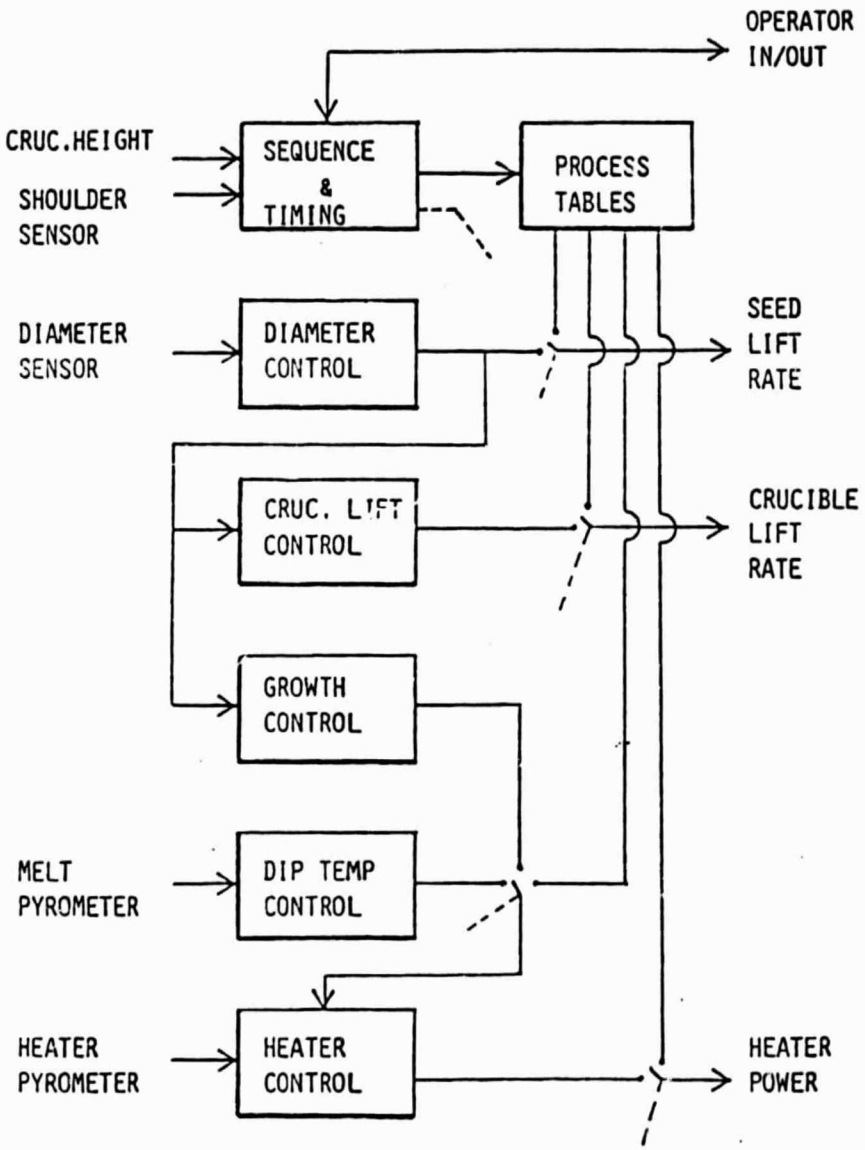

AGILE CONTROL ORGANIZATION

FIGURE 4-12

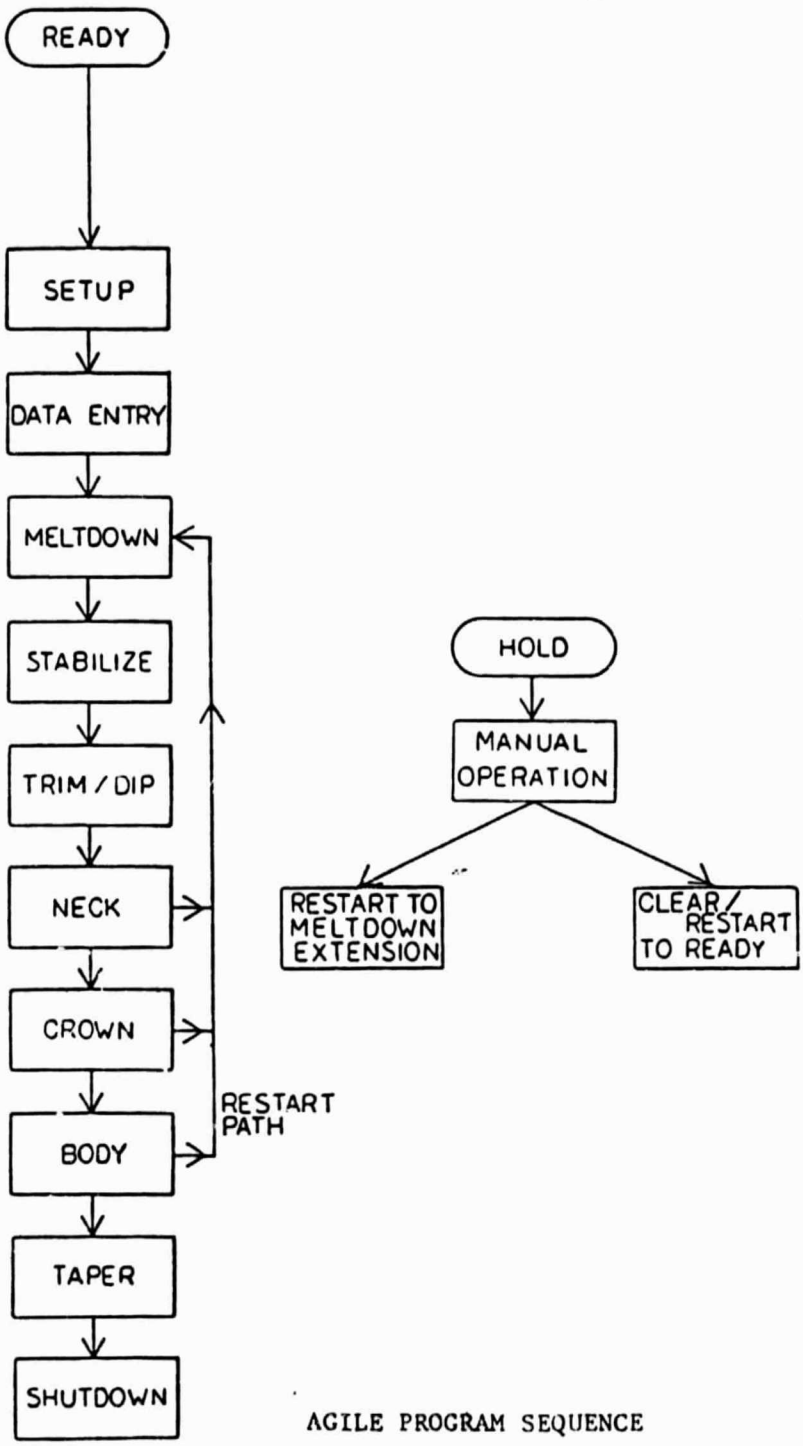

AGILE PROGRAM SEQUENCE

FIGURE 4-13

c. Diameter Sensor - The output of the sensor described in 4.2.3 is used as input to the Diameter Control loop during growth of the at-diameter crystal body.

d. Melt Pyrometer - This sensor output is used to automatically set the dip temperature as described in 4.2.1.

e. Heater Pyrometer - The standard heater pyrometer is mounted on the furnace tank. Its output is used as input to the heater control loop for control of heater power.

4.3.2.3 Functions

a. Sequence and Timing - Provides overall control of the program sequence and operator input-output. The dashed lines indicate logical switches within the program that determine the internal sources of control signals depending upon the step in the sequence. For example, the Seed Lift Rate is driven by the process tables during neck and crown growth and by the Diameter Control during body growth.

b. Diameter Control - This function is performed by a digital PID controller. Input to the controller is the digitally filtered output of the diameter sensor. The controller output is the Seed Lift Rate during growth of the crystal body.

c. Crucible Lift Control - The Crucible Lift Rate is calculated (from the crystal shoulder on) in a fixed ratio to the Seed Lift Rate. The ratio is provided by the operator as input data.

d. Growth Control - This function adjusts the set point of the Heater Control to maintain the long-term average of the Seed Lift Rate at a predetermined value.

e. Dip Temperature Control - Melt temperature is stabilized as described in 4.2.1.

f. Heater Control - Heater power is controlled by a PID loop with input from the heater pyrometer.

4.3.2.4 Outputs

The system provides outputs for Seed Lift Rate, Crucible Lift Rate, and Heater Power as shown in the Figure. As discussed earlier, these outputs are driven either by the process tables or by other process control functions within the Agile system as determined by sequence and timing.

The Agile system does not have control outputs for seed or crucible rotation, lift directions, or jog modes. These functions remain under the control of the operator, along with monitoring and control of water, vacuum, and argon utilities. Prompting messages regarding these functions are presented to the operator at appropriate points in the process.

4.3.3 Program Sequence

The principle steps in the program sequence are illustrated in Figure 4-13. The sequence proceeds as indicated by the arrowheads. The sequence may be interrupted (the Restart and Hold paths) by specific operator actions. The steps in the sequence are:

a. Setup - A timed sequence of messages is displayed to prompt the operator to perform certain operations or checks prior to crystal growth.

b. Data Entry - The operator is requested to enter specific parameters for the crystal growth process.

c. Meltdown - A four-step program in power level and time. The final step may be extended for fixed times by the operator in order to complete meltdown.

d. Stabilize - Melt temperature is stabilized to a preset value for seed dip. The crucible is automatically raised to the correct starting height for crystal growth.

e. Trim - Melt temperature may be annually trimmed. This is not normally required, but is permitted to correct for unusual circumstances.

f. Neck - A tapering neck is grown from a 10-step process table. The operator judges when the neck is adequately thin. A straight section of neck is then grown at constant pull speed.

g. Crown - A process table is also used to control crown growth. Crown growth proceeds until the output of the shoulder sensor exceeds a threshold, at which time the shoulder process steps are executed.

h. Body - The system enters Automatic Diameter Control (ADC) when the output of the diameter sensor exceeds a threshold. Body growth under ADC proceeds until a predetermined length of crystal is grown, at which time the Growth Control is turned on. During body growth, the Seed Lift Rate set point for the Growth Loop is automatically set as a function of ingot length. The settings are taken from a process table.

i. Taper - The final taper is grown automatically. The operator initiates taper growth in response to a prompt from the computer.

4.4 Test Results with Computer

A series of nominal 100 mm diameter crystals was grown from 12 and 18 kg melts during the sensor development program on the CG2000 RC grower. These growth runs led to the designs of melt temperature, body, and shoulder sensors later incorporated into the Mod 2000 design. System operation and reproducibility were verified by the growth of four 10 kg crystals from 12 kg melts with the use of identical process parameters in the Agile program. Two of these crystals are illustrated in Figure 4-14.

Measurement of these crystals yields a short term accuracy of diameter control that is better than $\pm$ 0.5 mm. Long term accuracy and reproducibility from crystal to crystal is approximately $\pm$ 2 mm. The long term errors are determined by errors in melt level, however, which reinforces the need for closed-loop melt level control.

ORIGINAL PAGE IS
OF POOR QUALITY

100 MM DIAMETER, 10 KG INGOTS GROWN WITH AGILE CONTROL

FIGURE 4-14

After integration with the Mod 2000 grower, testing continued but with the emphasis redirected to support of the process development. Two growth runs (Runs 13 and 14) were used to checkout the functioning of the Agile computer and sensors. These runs successfully demonstrated the principal control functions of the Agile system including neck, crown, and body growth. For other process development growth runs, variable growth conditions due to hot zone changes often precluded the use of the neck and crown portions of the Agile program which require a defined process. The Agile system was used routinely to control meltdown, stabilization, and body growth with satisfactory results as summarized in Section 4.0.

5.0 ANALYTICAL PROGRAM

The analytical program consisted of three general tasks:

1. Purity analyses of silicon material produced during 150 kg growth runs.
2. Solar cell fabrication and evaluation from selected samples of ingots, especially the 150 kg runs.
3. Furnace gas analyses.

The Technical Direction Memorandum issued by JPL in September of 1981 placed highest priority on the gas analyses; therefore, nearly all analytical efforts were performed in this area for the balance of the program.

5.1 Purity Analysis

Run 10 (150 kg) was selected for the preparation of samples for chemical analyses. The primary objective was to determine if impurity buildup in the melt would be sufficient to cause structure loss problems and a falloff of solar efficiency. Selected samples from grown ingots were prepared, as well as samples of a new crucible and the used crucible. Finally, a sample of the residual melt was analyzed.

The samples were sent to a testing laboratory for analysis by Spark Source Mass Spectrography (SSMS). Table 5-1 contains the results of the analyses.

Although the samples appeared to be very pure, the crucibles and residual melt did show notable amounts of calcium, iron, and aluminum consistent with our earlier experience.

When comparing the results from these samples with analyses from similar runs performed on earlier contracts, the general level of purity seems to have improved. However, the measured boron level is about one order of magnitude lower than it should be based upon the known dopant level and resistivity measurement (1.0-3.0 ohm-cm). Therefore, some doubt exists with regard to the accuracy of the analyses, and more extensive analyses should be performed for conclusive data. Earlier SSMS analyses were performed by Commercial Testing and Engineering Co., Inc.; whereas, the present samples were analyzed by Northern Analytical Laboratory.

IMPURITIES (CONCENTRATION IN PPMA)

Sample I.D.	Na	Mg	Ca	K	Cr	Fe	Cu	Mn	V	B	Al	P	Cl
10-1-T		0.01	0.02			0.1				0.01	0.01	0.01	0.01
10-3-M			0.01			0.1				0.01	0.01	0.01	
10-5-B			0.02		0.01	0.1	0.02			0.02	0.03	0.01	
10-R (Residual Melt)		0.01	1*			0.1				0.03	0.1	0.02	0.01
New Crucible 10-N (Lot #02244)			1	0.6		5	0.05	0.05		0.1	7	0.03	1
Used Crucible 10-U (Lot #02244)	1		2	0.6		5	0.05	0.1	0.02	0.2	5	0.02	1

*Inhomogeneous

IMPURITY ANALYSES

TABLE 5-1

There does not, however, appear to be any alarming buildup of impurities throughout the run in either the grown ingots or the residual melt.

5.2 Solar Cell Fabrication and Testing

Material from Run 10 was sent to Applied Solar Energy Corporation for fabrication and testing in accordance with their standard (baseline) method. Each of the five crystals produced during this 150 kg recharge run was sectioned such that material from the top, middle, and bottom of the crystal could be fabricated into 2 cm x 2 cm wafers for processing into solar cells. Each cell was identified according to the following "key":

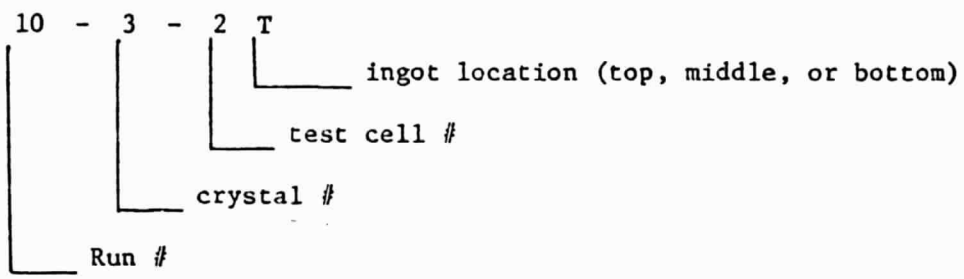

Thirty cells were fabricated and tested. Applied Solar provided one control cell. Of the thirty cells, four were duplicates to determine the repeatability of the fabrication and testing procedure.

These four cells were identified as follows:

I.D. #	Actual Sample
10 - 7 - 2 T	10 - 2 - T
10 - 7 - 3 T	
10 - 7 - 2 M	10 - 1 - M
10 - 7 - 3 M	

The cell efficiencies were tested under both AMO conditions and AM1 conditions. The testing results can be seen in Table 5-1.

As in previous long recharge runs, monocrystalline material produced average efficiencies 24% higher than polycrystalline material.

However, the average efficiencies of both monocrystalline and polycrystalline material was 24.4% and 28.3% higher respectively than cells fabricated in 1979-1980.[2] It is believed that the average efficiencies of the cells fabricated in 1982 are higher than those fabricated earlier because of improved cell fabrication methods, rather than improved material. As a matter of fact, the average efficiencies of the cells made from poly material in 1982 tested as high as the cells made from monocrystalline material in 1979 and 1980 (12.3%).

The results of the earlier work were corroborated with these results. Solar efficiency of monocrystalline material remains essentially constant to 150 kg in the continuous Czochralski process, as does efficiency of large-grained poly. The poly material is, however, somewhat less efficient.

The solar efficiency of the monocrystalline material was 15 to 16% AM-1 to 150 kg pulled.

The solar efficiency of the polycrystalline material was 11 to 13% AM-1 to 150 kg pulled.

Sample No.	Comments	Voc mV	Isc mA/cm^2	CFF %	AMO N %	AM1 N %
10-1-2T	Zero Dislocation	586	39.7	81	13.9	15.6
10-1-3T	Zero Dislocation	586	40.7	80	14.1	16.0
10-1-2M	Zero Dislocation	584	39.2	80	13.5	15.1
10-1-3M	Zero Dislocation	584	38.8	79	13.3	14.8
10-2-2T	Zero Dislocation	590	38.6	81	13.7	15.3
10-2-3T	Zero Dislocation	590	39.2	81	13.8	15.5
10-2-1B	Poly	562	34.4	80	11.4	12.7
10-2-3B	Poly	564	35.3	79	11.6	13.1
10-3-1T	Single	586	39.6	79	13.5	15.2
10-3-2T	Single	588	38.3	81	13.5	15.1
10-3-1M	Poly	558	34.8	79	11.3	12.7
10-3-2M	Poly	544	33.2	75	10.0	11.2
10-3-2B	Poly	564	35.2	78	11.5	12.8
10-3-3B	Poly	562	34.4	79	11.3	12.5
10-4-1T	Single/Poly	588	39.6	80	13.9	15.7

SOLAR CELL TEST DATA

TABLE 5-2 (A)

Sample No.	Comments	Voc mV	Isc_2 mA/cm	CFF %	AMO N %	AM1 N %
10-4-3T	Single/poly	586	38.6	80	13.4	15.0
10-4-1M	Poly	540	33.2	78	10.3	11.4
10-4-3M	Poly	536	32.4	76	9.8	11.0
10-4-2B	Poly	570	36.8	78	12.2	13.6
10-4-3B	Poly	560	35.7	76	11.2	12.6
10-5-1T	Single	588	38.2	82	13.6	15.1
10-5-3T	Single	588	38.6	81	13.6	15.2
10-5-3M	Poly	544	32.9	78	10.3	11.5
10-5-4M	Poly	546	32.8	79	10.5	11.8
10-5-2B	Poly	562	34.9	78	11.4	12.7
10-5-4B	Poly	562	34.8	79	11.5	12.8
4 Internal Controls						
10-7-2T	10-2-T	588	38.6	80	13.5	15.1
10-7-3T	10-2-T	588	38.3	81	13.4	15.0
10-7-2M	10-1-M	588	39.1	80	13.7	15.3
10-7-3M	10-1-M	588	39.6	79	13.7	15.3
External Control						
Applied Solar CZ Material		598	39.1	81	14.0	15.8

SOLAR CELL TEST DATA

TABLE 5-2 (B)

5.3 Furnace Gas Analysis

Although early silicon CZ growers were operated at about atmospheric pressure, most growers today are operated in the pressure range of 10 to 30 torr. A constant flow of protective gas is metered into the growth chamber (usually argon) and a mechanical vacuum pump maintains the desired pressure. The argon purge helps to provide the melt with a noncontaminating environment by sweeping away undesirable products of reactions that are ongoing throughout the crystal growth run. It also helps to minimize the deposition of silicon monoxide on the inside surfaces of the furnace chamber.

The objective of this portion of the program was to implement a method of quantitatively measuring gases suspected to exist in the ambient atmosphere of a silicon crystal grower. Possible species of gas (besides the argon purging gas) are CO, CO_2, N_2, H_2O, and H_2. CO and CO_2 might be the result of reactions between crucible and crucible support, or between graphite and silicon monoxide. The other species could indicate the possibility of air or water leaks into the growth chamber. Ultimately, it was hoped that gas analyses could be correlated to conditions of growth. The preferred method would measure either continuously, or would repeatedly analyze samples over a relatively short cycle time.

During portions of JPL Contract No. 954888 and 955270, a quadrupole residual gas analyzer (RGA) was used to analyze exhaust gases from a Hamco CG2000 crystal grower. Limited quantitative information from the RGA method led us to the conclusion that a gas chromatographic system (GC) would be the preferred analysis method for the present program. Several GC vendors were contacted and quotations received. However, no vendor could devise a satisfactory system for sampling the low pressure, low concentration gases in the crystal grower. Therefore, a consultant was retained to solve the sampling problem and verify the capabilities of the different GC manufacturers' equipment. This effort led to the conclusion that commercial type GC systems were not sensitive enough to measure the expected low concentrations of the gases of interest. The difficulty was associated with effectively seperating and analyzing oxygen, nitrogen, and argon in commercial GC equipment. Therefore, the initial concept

of one chromatograph doing the analyses of all significant gases was dropped and a new approach encompassing a modular or component system made up of several different types of gas analyzers was pursued. For carbon monoxide, hydrogen, and possibly other hydrocarbons, an inexpensive ethylene gas analyzer based on gas chromatographic principles could be used. It required modifications for it to function as a gas chromatograph, but these modifications were relatively simple and inexpensive when compared to the cost of a commercial GC.

Commercial sensors were found to be available for measuring oxygen and water vapor in low concentrations.

The analyzers capable of detecting low concentrations of nitrogen were expensive and, at best, untried in our application. Moreover, it was felt that the nitrogen concentrations in the ambient gases at the bottom of the crystal grower might be so low that they would be undetectable. For those reasons, nitrogen was dropped as a gaseous species to be analyzed.

The final gas analysis system was, therefore, comprised of the following gas analyzers:

1. An ethylene gas analyzer modified to perform as a gas chromatograph and detect very low concentrations of carbon monoxide and hydrogen.
2. An in situ oxygen analyzer capable of continuously monitoring the concentration of oxygen in the gases being sampled;
3. An in situ hygrometer capable of continuously monitoring the dew point of the gases being sampled. The dew point could then be converted to water vapor concentration levels.

In the Hamco CG2000, pure argon is introduced into the chamber continuously at the top. It flows generally downward over the melt and growing crystal and eventually is exhausted out a port in the lower portion of the chamber into the vacuum pump. It was decided to take samples from the exhaust line for analysis, although, in future work, it would be helpful to also sample incoming gas as well as gas in close proximity to the melt, for it is now believed that some of the products are formed in the heater/insulation region below the crucible and melt which do not affect the growing crystal.

Our approach to the gas analysis study was to assume that the incoming argon was of the purity specified by the manufacturer and that reactions taking place in the hot zone area were as predicted, and, in some cases, verified by thermodynamic analysis and corresponding literature, and therefore analyze gases in the lower portion of the crystal grower furnace tank at the exhaust exit. This approach we felt would allow us to best use our resources to answer the following questions:

- How do variations in crystal growth conditions and process parameters affect the quantities and types of gases produced in a vacuum type Czochralski crystal grower?
- Are high concentrations of certain gases detrimental to the growth of high quality (dislocation free) silicon crystals?
- What conditions can cause ambient gas concentrations detrimental to high quality crystal growth? Can these conditions be detected when they occur?
- Are there certain crystal growth procedures or process parameters that will minimize potentially detrimental concentrations of contaminant gases in a vacuum type Czochralski crystal grower?
- If contaminants in the ambient gas are unavoidable, can the hot zone be designed to minimize their effects?

5.3.1 Design, Construction, and Testing of Gas Analyzer

5.3.1.1 Design

A schematic showing the three analyzers and the sample gas flow pattern from the crystal grower to each analyzer is shown in Figure 5-1. The oxygen analyzer and GC have seperate calibration gas systems incorporated into their sample gas line.

The hygrometer did not require a calibration gas for reference or calibration. The output from the hygrometer control unit and the oxygen analyzer were continuously recorded on a Houston Instruments two-pen chart recorder, while the GC output was recorded on, integrated, and reported

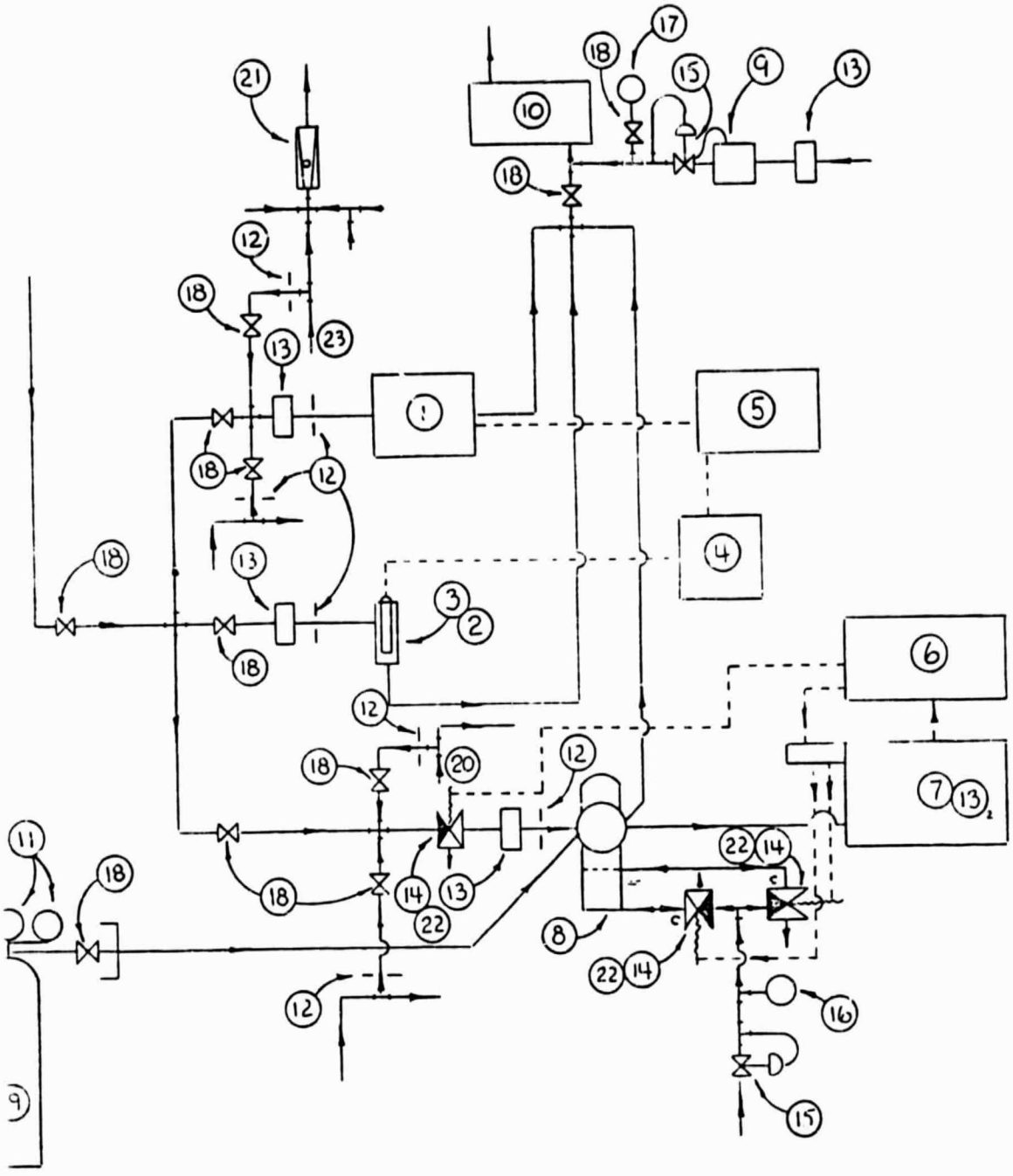

GAS ANALYSIS SYSTEM SCHEMATIC

(See following page for key)

FIGURE 5-1

GAS ANALYSIS SYSTEM

(Schematic Component Key)

Item	Description
1	Westinghouse Model 209 Oxygen Monitor
2	Panametrics 2830 Probe Flow-Through Housing
3	Panametrics Model M27R Model 700 Hygrometer M2 Probe
4	Panametrics Model 700 Single Channel Hygrometer
5	Houston Instruments Model B5218-5 Two-pen Recorder
6	Hewlett Packard Model 3390A Reporting Integrator and 19400A Sampler/Event Control Module
7	Bio-Gas Detector Model 12-110 Gas Chromatograph
8	Valco Ten-port 1/8" Multifunctional Rotary Sampling Valve, Actuator and Purge Housing
9	Moore Products Model 43-20L Subatmospheric Absolute Pressure Regulator and Model 63A Flow Controller
10	Precision Scientific Dual Stage Vacuum Pump
11	Matheson Dual Stage, High Purity Pressure Regulator
12	Orifices - Stainless Steel 1/8" OD or 1/16" OD Tubing
13	Mott Metallurgical Corp. Filters 6610-¼-10
14	Valco Digital Valve Interface
15	Norgren 0-100 psig Pressure Regulator
16	Norgren 0-100 psig Gauge
17	Mechanical Vacuum Gauge Leybold-Heracus DiaVac
18	On/off Valves for Vacuum Service
19	Cylinder of Matheson Air - Vehicle Emission Zero Type
20	Cylinder of High Purity Gas Mixture 2500 ppm CO in Argon
21	Dwyer Model RMA-150 Ratemaster Flowmeter
22	Three-way Skinner Solenoid Valve, 115 VAC Bubble Tight
23	Cylinder O_2

by a Hewlett Packard 3390A Integrator. The sampling system works on the principle of differential gas pressure flow. A small vacuum pump was used to produce a vacuum lower than that of the crystal grower and thus allow sample gases from the crystal grower to travel through the lines from the grower to a manifold. The manifold directs the sample gas flow to each of the three sensor areas of the analyzers. The sample gas exhausts through the vacuum pump after being analyzed. The system allows for isolation of any of the three analyzers by means of vacuum tight shutoff valves at the manifold. Stainless steel tubing was used to contain the flow of sample gas from the crystal grower to the manifold and from the manifold to the H_2O sensor. Copper tubing was utilized from the manifold to the oxygen analyzer and the GC system. Velocity of sample gas flow and therefore quantity of sample gas flow was determined by the capacity of the vacuum pump and the tubing size and constrictions of the sampling system.

A subatmospheric absolute pressure regulator and a flow controller were used to control the pressure in the sampling valve. This system was necessary because samples injected into the GC must be reproducible in volume, temperature, and pressure to be comparable on a quantitative basis.

Since the hygrometer and oxygen analyzers could be operated on a continuous basis without manual control or supervision, and since a typical crystal growth run lasts from sixteen to twenty-four hours (60 to 100 hours with recharge runs), the GC was designed to operate automatically through the use of the programmable H.P. 3390A Integrator, a H.P. 19400A Sampler/Event Control Module, a Valco digital valve interface, and a three-way solenoid valve. A ten-port rotary sampling valve provided a gas sample to the GC once every seven to eight minutes. A dual column system was used. The carrier gas used for this GC system is high purity air.

It was felt the gas analysis system should be mobile so that it could be transported to different crystal growers. Therefore, the system was designed and constructed to fit on a mobile cart (see Figure 5-2).

C-2

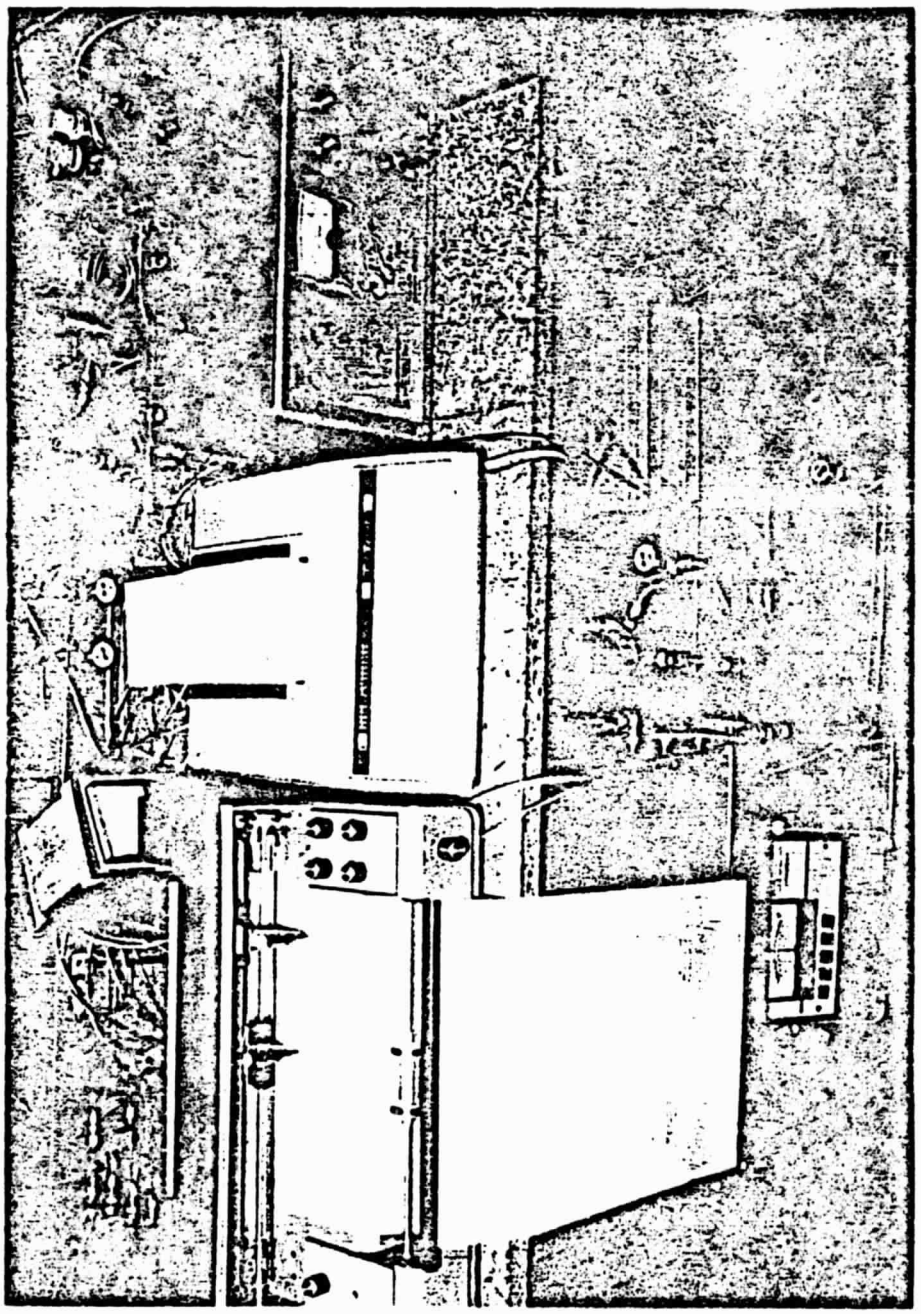

GAS ANALYSIS EQUIPMENT

FIGURE 5-2

5.3.1.2 Constuction and Test

In March, budget and schedule limitations on the project required postponment of some of the components, including the hygrometer, oxygen analyzer, and automatic controls. The balance of the construction was started in May with initial tests and calibration trials for the GC performed on the 28th of May.

The month of June was devoted to interfacing the gas analysis system with the Mod 2000 crystal grower, correcting external air leaks in a fitting on the rotary sampling valve, replacing an inactive second column on the GC, and general testing, calibrating, and debug of the total system.

Finally, on July 1, the first attempts were made to analyze gases from the crystal grower during a crystal growth run. Several more crystal growth runs were monitored during July along with a bakeout of graphite parts. Results and data interpretation are covered in Section 5.3.2.

Up to this time, the GC had been operated in the manual mode only. This meant that an operator had to stay at the gas analyzer bench and manually inject samples into the GC analyzer according to a set procedure. Moreover, all concentration calculations were made by comparing the peak height of a standard calibration gas with the peak heights of the sampled gases from plots on the two-pen recorder chart.

The integrator and hygrometer were received in October and interfaced with the GC. Trial runs were performed the last week in October. Results indicated the unit was functioning properly.

On November 19, the first crystal growth run was performed with the integrator operational. During this run, the hygrometer was also used to monitor moisture levels (dew points) continuously.

The oxygen analyzer was received in November, but was not installed on the gas analyzer bench until December due to the number of crystal growth runs performed during November and the learning curve necessary for the integrator and event control module. Attempts to automate the GC system were initially unsuccessful. A subminiature vacuum-tight solenoid valve still had not been received and it was discovered that the integrator

had come through without a special interconnect board necessary to interface it with the event control module.

During the month of December, five crystal growth runs were monitored with the gas analyzer. In each case, the hygrometer was run on a continuous basis and recorded. The GC was run on a manual basis injecting samples randomly throughout the run and analyzing the output on the integrator.

Cycle time data were accumulated with the integrator. A cycle time of seven to eight minutes was normal for a carrier gas flow rate of 24 cc to 25 cc/minute with regulated carrier gas tank pressure of approximately 13 psi.

The Hewlett Packard accessory kit for the H.P. 3390 Integrator was received on the seventh of December and sent to the local office for installation. It was discovered in December that the Humphrey solenoid valve was not bubble (leak) tight and could not be used in conjunction with the gas sampling system for the GC. A three-way Skinner valve was finally located that would do the job. The valve was installed along with the modified integrator the first part of January.

Although the oxygen analyzer performed well when bench tested (sampling air at one atmosphere), sufficient sample gas flow could not be achieved when the analyzer was connected to the gas analyzer bench sampling system. Further testing of the oxygen analyzer indicated that the pressure differential (ΔP) between the crystal grower and the controlled vacuum level of the gas analysis system was not sufficient to provide adequate flow of sample gas through the O_2 analyzer. With a ΔP of less than 50 torr, no flow was measured on the oxygen analyzer's flow meter. It required greater than a 300 torr pressure differential to meet the manufacturer's recommended flow rate, and a pressure differential greater than 200 torr was necessary to obtain a minimum flow rate specified by the manufacturer's technical staff. Further attempts to provide sufficient flow from the crystal grower to the oxygen analyzer using vacuum sources other than the pump on the gas analysis bench were unsuccessful. Therefore, as per the lease/buy arrangement with Westinghouse, the oxygen analyzer was sent back in February.

During the month of January, a great deal was accomplished to automate the GC system and further define the gases and their characteristic concentration patterns during bakeouts and crystal growth runs. Three long crystal growth runs were monitored in addition to two bakeouts.

By the end of January, the gas analysis system was operating automatically during growth runs without the aid of an operator. However, the integrator was reporting concentrations as area measured under curves. This area measurement had to be compared to the area measured under a calibration curve in order to denote the concentrations in parts per million (ppm). Therefore, the first two runs in February were devoted to developing a calibration table program in the integrator. This calibration table of standards can be used to compare concentrations of sample gases analyzed to the standards. The integrator can then report the sample gas concentration directly in parts per million.

Two problems were encountered at this point.

1. The shape of the curves produced by the integrator as a result of the GC detector signal contain a long, gradually decreasing tail. Not only did this adversely affect the area measurements under the curve, but it also produced an overlapping of the hydrogen curve with the start of the carbon monoxide curve. Corrections could be made for this by changing the integration program of the integrator. However, it was found that using peak heights rather than areas under curves proved to be a much more satisfactory method to use with our analysis equipment.
2. The other problem was associated with an electrically dead area of the GC analyzer below five percent of full scale meter deflection. In other words, when the signal from the GC detector was less than five percent of full scale deflection, the analyzer saw the signal as zero - no signal. This problem could be solved by either maintaining the baseline of the GC above the five percent full scale meter deflection or electrically bypassing the diode. Both procedures were used to eliminate the problem.

Although meaningful data were obtained prior to solving these two problem areas, the best gas analysis results were obtained during the month of March up to the end of the contract.

5.3.2 Gas Analysis Results

The system developed during this contract measured hydrogen, carbon monoxide, and water vapor. It is believed that these species represent the major contaminants, although oxygen, carbon dioxide, and nitrogen may be present in very small amounts. Silicon monoxide sublimes to a fine powder below about 1000° C and deposits on all cooler surfaces in the furnace, and no attempt was made to measure it quantitatively. Subjective observations of silicon monoxide deposits showed a correlation with CO measurements, i.e., heavy monoxide deposits corresponded with high CO concentrations. Also, it was observed that CO concentration increased when a water leak or an air leak was present. For these reasons, most emphasis was placed upon reliable measurements of CO.

F. Schmid, C.P. Khattak, T.G. Digges, Jr., and L. Kaufmann[6] compiled a list of potential chemical reactions that could occur in a vacuum type Czochralski crystal grower. This extensive thermodynamic analysis work was referenced to provide some insight into the possible reactions producing carbon monoxide gas, as well as other gases within the crystal grower. According to the authors, the following reactions could take place at the temperature and pressure conditions common for silicon crystal growth.

1) $2C + SiO \longrightarrow SiC + CO$
2) $C + SiO \longrightarrow Si + CO$
3) $3C + 2SiO \longrightarrow 2SiC + CO_2$
4) $C + SiO_2 \longrightarrow SiO + CO$
5) $3C + SiO_2 \longrightarrow SiC + 2CO$
6) $CO + SiO \longrightarrow SiC + 2SiO_2$

Reactions 1, 2, 4, and 5 produce carbon monoxide; however, the most probable reactions are 4 (crucible and crucible support reaction) and 1 (reaction of silicon monoxide with graphite parts of the hot zone where the temperature is appropriate).

It is not the intention of this report to explain the chemical reactions taking place in the crystal grower or why certain gaseous species increase or decrease in concentrations at different periods of the crystal growth cycle. The data are presented with possible interpretations; however, a more extensive experimental program would be required to develop a model of the gas environment in crystal growth. Measurements of gas concentrations are believed to be accurate to ± 10%.

A typical plot of carbon monoxide and hydrogen concentration as a function of time into a silicon crystal growth run can be seen in Figure 5-3. Hydrogen concentration is indicated by the dotted line; whereas, the carbon monoxide concentration is represented as the solid line. This run was started at 11:00 AM (power on) and completed the following day at 1:45 PM (power off). The meltdown was complete at 1306 hours of the first day and one meltback was performed from 1715 hours to 1750 hours the first day.

Hydrogen concentration was greatest during the first hour just before the furnace temperature had reached the melting point of silicon. As the silicon started to melt, the power to the heater was reduced somewhat, resulting in a rapid decrease in hydrogen concentration. The CO concentation, on the other hand, continued to increase as more silicon melted. A solid silicon bridge dropped into the melt at 12:35 causing a reduction in CO. However, the CO concentration started increasing again as the meltdown proceeded until the power level was decreased significantly prior to complete meltdown at 1304. From 1330 to 1700, melt stabilization, neck, crown, and a body growth of approximately three inches was accomplished. At that point, structure loss occurred and the crystal was melted back. Meltbacks require the furnace temperature to be increased and the CO level increased accordingly. The second crystal growth cycle continued until a 31.6 kg crystal had been grown.

A calibration check was performed between 0700 and 0800 the following morning. This check indicated that the measured CO concentration was 30% lower than the actual known concentration of the standard. Therefore, concentration levels at this time, although correct in their relative pattern of change, are actually 30% lower than they should be.

ORIGINAL PAGE IS
OF POOR QUALITY

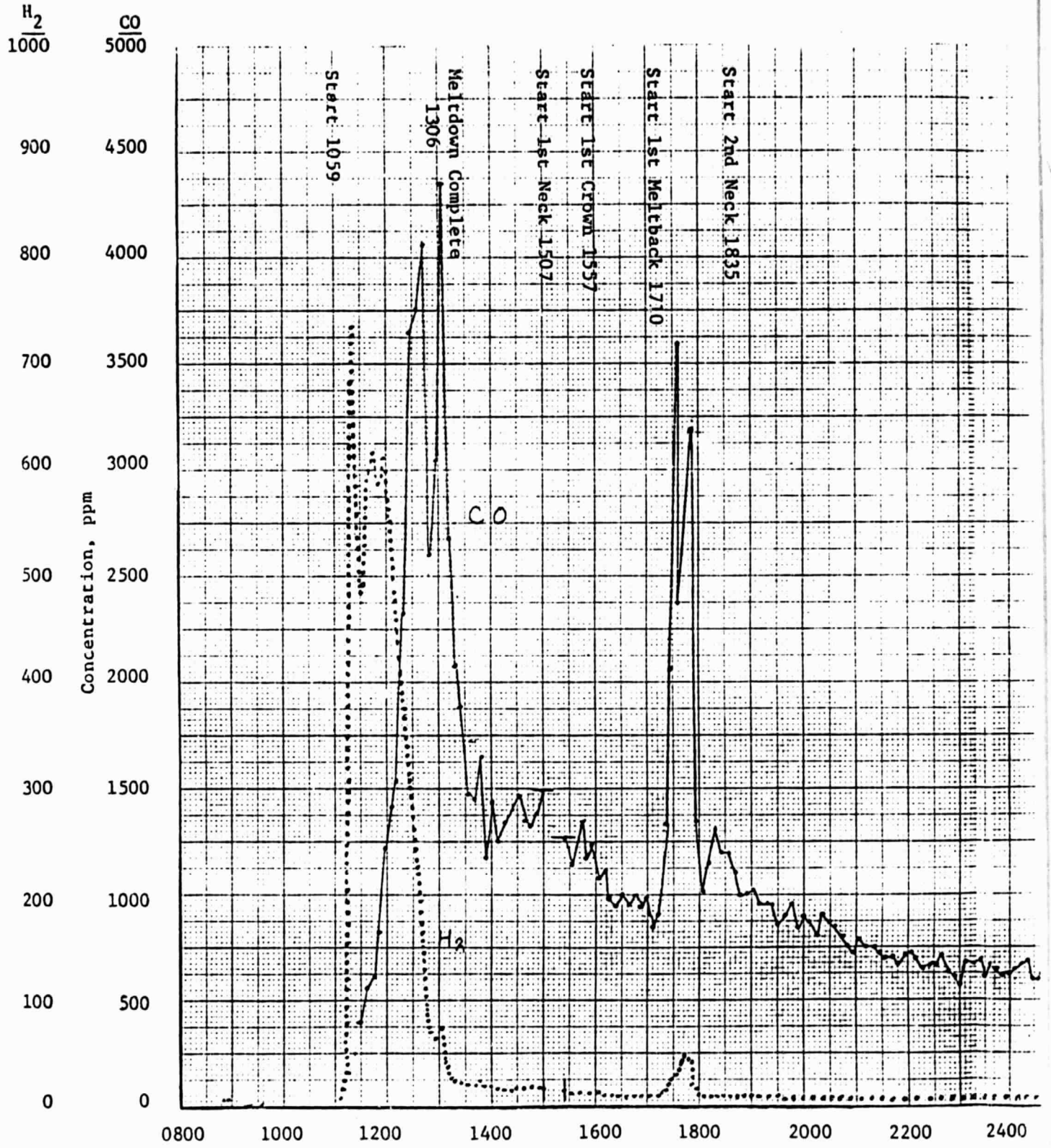

FIGURE

H_2 AND CO CONCENTRAT

ORIGINAL PAGE IS
OF POOR QUALITY

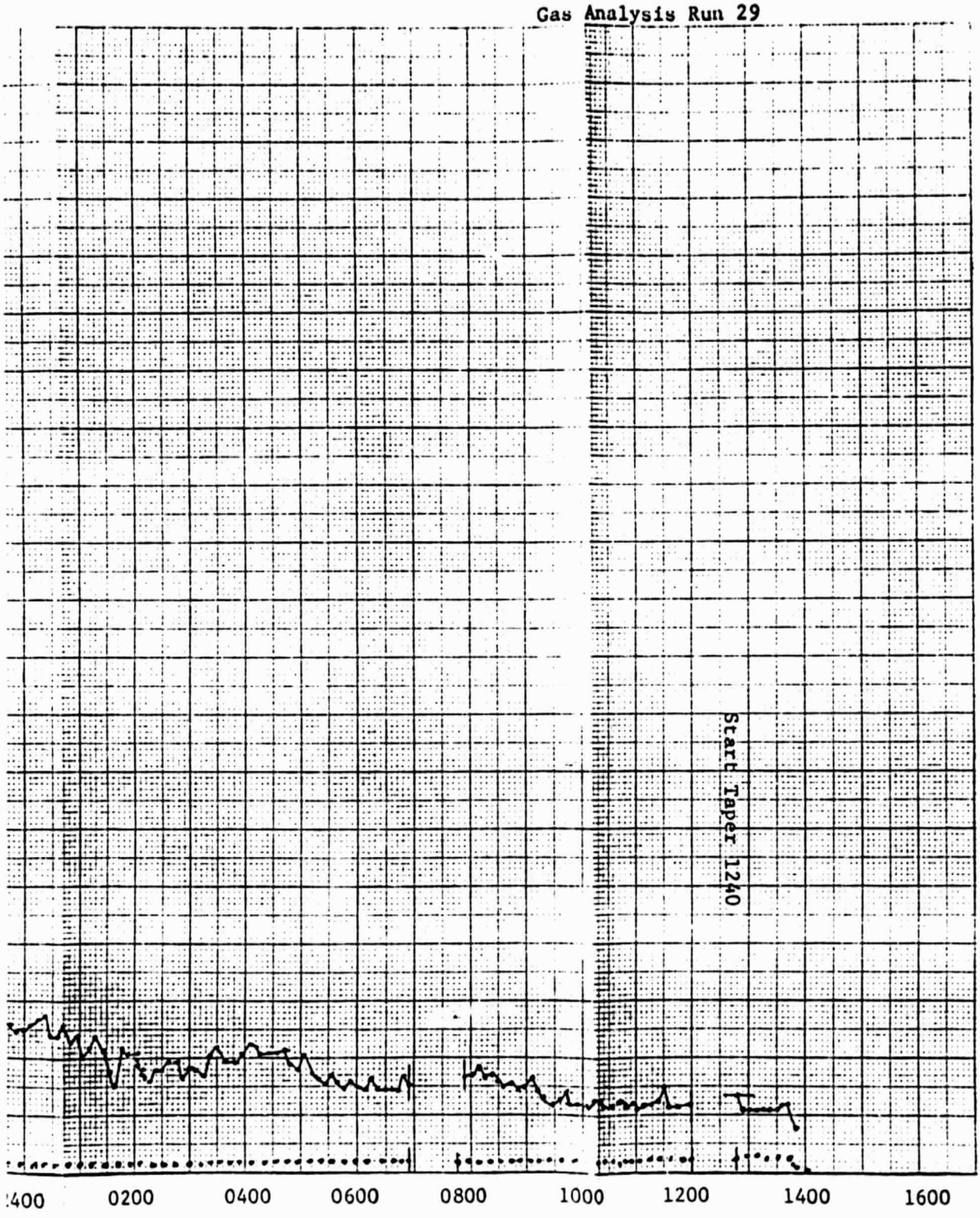

.OCK TIME

.GURE 5-3
'TRATION DURING RUN 29

There is apparently a slow calibration drift in the system which is not understood at this time. However, it is not a serious problem and can be easily corrected by occasional recalibration of the integrator "calibration table." Recalibration is accomplished by running the calibration gas standard again and entering the new value into the calibration table.

The overall pattern of carbon monoxide and hydrogen concentration was similar for all crystal growth runs. Certain conditions influence the concentrations substantially, however. Factors affecting carbon monoxide concentrations as observed during a normal crystal growth cycle follow:

a) Little or no CO is detected during the initial stages of the meltdown as the silicon and hot zone parts are heating up.

b) A rapid increase in the CO concentration is observed when the silicon starts to melt.

c) Continued increase in CO concentration occurs as more silicon melts and the furnace temperature rises.

d) Maximum CO concentration appears at the end of the meltdown just before heater power is decreased.

e) Unusually high concentrations of CO are seen if the melt is super-heated following meltdown.

f) CO concentration gradually decreases as the melt temperature cools to seed dip temperatures following meltdown.

g) Continued decreases in CO concentration occur as the crucible is raised to the start height for crystal growth and the melt is cooled more.

h) CO concentration decreases as the crucible is slowly raised out of the hot zone during crystal growth.

i) CO concentration is sensitive to furnace temperature changes (power changes) during any stage of the growth cycle.

The characteristic pattern for hydrogen gas concentration is as follows:

a) Rapid H_2 increase in the beginning stages of the meltdown when the power is increased to the normal maximum during meltdown. This peak increases to a maximum about thirty minutes into the meltdown and then slowly decreases. It

continues to decrease even as the CO concentration starts increasing dramatically when the silicon starts to melt.

b) H_2 concentration decreases throughout the remainder of the crystal growth.

c) Large changes in temperature influence the concentration of H_2 somewhat. Higher temperature increases the concentration. This effect is much more evident in the early stages of the crystal growth run than the later stages.

The moisture level parallels those of hydrogen during the first stages of meltdown.

Figure 5-4 shows a silicon crystal growth run that included several meltbacks of beginning crystals (during the first twelve hours) and a recalibration of the GC late into the run. The sharp peak at approximately 1300 hours the second day was the result of a large power increase to melt back a wall freeze. The discontinuity at 0800 points out the problem experienced with the inability of the GC to remain in calibration over a long period of continuous run time and the brief procedure of recalibration to correct the problem.

Figure 5-5 shows very clearly the carbon monoxide and hydrogen gas concentrations as a result of a rather severe air leak in the top portion of the crystal grower. This run was a recharge run and the graph begins during the last twelve hours of the growth of the first crystal. At approximately 2300 hours of the first day near the end of the growth of the first crystal, a recalibration was performed showing a slight increase in the average CO reading. During the recharging operation, when the seed rotation direction was reversed, a seal failed and a large air leak opened up. The sharp increases and decreases of carbon monoxide and hydrogen concentrations experienced during the recharging operation, approximately 0500 to 0740 hours, were associated with opening and closing of the isolation valve. (The air leak was effectively eliminated when the valve was closed.) Variations in the high concentration of carbon monoxide and hydrogen during the growth of the second crystal are most likely due to variations in the leak rate of the air, with some fluctuation brought about by temperature changes.

*It should be noted that the concentration scales used on the

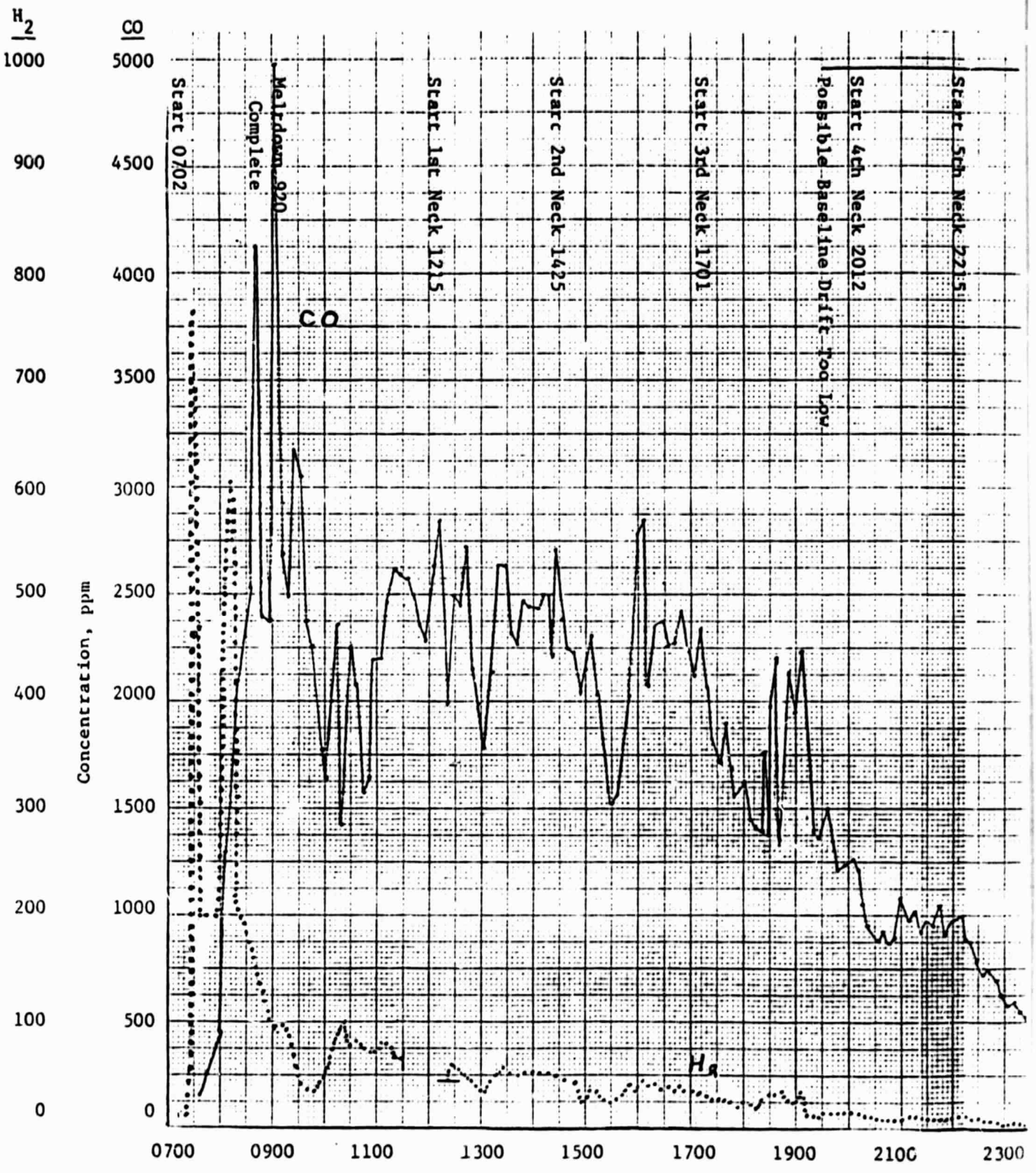

FIGURE 5-4

H_2 AND CO CONCENTRATION DUR

ORIGINAL PAGE IS
OF POOR QUALITY

Gas Analysis Run 25

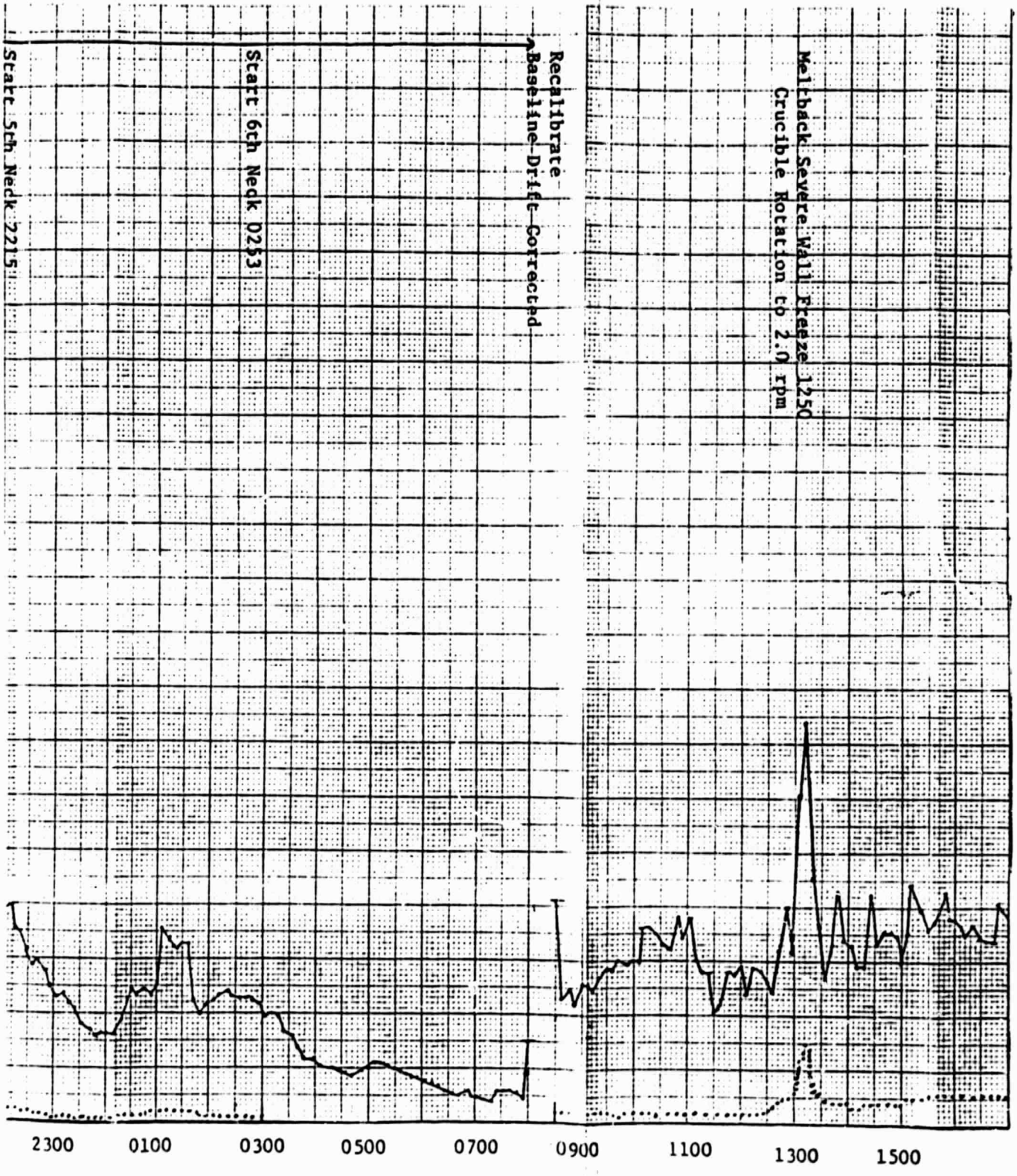

TIME

5-4

ION DURING RUN 25

ORIGINAL PAGE IS
OF POOR QUALITY

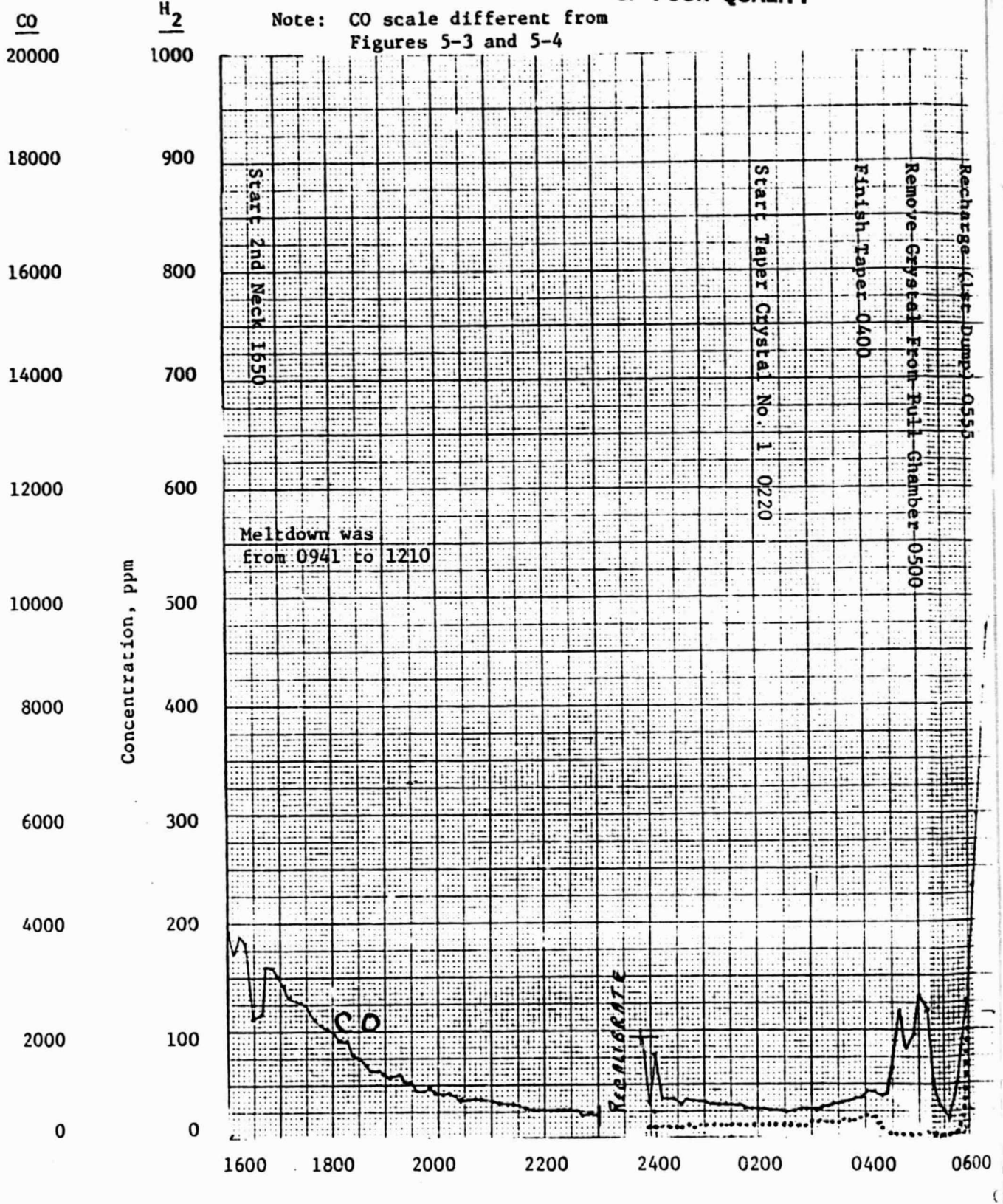

H_2 AND CO CONC

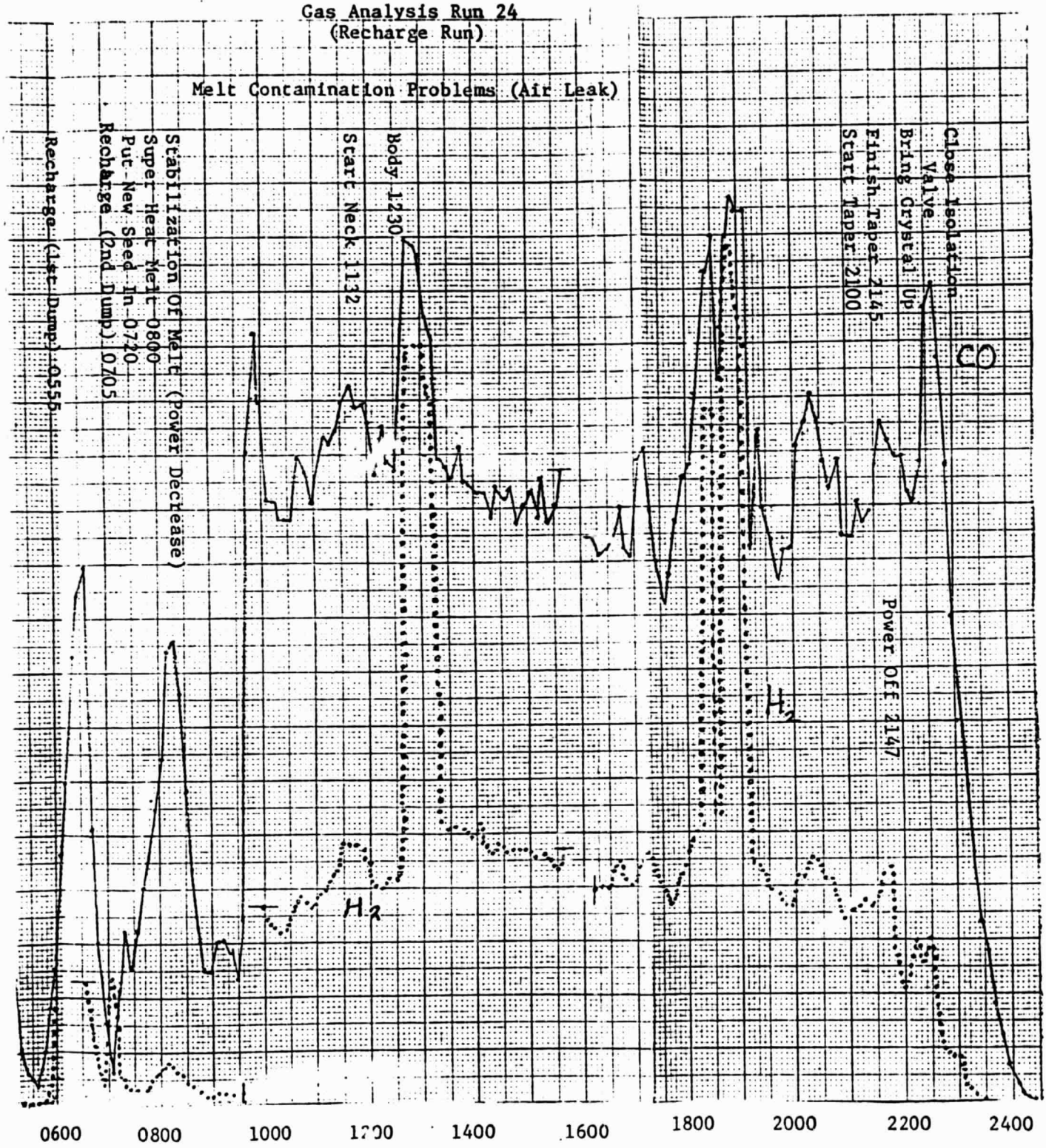

FIGURE 5-5

O CONCENTRATION DURING RUN 24

vertical axis of the graph are considerably higher than those of the previous two graphs.

Some limited experimentation was done during January which indicated that small air leaks may be detectable on the GC. Small amounts of air were allowed to enter the grower for a short period of time (2-3 seconds) with resulting small but noticeable increases in the measured CO concentrations. Although the CO increases were small for these minute quantities of air injection when using the 10 ppm range of the GC, the higher sensitivity 1 ppm range showed more distinct peaks. It is concluded that small intermittent leaks may be detectable but that air leaks occurring in a crystal grower that are of a continuous nature will result in increased base-line CO concentrations and may not be detected. Temperature changes will produce far greater variations in carbon monoxide and hydrogen concentrations which will probably mask small air leaks that may occur in the crystal grower. This would be another basis for more than one gas sampling location. Small air leaks might be more detectable if sampling was made above the melt rather than at the exhaust.

Moisture levels of ambient gases within the crystal grower followed a pattern similar to H_2. The pattern showed decreasing moisture levels during the initial room temperature purge step, leveling off of moisture levels when furnace power was turned on at a low level, and, finally, rapidly increasing moisture levels when the power level was raised to rapidly heat the silicon to the melting point. The moisture levels then decrease rapidly when the power level is decreased at the time silicon starts melting. Moisture levels continue to decrease throughout the remainder of the crystal growth run.

Figure 5-6 shows the water vapor concentration in ppm as a function of time into Run 24, a recharge run. Following a short warm-up and argon purge cycle, the power was turned on at 0941. The power level was kept relatively low (50 kW) for the first ten to fifteen minutes then rapidly increased to 110 kW for maximum safe heat-up rate. During this maximum heat-up period, the moisture level rose very rapidly and was observed as high as 12,550 ppm. Moisture concentration then decreased during the meltdown cycle almost as rapidly as it had increased. The increase in moisture usually coincides with the rapid rise of hydrogen concentrations

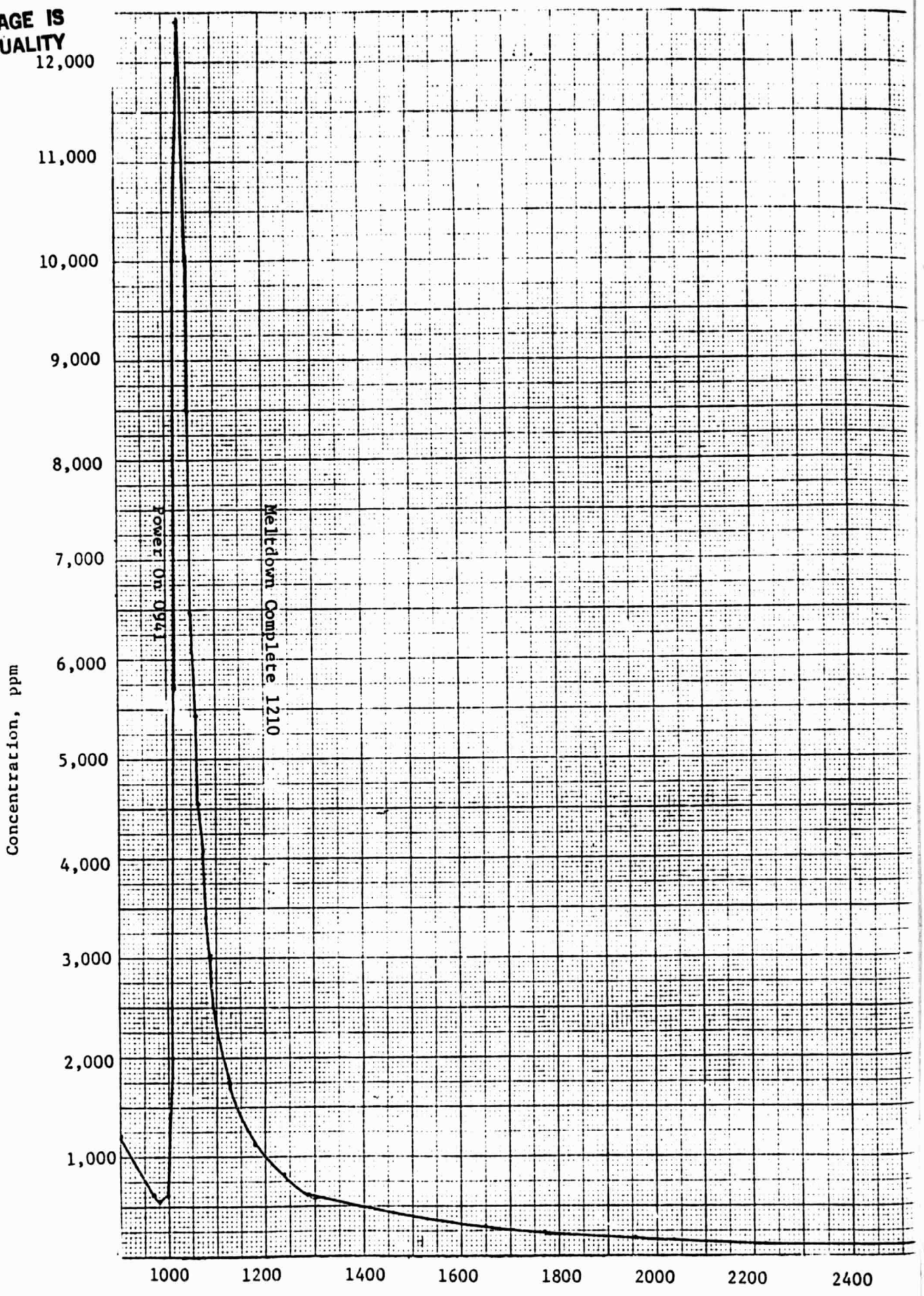

FIG

WATER VAPOR CONCEN

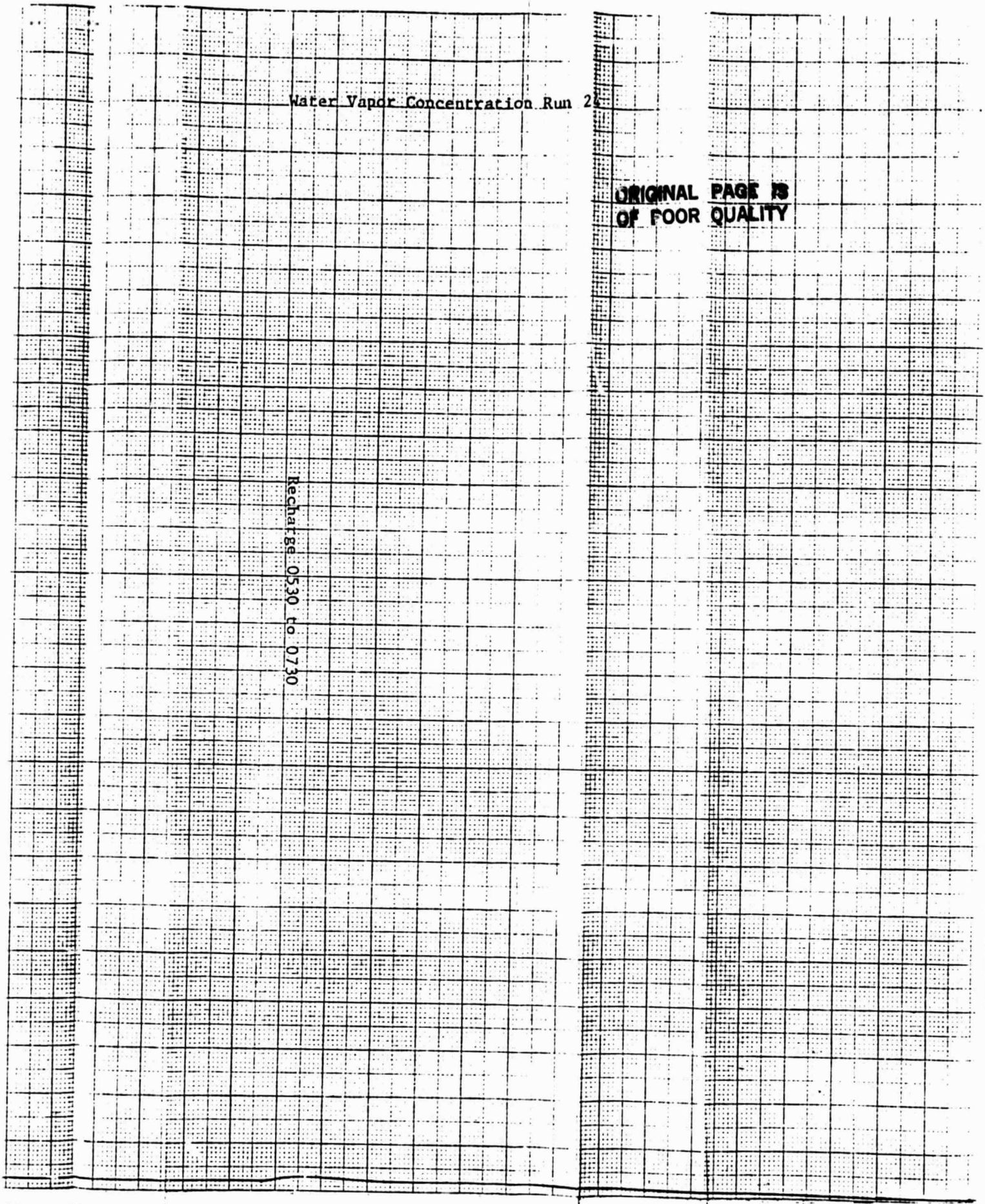

FIGURE 5-6
CONCENTRATION DURING RUN 24

during the early stages of the meltdown.

An interesting result of the moisture concentration studies was that runs made immediately following bakeouts or other runs, when the furnace had been loaded with silicon shortly after the grower was opened (and was still warm), yielded lower maximum concentrations of moisture during the early stages of meltdown and faster decreases in moisture after the maximum levels had been reached. This suggests that moisture in the furnace is the release of adsorbed water from atmospheric humidity.

Experimental evidence has shown that graphite hot zones must be "baked out" prior to crystal runs for the best results. Several bakeout runs were performed during this program and gas analyses were made on them. Comparison of the bakeouts with the crystal growth runs has yielded a better understanding of the importance of the bakeout. It was noted first that bakeouts of new graphite hot zone parts yielded considerably more CO than previously baked out (used) graphite parts.

Following Run 21, it was decided to convert the crystal grower to the larger hot zone capable of accepting 16" diameter crucibles. Since much of the graphite to be used was new, it was necessary to perform a thorough bakeout of these new parts prior to making any crystal growth runs. Now that the GC was automated, it gave us an ideal opportunity to measure gas atmosphere data during a bakeout. Moreover, since much of the graphite was new, this data could also be compared to data of bakeouts of old and previously baked out graphite.

It is customary to bake out new graphite parts over a longer period of time than previously baked out graphite and in steps of increasing temperature. Since there is a much larger quantity of volatiles in new graphite as opposed to previously baked out graphite, a prolonged step temperature bakeout is performed to liberate volatiles at each increasing temperature plateau. This can be evidenced by high concentrations of the analyzed gases (carbon monoxide and Hydrogen) at one temperature plateau, decreasing over a period of time at that temperature, but again, increasing to the high concentration levels when the temperatue is elevated to the next plateau. A total of three days (5-7 hours/day) were required to bake out this new graphite to a satisfactory purity as indicated by the gas analyzer. Each day, a higher temperature plateau was used.

The gas analysis data generated the second and third days of the bakeout can be seen on the graphs in Figures 5-7 and 5-8. Figure 5-7 is a plot of the carbon monoxide concentration as a function of time, while Figure 5-8 plots hydrogen concentration as a function of time. Both the second bakeout day (1/22/82) and the third bakeout day (1/25/82) are plotted on the same graph. In this way, comparisons can be made and readily seen on the same graph. It should be noted that, between the 22nd and the 25th, the crystal grower and hot zone were kept under vacuum except for a short period of time (approximately one hour) used to clean the furnace and vacuum the graphite.

The second day's temperature plateau was significantly above the normal crystal growth temperature. The CO concentration rose sharply following the first half hour of the bakeout when the temperature was relatively low and increasing slowly. At 11:00 AM, the power was raised to increase temperature more rapidly and resulted in the dramatic increase in carbon monoxide until the plateau temperature was reached at approximately 12:00 noon. At this time, automatic temperature control was used to maintain the temperature at this plateau. This resulted in a small decrease in the power to the heater. Once the power was stabilized, it remained at this level throughout the remainder of the bakeout. Once the automatic temperature control was initiated, the CO concentration levels dropped rapidly and continued to decrease throughout the remainder of the bakeout.

The third day's bakeout repeated the pattern of the second day's bakeout: a sharp increase in CO concentration during the rapid rise in temperature to the new plateau (meltdown temperature level), then a rapid, continuous decrease in CO concentration throughout the remainder of the bakeout once the plateau was reached and automatic temperature control was initiated. It is interesting to note, however, that the maximum concentration level of CO reached the third day was higher than that reached the second day. Moreover, a break in the decreasing concentration trend can be observed at 1510 hours. This CO concentration increase is due to an 8% temperature increase made at that point in the bakeout.

Although the carbon monoxide concentration plots are similar for both days, the hydrogen concentration plots are quite different. The plot in Figure 5-8 shows a much higher concentration of hydrogen during

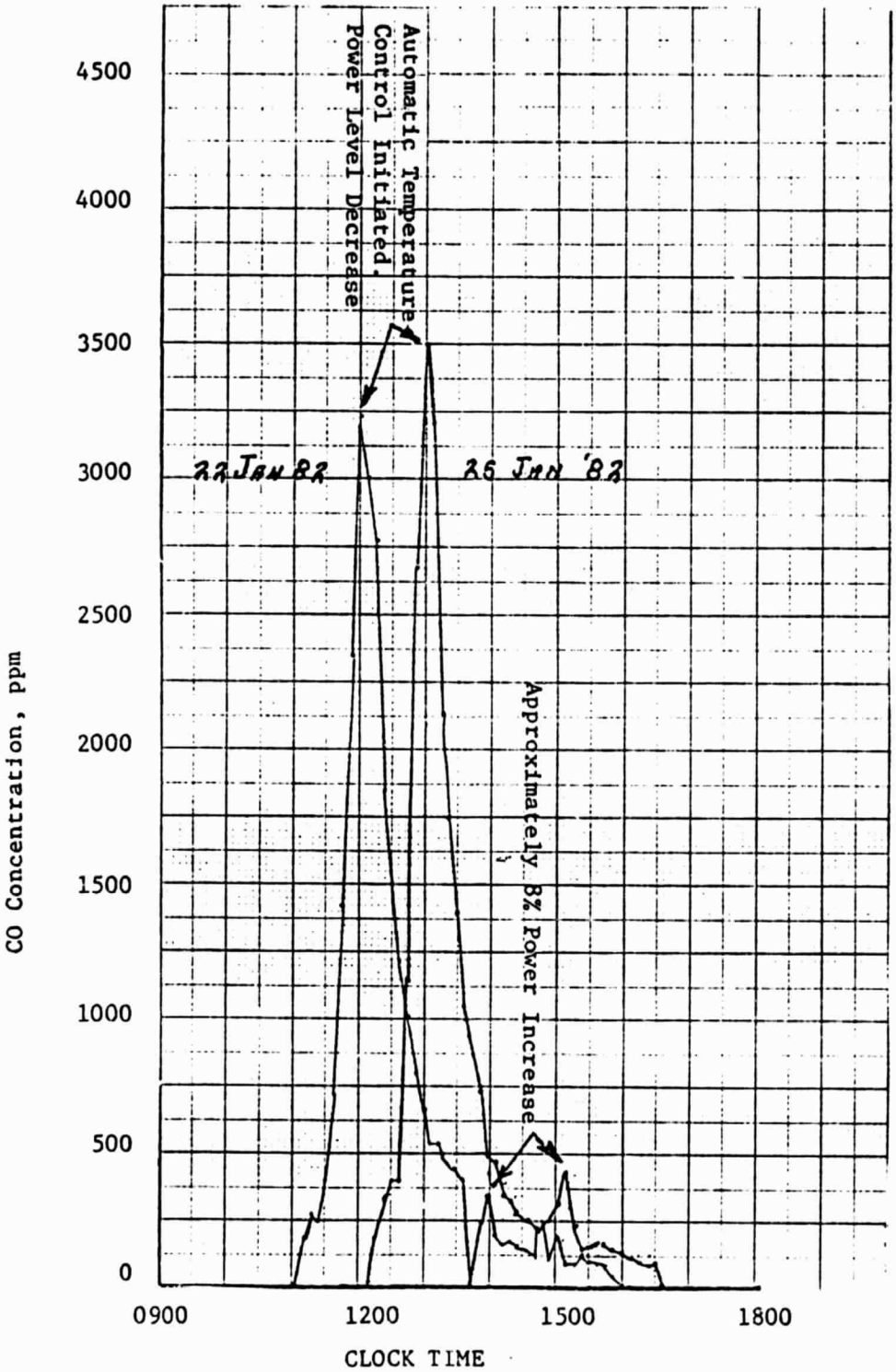

FIGURE 5-7

CO CONCENTRATION DURING BAKEOUT OF NEW GRAPHITE

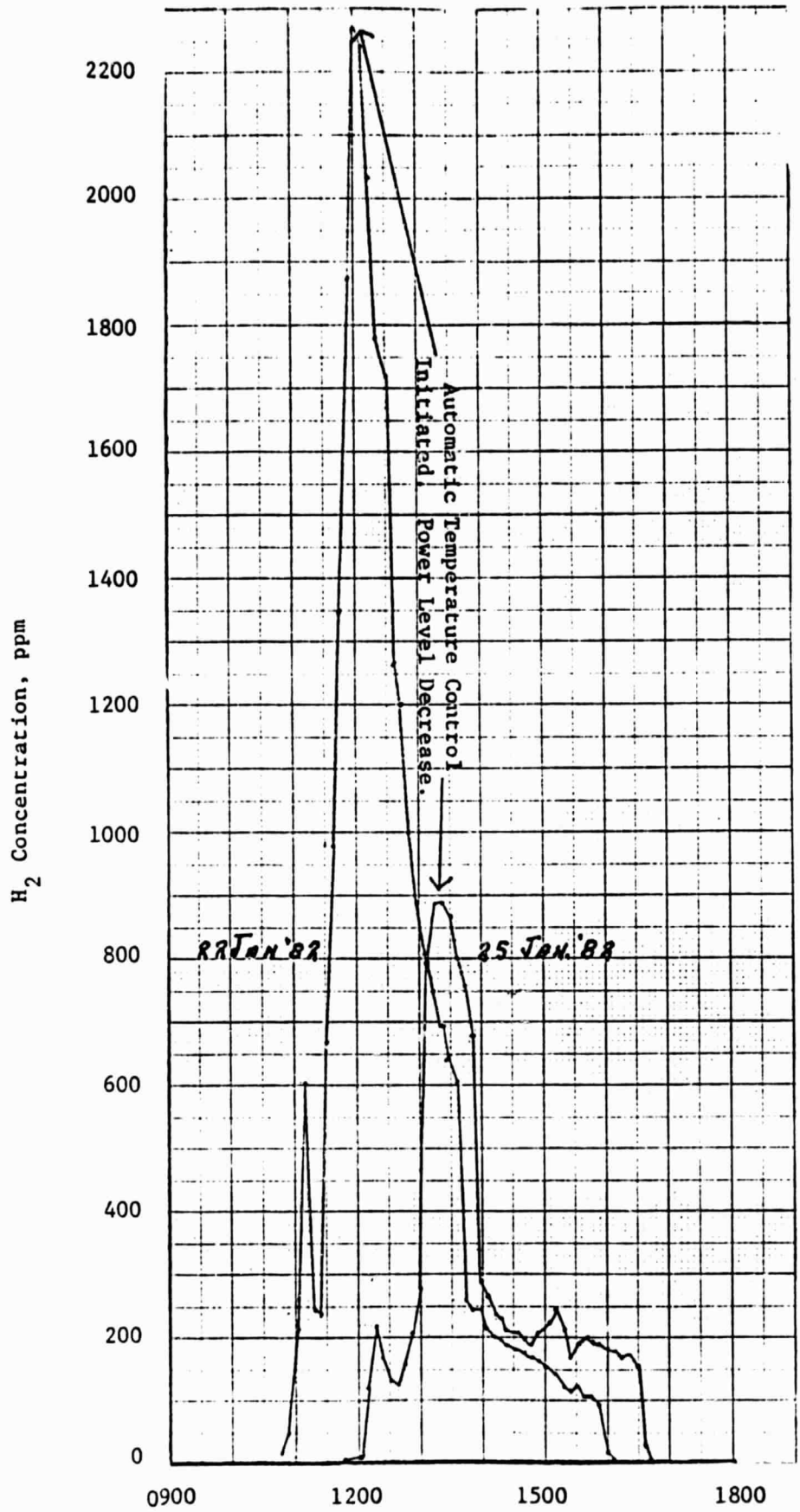

FIGURE 5-8

H_2 CONCENTRATION DURING BAKEOUT OF NEW GRAPHITE

the second day's bakeout than during the third day's bakeout, even though the third day's bakeout was at a significantly higher temperature.

It should be noted that on the hydrogen analysis of January 22 (Figure 5-8) there is an inconsistency in the smoothness of the curve. A sharp decrease in the hydrogen concentration was experienced between 11:10 AM and 11:30 AM. However, at 11:30 AM, the concentration started again to rise very rapidly and attained its maximum concentration in the next half hour. This sharp turnaround and increase in hydrogen concentration corresponds to a 7% power increase at 11:30 AM and a temperature higher than the first day's bakeout plateau at 11:34 AM. The peak concentration corresponds to the time (12:04 PM) the automatic temperature control was initiated.

Dew point measurements taken by the hygrometer during this bakeout indicate an increasing moisture level through the first half hour, then a decrease until the previous day's bakeout temperature plateau was surpassed. The moisture level then increased again until shortly after automatic temperature control was initiated. The moisture concentration levels parallel the hydrogen concentrations during this bakeout.

Since the crystal grower was not opened between the first day's bakeout (1/21/82) and the second day's bakeout (1/22/82), it can be assumed that water vapor from the air did not contribute to the moisture levels recorded during the second day's bakeout.

Although the third day's bakeout hydrogen concentration plot looked similar to the second day's bakeout, the correlation between increases and decreases in moisture level is not present. The moisture level peaks in the early stages of the bakeout (12:15 PM - 12:30 PM), then decreases continuously for the remainder of the bakeout. There is no change of direction when the previous day's bakeout temperature plateau is reached and surpassed. However, the hydrogen concentration, which had started to decrease with the decreasing of the moisture level, again started its sharp increase close to the previous day's bakeout temperature plateau. As can be seen, the hydrogen concentration levels, although significantly lower than the second day's bakeout, peaks about the time the automatic temperature control was initiated for that bakeout's temperature plateau. The hydrogen concentration level peaked upward again when the power level (temperature) was increased by 8% at 1510 hours.

Following each day's bakeout, a black powdered coating was observed on the cold stainless steel furnace tank walls and furnace tank top plate. This is normal for new graphite but is rarely seen with used, well-baked-out graphite.

Figure 5-9 is a graph of a bakeout performed on previously used graphite. The CO and H_2 lines are combined on the same graph and are not very distinguishable. However, the important point here is to note the differences in the maximum concentrations of these two gaseous species when compared to Figures 5-7 and 5-8. The maximum CO levels were approximately 1/6 those of the bakeout on 1/25/82 and the hydrogen levels were a little more than half the maximum concentrations recorded during the bakeout of 1/22/82.

It is felt that the high initial concentration of hydrogen during bakeouts is caused by the same mechanism which causes high hydrogen concentrations during the initial meltdown stages of crystal growth, that is, the release of water vapor absorbed by certain parts of the crystal grower hot zone and its reaction with hot graphite. However, new graphite that has never been baked out before, contains additional volatiles which increase the concentration levels of both CO and H_2.

Figure 5-10 is another illustration of the CO and H_2 concentrations during a bakeout of used graphite hot zone parts. The graph represents a two-day bakeout and is typical of the lower concentrations seen during bakeouts of used graphite (be sure to compare concentration scales for all graphs).

One area of gas analysis that was not explored and could shed further light on the chemical reactions taking place in the crystal grower during silicon crystal growth is to analyze the ambient gases produced during a normal meltdown cycle using a fused quartz crucible with no silicon in it. With no silicon to react with the fused quartz crucible, the reactions between the quartz and the graphite could be studied in more detail.

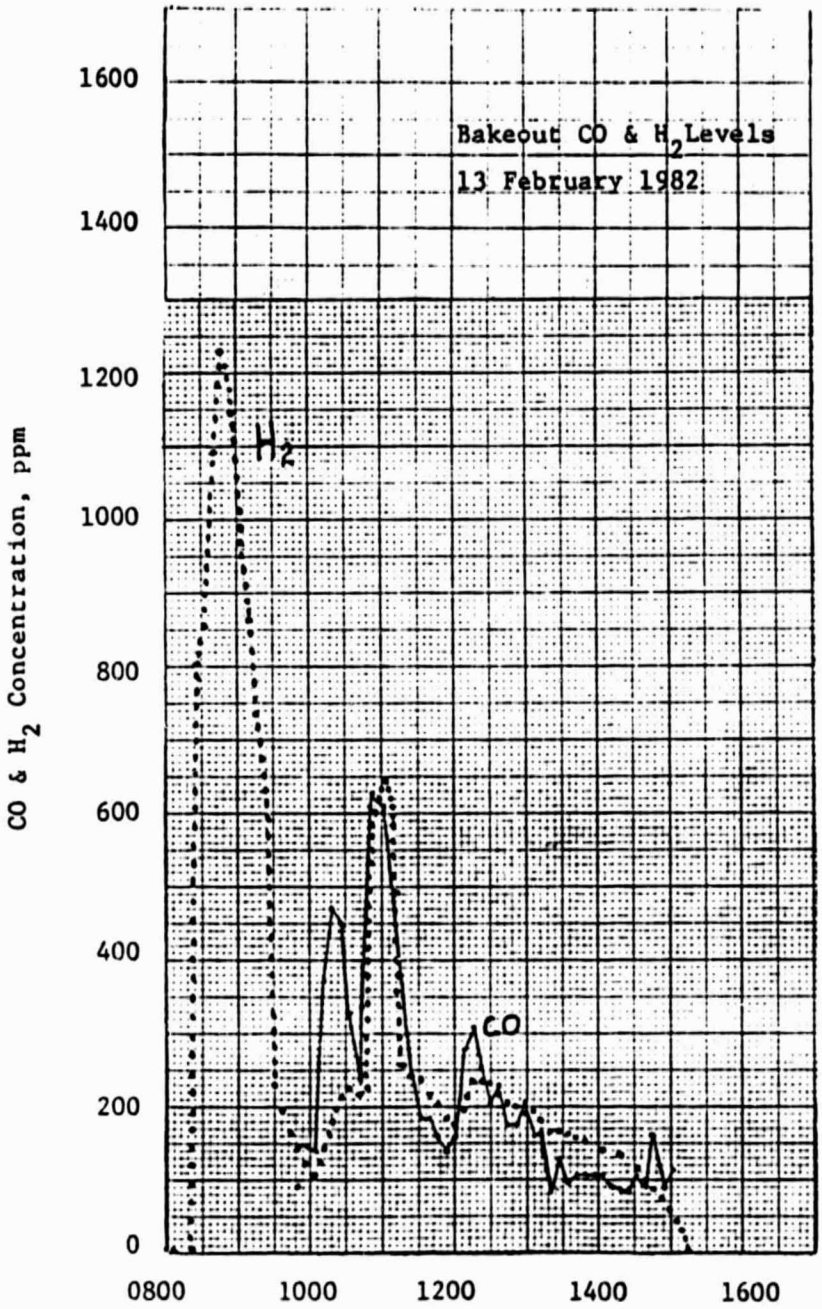

FIGURE 5-9

H_2 AND CO CONCENTRATION, BAKEOUT OF USED GRAPHITE

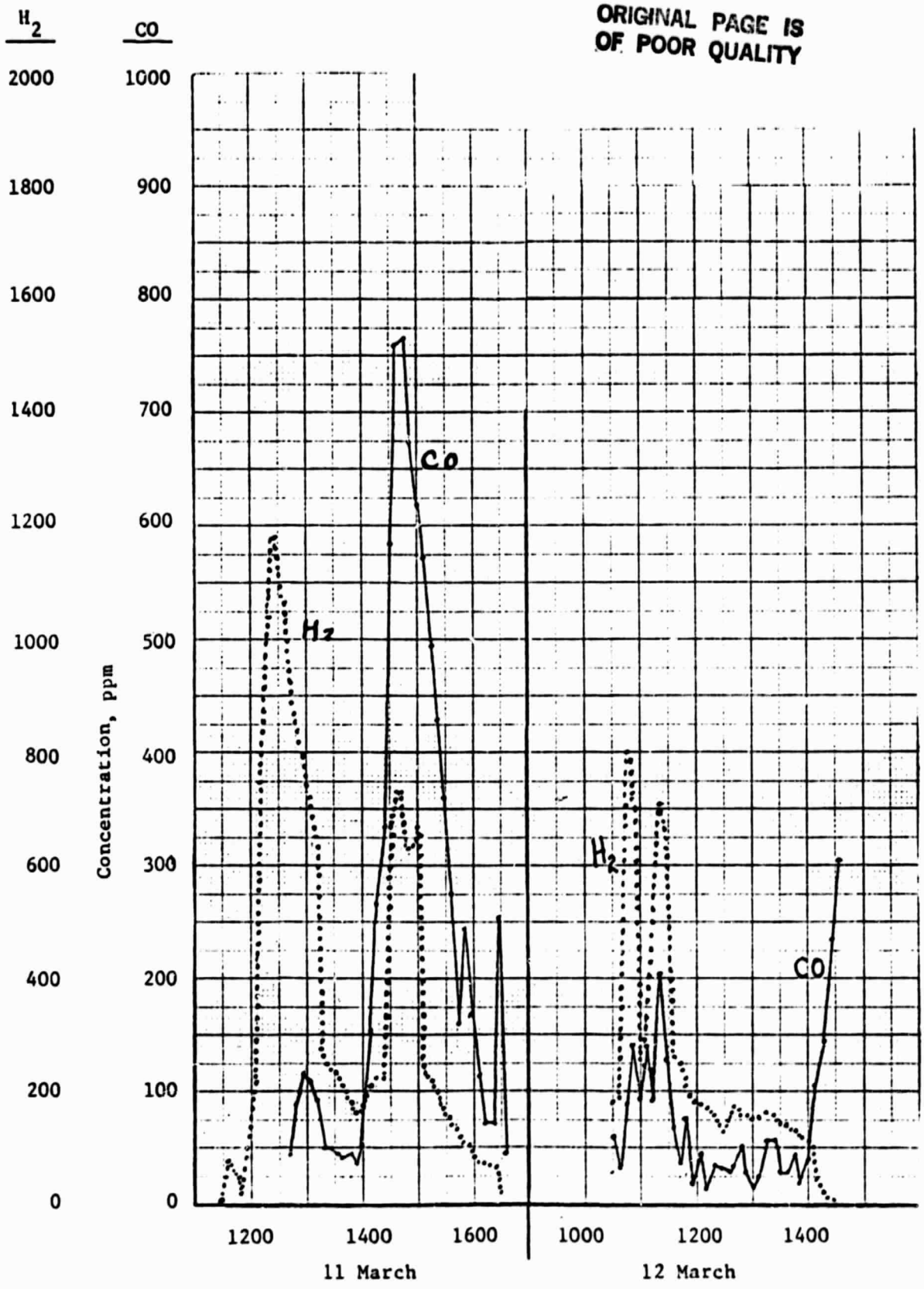

FIGURE 5-10

CO AND H_2 CONCENTRATION DURING BAKEOUT

6.0 ECONOMIC ANALYSIS

6.1 Three Schemes Analyzed

An add-on cost projection based on the program throughput goal of 2.5 kg/hr is shown in Table 6-1. Three schemes were considered for growing 150 kg from 406 mm (16") diameter crucible in the prescribed cycle time of 60 hrs. Scheme 1, pulling five crystals each of 30 kg, should be achievable from a 381 mm (15") crucible, and, therefore, better utilization of the 406 mm crucible size would be afforded by schemes 2 and 3. The advantage of pulling 150 kg as 4 x 37.5 kg crystals or 3 x 50 kg crystals, is the reduction in the number of recharge operations required. This is not immediately obvious in the final add-on costs shown in Table 6-1, because the fixed cycle time dictates that the greater the number of crystals grown, to achieve 150 kg, the higher must be their average pull rate.

A better illustration of the add-on cost difference between growth schemes is provided when the crystal growth rate is similar (for a given nominal crystal diameter). An intermediate analysis for 5 x 30 kg crystals grown from a 381 mm (15") crucible, based on actual growth parameters, produced an add-on cost of $25.51/kg (or ¢18/pk. watt) for an average pull rate of 7.6 cm/hr. Whereas, the program best case analysis, for 4 x 37.5 kg crystals from a 406 mm crucible with a mean pull rate of 8 cm/hr., produced an add-on cost of $23.17/kg (See Table 6-2).

6.2 Cheapest Machine Analysis

Because of the effectiveness of multiple crystal growth in reducing materials cost, the largest component of total annual (add-on) cost now is that due to capital equipment. Table 6-2 shows an annual equipment cost component of $141,109 which represents 43% of the total annual cost, compared to the materials cost contribution of 31%. Clearly a decrease in the cost of the capital equipment will directly affect add-on cost and a measure of sensitivity is given in Table 6-3.

TABLE 6-3

% Reduction in Equipment Cost	Add-on Cost $/kg
0	23.17
5	22.67
10	22.17
15	21.67
25	20.67
30	20.18

As an example, a 25% reduction in equipment cost would produce a $2.5/kg reduction in add-on cost.

In looking for ways to reduce the cost of a grower required to produce solar grade material, a first question might be, "How does this requirement differ from that for producing electronic grade material?" In terms of machine functions and controls, the answer is, "Hardly at all." In fact, because of the recharge requirement, the growth of solar grade material might be considered a slightly more demanding application. Thus there are no basic functional or design differences in a standard Czochralski grower which can be dispensed with. However, there are still areas in which a measure of cost reduction can be achieved, and these are:

(i) Elimination of redundant controls - The use of microprocessor control has resulted in some duplication such that both digital and analogue versions of the diameter controller, heater controller, and growth controller are presently available. Elimination of a set of analogue controllers is a reasonable cost saving step.

(ii) Value Engineering - A properly undertaken exercise should identify those components which are not absolutely necessary, e.g., water flowmeters, and those which could be bought at reduced cost or manufactured from cheaper materials.

(iii) Quantity price breaks - In arriving at capital equipment cost, a 5% discount for quantities of 5 to 9 machines has been used. Further discounting would apply if quantities greater than ten are considered.

An estimate of cost reduction likely in the above mentioned categories is as follows:

(i) $6,000

(ii) $4,000

(iii) $15,500

These costs are per operating unit and are quoted in 1980 dollars. Total saving of $25,500 represents a 10.3% cost reduction, and this equates to an add-on cost decrease of $1.03/kg ($23.17/kg $\rightarrow$ $22.14/kg).

TABLE 6-1

ECONOMIC ANALYSIS
CG ADD-ON COST PROJECTIONS BASED ON
GROWER THROUGHPUT GOAL OF 2.5 KG/HR

CONDITIONS	1	2	3
Crucible Diameter (cm)	40.6	40.6	40.6
Crystal Diameter (cm)	15.24	15.24	15.24
Total Poly Melted (kg)	158	158	158
Total Crystal Pulled (kg)	150	150	150
Avg. Straight Growth Rate (cm/hr)	10.3	8.9	7.8
Pulled Yield (%)	94.9	94.9	94.9
Yield After CG (% of Melt)	83.5	85.4	87.3
Individual Crystal Wt. (kg)	30	37.5	50
No. Crystals/Crucible	5	4	3
Cycle Time (hr)	60	60	60

PROCESS CYCLE TIMES

OPERATION	TIME (MINS)		
1. Preparation			
Load Polysilicon	15	20	25
Close Furnace	5	5	5
Pump Down	15	15	15
Melt Down	105	115	135
Subtotal	140	155	180
2. Growth Cycle (Initial)			
Lower Seed	*	*	*
Stabilize Temp.	30	30	30
Neck Growth	20	20	20
Crown Growth	55	55	55
Straight Growth	347	515	795
Taper End	60	60	60
Subtotal	512	680	960
3. Recharge/Growth Cycle	(X4)	(X3)	(X2)
Cool Crystal	30	30	30
Remove Crystal	10	10	10
Load Hopper, Vac Down (X2)	60	60	60
Lower Hopper (X2)	10	10	10
Dump and Melt	80	85	90
Lower Seed	*	*	*
Stabilize Temp.	30	30	30
Neck Growth	20	20	20
Crown Growth	55	55	55
Straight Growth	347	515	795
Taper End	60	60	60
Subtotal	702	875	1160
	(X4) 2808	(X3) 2625	(X2) 2320

TABLE 6-1 (CONT'D)

4. Shut Down Cycle	1	2	3
Cool Furnace	80	80	80
Remove Crystal	**	**	**
Clean, Set Up	60	60	60
Subtotal	140	140	140
Total Cycle Time (Mins)	3600	3600	3600

*Completed during Melt Stabilization Time
**Completed during Furnace Cooling Time

Growth Rate Calculation

Grow Diameter (cm)	15.75	15.75	15.73
Straight Crystal Wt (kg)	27	34.5	47
Straight Growth Time (hr)	5.78	8.58	13.25
Avg. Growth Rate (kg/hr)	4.67	4.02	3.55
Wt per Unit Length (kg/cm)	0.454	0.454	0.454
Avg. Pull Rate (cm/hr)	10.3	8.89	7.82

SAMICS/IPEG INPUT DATA AND COST CALCULATION

INPUT DATA ($ 1980)	1	2	3
1. Capital Equipment Cost (EQPT)	$ 247,560	$ 247,560	$ 247,560
2. Floor Space (SQFT)	120	120	120
3. Annual Direct Salaries			
Prod. Operator (0.65 man @$13160/yr)	8,554	8,554	8,554
Elect. Tech (0.3 man @$16940/yr)	5,082	5,082	5,082
Inspector (0.1 man @$11550/yr)	1,155	1,155	1,155
Total (DLAB)	$ 14,791	$ 14,791	$ 14,791
4. Direct Materials Usage based on Machine Utilization of 85% = 124 cycles/yr			
Crucibles 16 x 12 @$345	42,780	42,780	42,780
Seeds ($20 each)	2,480	2,480	2,480
Dopant ($25/cycle)	3,100	3,100	3,100
Argon (60 ft/hr at $0.05/ft^3)	22,320	22,320	22,320
Graphite (4 sets 16" graphite parts per yr @$8,889/set)	35,556	35,556	35,556
Materials Total (MATS)	$ 106,236	106,236	$ 106,236

TABLE 6-1 (CONT'D)

5. Utilities	1	2	3
Electricity @$0.04/kw hr			
Meltdown @100 kw	3,513	3,058	2,604
Avg. Grow @75 kw	18,600	18,910	19,220
Water @0.7¢/ft^3	12,106	12,106	12,106
30 gpm for 97% cycle			
Utilities Total (UTIL)	$ 34,219	$ 34,074	$ 33,930

IPEG Price	5 x 30 kg crystals	4 x 37.5 kg crystals	3 x 50 kg crystals
C1 EQPT x $0.57/yr = $EQPT	141,109	141,109	141,109
C2 SQFT x $109/yr = $SQFT	13,080	13,080	13,080
C3 DLAB x $2.1/yr = $DLAB	31,061	31,061	31,061
C4 MATS x $1.2/yr = $MATS	127,483	127,483	127,483
C5 UTIL x $1.2/yr = $UTIL	41,063	40,889	40,716
Total Annual Cost	$ 353,796	$ 353,622	$ 353,449
Quan (total Charged x Yield after CZ)(kg)	16,360	16,732	17,104
Add-On Cost ($/kg)	21.62	21.13	20.66
Add-On Cost (¢/Peak Watt) (Assumes 1 kg = 1 M^2)	15.25	14.90	14.57

TABLE 6-2

CZ ADD-ON COST BASED ON BEST MOD CG 2000
PROCESS PARAMETERS

CONDITIONS

Crucible Diameter (cm)	40.6
Crystal Diameter (Grnd) (cm)	15.24
Total Poly Melted (kg)	155
Total Crystal Pulled (kg)	150
Avg. Straight Growth Rate (cm/hr)	8.0
Pulled Yield (%)	96.7
Yield After C.G. (% of melt)	86.9
Individual Crystal Wt. (kg)	37.5
No. Crystals/Crucible	4
Cycle Time (hr)	70.75

TABLE 6-2 (CONT'D)

PROCESS CYCLE TIMES

OPERATION	TIME (MINS)
1. Preparation	
Load Polysilicon	20
Close Furnace	10
Pump Down	20
Meltdown	150
Subtotal	200
2. Growth Cycle (Initial)	
Lower Seed	*
Stabilize Melt	60
Neck Growth	25
Crown Growth	60
Straight Growth	595
Taper End	60
Subtotal	800
3. Recharge/Growth Cycle (X3)	
Cool Crystal	30
Remove Crystal	10
Load Hopper/Pump Down (X2)	60
Lower Hopper and Dump (X2)	15
Meltdown	120
Replace Seed and Lower	*
Stabilize Melt	60
Neck Growth	25
Crown Growth	60
Straight Growth	595
End Taper	60
Subtotal	1035
(X3)	3105
4. Shut Down Cycle	
Cool Furnace	80
Remove Crystal	**
Clean, Set Up	60
Subtotal	140

Total Cycle time of 4245 mins = 70.75 hr.

* Completed during melt stabilization time
** Completed during furnace cooling time

TABLE 6-2 (CONT'D)

GROWTH RATE PARAMETERS	
Grow Diameter (cm)	15.5
Straight Crystal Wt. (kg)	34.9
Straight Growth Time (hr)	9.92
Avg. Growth Rate (kg/hr)	3.52
Avg. Pull Rate (cm/hr)	8.0
Wt. Per Unit Length (kg/cm)	0.44

SAMICS/IPEG INPUT DATA AND COST CALCULATION

INPUT DATA ($ 1980)

1.	Capital Equipment Cost (EQPT)	$ 247,560
2.	Floor Space (SQFT)	120
3.	Annual Direct Salaries:	
	Prod. Operator (0.65 man @ $13160/yr)	8,554
	Elect Tech (0.3 man @ $16,960/yr)	5,082
	Inspector (0.1 man @ $11,550/yr)	1,155
	TOTAL (DLAB)	$ 14,791
4.	Direct Materials Usage Based on Machine Utilization of 85% = 105 cycles/yr:	
	Crucibles @ $345 ea.	36,225
	Seeds ($20/cycle)	2,100
	Dopant ($25/cycle)	2,625
	Argon (60ft^3/hr @ $0.04/ft^3)	17,325
	Graphite (3 sets/yr)	27,339
	TOTAL (MATS)	$ 85,614
5.	Utilities	
	Electricity @ $0.04/kw hr	
	Meltdown @ 100 kw	3,570
	Avg. Grow @ 70 kw	17,370
	Water @ c0.7/ft^3	
	30 gpm for 97% cycle	12,130
	TOTAL (UTIL)	$ 33,070

IPEG Price $ X #&.% kg crystals

C1 EQPT x $0.57/yr = $ EQPT	141,109
C2 SQFT x $109/yr = $ SQFT	13,080
C3 DLAB x $2.1/yr = $ DLAB	31,061
C4 MATS x $1.2/yr = $ MATS	102,736
C5 UTIL x $1.2/yr = $ UTIL	39,684
TOTAL ANNUAL COST	$ 327,670

TABLE 6-2 (CONT'D)

QUAN. (Total Charged x Yield After C.G.) kg	=	14,143
Add-on Cost $/kg	=	23.17
Add-on Cost ¢/pk. watt	=	16.34
(Assumes 1 kg = 1 m^2)		
Machine Throughput kg/hr	=	2.12

7.0 SUMMARY

Previous JPL/DOE contracts at Kayex as well as other contractors helped to identify (1) the preferred method for continuous growth and (2) the areas where further cost cutting was feasible. With background information from these previous efforts, the hopper method of periodic recharging with lump silicon was chosen, and the following areas were chosen for further development work for the purpose of reducing the add-on cost and demonstration of technology readiness:

1. Growth of 150 kg from one crucible by serial ingot growth with periodic recharging.
2. Increased throughput to 2.5 kg/1 hr by improved growth rate, larger diameter (150 mm), and faster recharge cycling.
3. Improved automation for lower labor cost and better yields.
4. Identification of equipment cost items which might be reduced.
5. Better understanding of process parameters as they relate to yields, crucible/silicon interactions, and melt contamination.

The program consisted of several tasks:

1. Equipment construction and test
2. Process Development
3. Automation
4. Analytical Study
5. Documentation

7.1 Equipment Construction

A Hamco CG2000RC design was chosen as the basic equipment for the work. Certain modifications were made to the design including larger capacity, interfacing for automation, chamber modifications for sensors, and a variety of miscellaneous improvements based upon our past experience with the CG2000RC. The equipment was designed as part of contract JPL/DOE 958888 and constructed in the first four months of this contract. It was put through a testing/debugging program and met all design specifications.

7.2 Process Development

In the process development task, a considerable amount of time was directed toward obtaining quality ingots from the larger melt size with the larger (150 mm) diameter while also attempting to achieve improved growth rates. Persistent problems with structure loss and spiral-shaped crystals at the higher growth rates were only partially solved by the end of the program. Specific achievements in the process development area are as follows:

1. A 150 kg growth run was demonstrated by growing 5 x 30 kg ingots. A throughput of about 1.5 kg/hr was achieved.
2. A 37.5 kg crystal, completely dislocation free, was grown from a 40 kg melt demonstrating the feasibility of producing 150 kg by growing 4 ingots, with a resulting improvement in throughput because of one less recharging cycle.
3. The beneficial effect of a radiation shield was confirmed in terms of improved growth rate and improve crystal cleanliness due to the purging control effect of the shield.
4. The spiral growth effect with large melts was reduced substantially although not eliminated by control of melt level, growth rate, and the use of the radiation shield. Thermal instability of large melts appears to remain as a problem to be addressed.
5. Proposed new crucible designs may reduce or control crucible/melt interactions which are theorized to result in structure loss. Crucibles with a bubble-free inner layer may improve yields. These are, however, presently available only to a maximum size of 12-inch (305 mm) diameter, smaller than those being used on this contract.

7.3 Automation

Implementation of sensors for melt temperature, shoulder and diameter, and melt level was completed. The melt temperature sensor, after suitable electronic filtering, was interfaced with the Hamco Agile

system to provide closed-loop melt temperature trimming prior to reading.

The melt level sensor was demonstrated. Although it was found to track melt level accurately, closed-loop control of melt level was not implemented.

A shoulder/diameter sensing pair of pyrometers was used to automate the crown/shoulder growth. This was found to provide improved reproducibility for 100 mm crystals from 12 kg melts. The system was not fully developed for larger melts and diameters because of the various parameters and hot zone changes which were part of the process development. task.

The Hamco Agile system was interfaced successfully to the Mod CG2000 and used for most of the runs on the contract.

7.4 Analytical Study

Solar cells from the 150 kg run were fabricated and tested by Applied Solar Energy Corp. The solar efficiency of the monocrystalline material was 15 to 16% AM-1 for the complete run, whereas that of polycrystalline material was 11 to 13%. This lower efficiency of polycrystalline material was consistent with earlier results. Little or no reduction in efficiency was observed from the beginning to the end in this long run.

Chemical analyses of silicon and crucible showed somewhat improved purity over earlier contracts. Residual melt impurities were primarily calcium, iron, and aluminum. More extensive analyses should be performed in order to draw reliable conclusions.

The bulk of the analytical work related to gas analysis of the ambient gas in the growth chamber. Carbon monoxide, water vapor, and hydrogen were found to vary through the run according to temperature and stage of the run. Carbon monoxide was found to be especially indicative of the quality of the run. Its concentration is a function of temperature as well as chamber leaks or contamination from graphite.

Equipment was designed, built, and operated from the automatic analyses of the three mentioned gases.

7.5 Documentation and Technology Readiness Demonstration

An economic analysis is presented in this report covering the add-on cost of CZ growth for three schemes of growth. Additionally, the sensitivity of equipment cost to add-on cost is presented. A decrease in equipment cost would clearly have an important impact on growth costs now that continuous CZ has reduced the material cost substantially.

A series of 15 runs was conducted utilizing the new Hamco CG6000 crystal grower, embodying most of the features of the Mod CG2000 as well as a number of additional improvements brought about by process development experience and automation results both from this work and other company-funded projects.

The commercial machine was demonstrated to be capable of the growth of large-charge, quality crystal ingot at throughput rates essentially equivalent to those demonstrated with the Mod 2000. The T.R. provision of the contract is satisfied since this machine, with the process, is offered for sale to the industry.

REFERENCES

1. Rea, S.N., Continuous Czochralski Process Development, Texas Instruments DOE/JPL Contract No. 954887.

2. Wolfson, R.G. et. al., Development of Advanced Methods for Continuous Czochralski Growth, Varian Associates DOE/JPL Contract No. 954884.

3. Fiegl, G., Continuous Liquid Feed Czochralski Growth, Siltec Corporation DOE/JPL Contract No. 954886.

4. Runyan, W.R., Silicon Semiconductor Technology, McGraw-Hill, New York, 46, (1965).

5. Kobayaski, N., J. Crystal Growth, 52, 425, (1981).

6. Schmid, F., Khattak, C., Digges, T.G. Jr., and Kaufman, L., J. Electrochemical Society, 126, 935-938, June, (1979).

7. Johnson, C.M., Continuous Czochralski Growth, Kayex Corporation DOE/JPL Contract No. 954888, Final Report, December (1980).